Novel anti-inflammatory targets and mechanisms of boswellic acids and celecoxib

Dissertation
zur Erlangung des Doktorgrades
der Naturwissenschaften

vorgelegt beim Fachbereich
Chemie, Biochemie und Pharmazie
der Johann Wolfgang Goethe-Universität
in Frankfurt am Main

von
Lars Tausch
aus Bad Nauheim

Frankfurt am Main (2008)
(D30)

vom Fachbereich Chemie, Biochemie und Pharmazie der Johann Wolfgang Goethe – Universität als Dissertation angenommen.

Dekan:	Prof. Dr. Harald Schwalbe
Gutachter:	Prof. Dr. Dieter Steinhilber
	Prof. Dr. Oliver Werz
Datum der Disputation:	29.08.2008

Meiner Familie!

Lieber einsam mit den Freien fallen, als mit den Massen im Triumphe ziehen!

Table of contents

1 Abbreviations and reagents

1.1 Abbreviations

[^{3}H]-AA	tritium labelled arachidonic acid
AB	antibody
A(β)-BA	3-*O*-acetyl-β-boswellic acid
(A)KBA	3-O-(acetyl-)-11- keto boswellic acid
ADP / ATP	adenosine diphosphate / adenosine triphosphate
Akt / PKB	protein kinase B
2-APB	2-aminoethyldiphenyl borinate
AUC	area under the curve
(β)-BA	β-boswellic acid
BAs	boswellic acids
BAPTA/AM	1,2-bis(aminophenoxy)ethane-N,N,N`,N`-tetraacetic acid tetrakis / acetoxymethylester
BS	*Boswellia serrata*
BSA	bovine serum albumin
B.*spec.*	*Boswellia species*
$[Ca^{2+}]_i$	intracellular Ca^{2+} concentration
$CaCl_2$	calcium chloride
CatG	cathepsin G
CD62	cell surface protein 62
CDC	cinnamyl-3,4-dihydroxy-alpha-cyanocinnamate
CGI	cathepsin G inhibitor
CLP	coactosine-like protein
COPD	chronic obstructive pulmonary disease
COX	cyclooxygenase
CpG-DNA/-ODN	cytosine/guanine-rich DNA fragments / -oligodesoxynucleotides
$cPLA_2$	cytosolic phospholipase A_2
CytB	cytochalasin B
DAG	diacylglycerol
DMEM	Dulbecco´s modified Eagle medium
DMSO	dimethylsulfoxide

DNA-PK(I)	DNA-dependent protein kinase (inhibitor)
DTT	dithiothreitol
EC_{50}	effective concentration (50% of stimulation or inhibition)
EDTA	ethylenediaminetetraacetate
EGF	endothelial growth factor
eNOS	endothelial nitric oxide synthase
ERK	extracellular signal-regulated kinase
ETP	endogenous thrombin potential
FCS	fetal calf serum
FLAP	5-LO-activating protein
fMLP	N-formyl-methionyl-leucyl-phenylalanine
FPP(s)	farnesyl-pyrophosphate (synthase)
Fura-2/AM	[1-[2-(5-carboxyoxazol-2-yl)-6-aminobenzofuran-5-oxyl]-2-(2`-amino-5`-methyl-phenoxy)ethane-N,N,N`,N`-tetraacetic acid, pentaacetoxymethylester]
Glut-(K)BA	3-*O*-glutaroyl-11-(keto)-boswellic acid
GPCRs	G protein-coupled receptors
GSH	glutathione
HL-60	human leukemia cell line
HLE	human leukocyte elastase
H(P)ETE	hydro(per)oxyeicosatetraenoic acid
HPLC	high performance liquid chromatography
IC_{50}	inhibiting concentration (50% of inhibition)
IGF-1	insulin-like growth factor
IgG / IgM	immunoglobuline G / M
IκB	inhibiting factor of kappa B
IL-6	interleukin 6
IKK	IκB-kinase
IMAC	ion metal affinity chromatography
IP_3	inositoltrisphosphate
IPP	isopentenylpyrophosphate
IPTG	isopropyl-β-D-thiogalactopyranoside
(K)BA-Seph	11-(keto) boswellic acid coupled to Sepharose
LB-medium	Luria Broth base - medium

LNCaP	human prostate cancer cell line
5/12-LO	5/12-lipoxygenase
LPS	lipopolysaccharide
LTs	leukotrienes
M9	minimal medium 9
MALDI-TOF-MS	matrix-assisted laser desorption ionisation – time of flight – mass spectrometry
MAPK	mitogen-activated protein kinase
MCF-7	human mamma carcinoma cell line
11-me-BAs	11-methylene-boswellic acids
MFI	mean channel fluorescence intensity
MM6	human monocytic cell line
MQ	Milli Q water
MS	mass spectrometry
mTOR	mammalian target of rapamycin (kinase)
MWCO	mol weight cut off
NFκB	nuclear factor κ B
NMR	nuclear magnetic resonance spectroscopy
NSAIDs	non-steroidal anti-inflammatory drugs
OD	optical density
p12-LO	platelet-type 12-lipoxygenase
PAC-1	cell surface protein
PAF	platelet-activating factor
PAR-4	protease-activated receptor 4
PBS	phosphate-buffered saline
PDGF	platelet-derived growth factor
PDK-1	3-phosphoinositol-dependent kinase
PGC buffer	PBS plus 1 mg/ml glucose plus 1 mM $CaCl_2$
PG	prostaglandin
PI3K	phosphatidylinositol 3 kinase
PIP_3	phosphatidylinositol-trisphosphate
PKA, PKB, PKC	protein kinase A, B, C
PLC	phospholipase C
PMNL	polymorphonuclear leukocytes

PMSF	phenylmethylsulfonylfluoride
PRP	platelet rich plasma
pTyr	phosphotyrosine
r12-LO / his12-LO	recombinant 12-lipoxygenase / 6-his-tagged 12-lipoxygenase
Rap 1b	Ras-related protein 1b
RBL-1	rat basophilic leukemia cell line
RFU	relative fluorescence units
ROS	reactive oxygen species
RT	room temperature
RTK	receptor tyrosine kinases
SDS	sodium dodecylsulfate
SDS-b	2x SDS loading buffer
SDS-PAGE	SDS-polyacrylamide gel electrophoresis
Seph	EAH-Sepharose 4B
Suc-AAPF-pNA	N-succinyl-alanyl-alanyl-prolin-phenylalanine-p-nitroanilide
TBS	tris-buffered saline
TCM	traditional Chinese medicine
TFA	trifluoro acetic acid
TG	thapsigargin
TGFβ	transforming growth factor beta
TNFα	tumour necrosis factor alpha
TRAP	thrombin receptor-activating peptide
TXA_2	thromboxane A_2
WB	western blot
w/o	without

1.2 Reagents

- Boswellic acids (BAs) were prepared by Dr. J. Jauch [1] (Saarbrücken)
- *Boswellia serrata* (BS) extracts were generous gifts from Burg-Apotheke, Königstein, Germany and Pharmasan GmbH, Freiburg, Germany
- Celecoxib, etoricoxib, rofecoxib were sythesized by WITEGA Laboratories Berlin-Adlerhof GmbH, Germany
- Insulin was a generous gift from Aventis Deutschland GmbH, Frankfurt, Germany
- 5-LO antibody was provided by Dr. O.Rådmark, Stockholm, Sweden
- 12-LO antibody was provided by Dr. C.Funk, Kingston, Canada
- TGFβ was prepared from human platelets as described [2]
- BAPTA/AM, Fura-2/AM were from Alexis Corp, Lausen, Switzerland
- Ampicillin, Coomassie brilliant blue G250, IPTG, leupeptin, oxalacetic acid, were from Applichem, Darmstadt, Germany
- Antibodies against CD41-PC7, CD62-PE, and PE-labelled isotype IgG1 control were purchased from Beckman Coulter, Krefeld, Germany
- Antibodies against PAC1-FITC and FITC-isotype IgM and matrigel were from Becton Dickinson Biosciences, Freiburg, Germany
- CatG antibody, CDC and fluorescence dye secondary antibodies (Rockland Inc.) were from Biomol GmbH, Hamburg, Germany
- Bradford and Lowry reagents were from Biorad, München, Germany
- α-Cyano-4-hydroxycinnamic acid was purchased from Bruker Daltonics Inc., Manning Park Billerica, MA, USA
- Alendronate, cathepsin G inhibitor I, chymotrypsin, DNA-PK inhibitor, elastase, PP2, PP3; Protein kinase assay kit (non-radioactive); staurosporine, SU6656 and tryptase were from Calbiochem, Schwalbach/Ts., Germany
- 5-HETE, LTB_4 and zileuton were from Cayman chemical company, Ann Arbor, MI, USA
- Antibodies against Akt and pAkt, pBad, DNA-PK, Ras; Akt1 kinase and Akt kinase assay kit were from Cell Signaling / New England Biolabs, Frankfurt, Germany
- Boc-Ala-Ala-Nva-SBzl, Cathepsin G, elastin-sepharose, N-Suc-AAPF-pNA, proteinase 3 were from Elastin Products Company Inc., Owensville, MS, USA
- α-Amyrin and ursolic acid were from Extrasynthèse, Genay, France

- [^{3}H]-arachidonic acid, [^{32}P]-ATP, CM Sephadex C-50, EAH-Sepharose 4B, [^{14}C]-isopentenylpyrophosphate, TNFα release kit, nitrocellulose and PVDF membrane were from GE Healthcare, Amersham Bio-Sciences, Freiburg, Germany
- Plastic/PS-materials were from Greiner bio-one GmbH, Frickenhausen, Germany
- DMEM, glutamine, LB, LPS, penicillin/streptomycin, RPMI were from Invitrogen GmbH, Karlsruhe, Germany
- WB blocking buffer, fluorescence dye secondary antibodies were from LiCor Biosciences GmbH, Bad Hombug, Germany
- Grams violet, β-mercaptoethanol, methanol, trifluoracetic acid were from Merck Chemicals, Darmstadt, Germany
- Collagen reagent Horm was from Nycomed, Singen, Germany
- CpG ODN 1018 were from Operon biotechnologies GmbH, Köln, Germany
- Nycoprep and sodium pyruvate were from PAA, Pasching, Austria
- Optiphase HiSafe scintillation liquid was from Perkin-Elmer Deutschland, Rodgau-Jügelsheim, Germany
- DNA-PK, DNA-PK peptide substrate were from Promega Deutschland GmbH, Mannheim, Germany
- Ni^{2+}-NTA resin was from Qiagen GmbH, Hilden, Germany
- Trypsin (sequencing grade) was from Roche, Mannheim, Germany
- Antibodies against β-actin, cPKC, pTyr were from Santa Cruz Biotechnology, Heidelberg, Germany
- ATP, glucose, GSH, PBS were from Serva, Heidelberg, Germany
- ADP, arachidonic acid, ASS, ATP-agarose, N-α-benzoyl-DL-arginine-pNA, bromophenolblue, BWA4C, chymase, cytochalasin B, dextran, diclofenac, DMSO, DTNB, DTT, farnesol, fatty acid free BSA, FCS, fMLP, geranylpyrophosphate, γ-globulin, ionomycin, ionophore A-23187, isopentenylpyrophosphate, lysozyme, N-methoxysuc-AAPV-pNA, m-3M3FBS, n-octyl-β-glucopyranoside, non essential amino acids, NP-40 (Igepal), PAF, PEG 4000, PGB_1, phosphatidylcholine, SDS, soybean trypsin inhibitor, sucrose, thapsigargin, thrombin, triethanolamine, trypan blue, Tween 20, Tx-100, U-73122, U-73343, wortmannin, zileuton and all other chemicals were purchased in analytical grade from Sigma-Aldrich Chemie, Steinheim, Germany
- Vivaspin cut-off columns were from Vivascience AG, Hannover, Germany

2 Introduction

2.1 Boswellic acids in traditional medicine and treatment of chronic diseases

Frankincense, the gum resin of the *Boswellia serrata* (BS) tree **(fig.211)**, was known to ancient civilisations and is still used for ritual purposes in the Catholic Church and traditional ceremonies in Northern Africa. The first documentation of incense was the Papyrus Ebers written at the time of Pharao Amenophes I around 1500 BC [3]. The gum resin extracts of BS have traditionally been applied in folk medicine for centuries to treat various chronic inflammatory diseases, and experimental data from animal models and clinical studies on humans confirmed an anti-inflammatory potential of lipophilic BS extracts, for review see [4-7]. Detailed analysis of the ingredients of these extracts revealed that the pentacyclic triterpenes boswellic acids (BAs) **(fig.212)** possess pharmacological activities which may be responsible for the respective anti-inflammatory properties [6]. Among the pentacyclic triterpenes, derivatives of tirucallic acid, dehydro boswellic acid and lupeolic acid are major ingredients with pharmocological effects.

A number of relevant targets of BAs including 5-lipoxygenase (5-LO) [8], platelet-type 12-LO (p12-LO) [9], human leukocyte elastase (HLE) [10], toposiomerase I and II [11] and IκB kinases (IKK) [12] were identified. BAs induce apoptosis in tumour cells, [13, 14] accompanied by decreased

figure 211: Leaves and blossoms of the boswellia serrata tree [15]

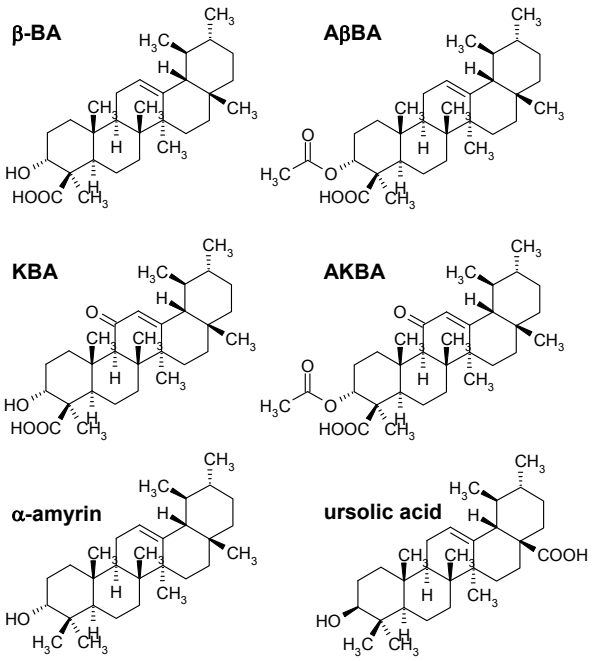

figure 212: Structures of the four major β-boswellic acids and two related pentacyclic triterpenes

extracellular signal-regulated kinase (ERK) phosphorylation [16] and enhanced caspase activity [14]. BAs differentially interfere with signalling molecules and pathways related to inflammatory processes and tumour growth including Ca^{2+}-influx, mitogen-activated protein kinases (MAPK) and Akt [17, 18]. Colon cancer proliferation is inhibited by BAs due to a p21-dependent pathway [19]. All these effects are dependent on the structure of the BAs, since 11-keto-BAs have different targets than 11-me-BAs.

Several functional effects of BS extracts on animals and humans have been described; however, the underlying molecular mechanisms still seem to remain unclear. The extracts reduce carrageenan-induced oedema and chemical-induced colitis in rats and mice [20] and several studies on humans investigated the effectiveness of BS extracts in chronic inflammatory diseases like arthritis, Crohn´s disease and ulcerative colitis. In a placebo-controlled (randomized, double-blind) study of patients with osteoarthritis, all patients (n = 30) receiving drug treatment reported a decrease in knee pain, increased knee flexion and increased walking distance, which is statistically significant and clinically relevant [21]. The effect of BS extract (3 x 350 mg/d) was compared to sulfasalazine treatment (3 x 1 g/d) in patients suffering from ulcerative colitis grade II and III. All clinical parameters improved and 82% of treated patients went into remission; in the case of sulfasalzine, the remission rate was 75% [22]. Studies in patients with Crohn´s disease led to similar results: BS extracts were either as effective or even more effective than mesalazine or sulfasalazine [23, 24]. BS extracts (H15®) were successfully tested for cancer treatment in palliative therapy of patients with brain tumours and radiochemotherapy-related leukoencephalopathy. Oedema were reduced and all patients with leukoencephalopathy improved clinically for several months [25]. Due to these results, the medicinal product H15® (containing BS extract) was designated by the EMEA as an orphan drug and is approved in part of Switzerland for the treatment of peritumoral brain oedema.

It is generally believed that the anti-inflammatory properties of BAs are mainly due to interference with 5-LO product synthesis [4, 5] and also to interference with the nuclear factor κ B (NFκB) signalling pathway [12]. Moreover, BAs modulate central signal transduction pathways such as Ca^{2+} signalling and MAPK activation [17], relevant for diverse functions of inflammatory cells. Despite these numerous putative target molecules of (11-keto-)BAs, the pharmacological relevance of the interactions with these targets is a matter of debate. Most of these interactions occur at relatively high concentrations that are far above the plasma levels of (11-keto-)BAs (<1 μM) reached following oral application of a standard dosage of *B. spec*

extracts, and are considered not relevant *in vivo* [26, 27]. In summary, direct interactions of BAs with high-affinity targets that are pharmacologically relevant *in vivo* still remain to be shown.

2.2 Cathepsin G; a neutrophil serine protease and its role in disease

Cathepsin G (CatG) is a neutral serine protease with a molecular weight (MW) of 25.8 kDa, mainly expressed in pro-inflammatory leukocytes (i.e. polymorphonuclear leukocytes (PMNL) and macrophages), where it is stored in azurophilic granules in their active form and released upon exposure to inflammatory stimuli by degranulation [28, 29]. Neutrophil infiltration, which is mediated by CatG, is a common pathological feature in acute inflammatory disorders and is necessary for phagocytosis and eradication of microorganisms [30]. It was demonstrated that CatG is crucial for resistance against infection with Staphylococcus aureus [31]. In addition, CatG contributes to protection against certain fungal infections [32, 33]. However, neutrophils are also present in inflammatory diseases which are not caused by microorganisms, and active CatG is detectable at sites of inflammation [30]. It is known that ligation of cell-surface receptors, such as β_2-integrins, activates a cascade of cytoplasmic signalling molecules and triggers an influx of calcium ions (Ca^{2+}). The increase in the intracellular concentration of Ca^{2+} ($[Ca^{2+}]_i$) mediates the fusion of granules to the plasma membrane [34]. Once released, neutrophil serine proteases are potentially fully active because they function optimally in a neutral environment. Biochemical studies indicate that CatG preferentially hydrolyses peptide bonds after aromatic amino-acid residues [35]. Following release into the plasma, it cleaves extracellular matrix proteins including laminin, proteoglycans, collagen, fibronectin and elastin, implying a role in local destruction of connective tissue at sites of injury [36]. Under normal circumstances, this extracellular protease activity is inhibited by serpins, which are endogenous serine protease inhibitors that form complexes with these extracellular proteases. Therefore, anti-chymotrypsin binds to and inhibits CatG [35, 37]. In addition, neutrophil elastase and CatG are also inhibited by secretory leukocyte protease inhibitor [37]. It was recognized several years ago that serpins not only inhibit proteolysis but also prevent recruitment of inflammatory cells [38, 39]. Although the role of CatG in host defence is acknowledged, neutrophil serine proteases have also been implicated in various non-infectious, inflammatory processes. In support of this idea, inhibition of neutrophil serine proteases has been shown to reduce neutrophil infiltration and neutrophil-mediated injury [40-42], and mice with a CatG

deficiency are resistant to experimental arthritis [43, 44]. Based on these properties, CatG is implicated in many inflammatory disorders including asthma, chronic obstructive pulmonary disease (COPD), emphysema, reperfusion injury, psoriasis and rheumatoid arthritis [30]. In addition, CatG may stimulate platelets via the protease-activated receptor (PAR)-4 for aggregation and secretion [45]. Truncation of chemokines and cytokines by CatG increased its monocyte chemotactic activity about 1,000-fold [46]. Another study by Sun et al. demonstrated that CatG is a chemotactic agonist for the G protein-coupled formyl peptide receptor (FPR) [47]. CatG binds FPR with low affinity, inducing a modest Ca^{2+} flux and weak activation of MAPK. However, the stimulation with CatG of cells that express FPR induced the translocation of protein kinase C ξ (PKCξ) from the cytoplasm to the plasma membrane, which is essential for FPR-dependent chemotaxis. Therefore, extracellular CatG might contribute to leukocyte recruitment *in vivo* by binding to FPR on neutrophils and monocytes [48]. The agonistic activity of CatG on FPR might not depend on proteolysis, since no small and soluble molecules were released during the interaction of the enzyme with the receptor [48, 49].

2.3 DNA-dependent protein kinase and Akt

Human DNA-dependent protein kinase (DNA-PK) and the protein kinase B (Akt/PKB) are important signal transducers for growth, survival and apoptosis[50-52]. DNA-PK is a nuclear serine/threonine protein kinase that, when activated by DNA [52], phosphorylates several DNA-binding substrates, including the tumour suppressor protein p53 [50]. DNA-PK and Akt signalling pathway has emerged as a critical mediator of diverse cellular processes including metabolism, gene expression, migration, angiogenesis, proliferation and cell survival. Since Akt is tightly controlled, the consequences of its deregulation have been implicated in the development of cancers and diabetes [53, 54]. The activity of Akt is markedly stimulated in a phosphatidylinositol 3-kinase (PI3K)-dependent manner. Akt is phosphorylated at Thr-308 by the PI3K-activated 3-phosphoinositol-dependent kinase (PDK1). However, active Akt does not only depend on Thr-308 phosphorylation, but is also phosphorylated at Ser-473. The responsible kinase remained unclear for a long time, but was recently identified as DNA-PK **(fig. 213)** [55].

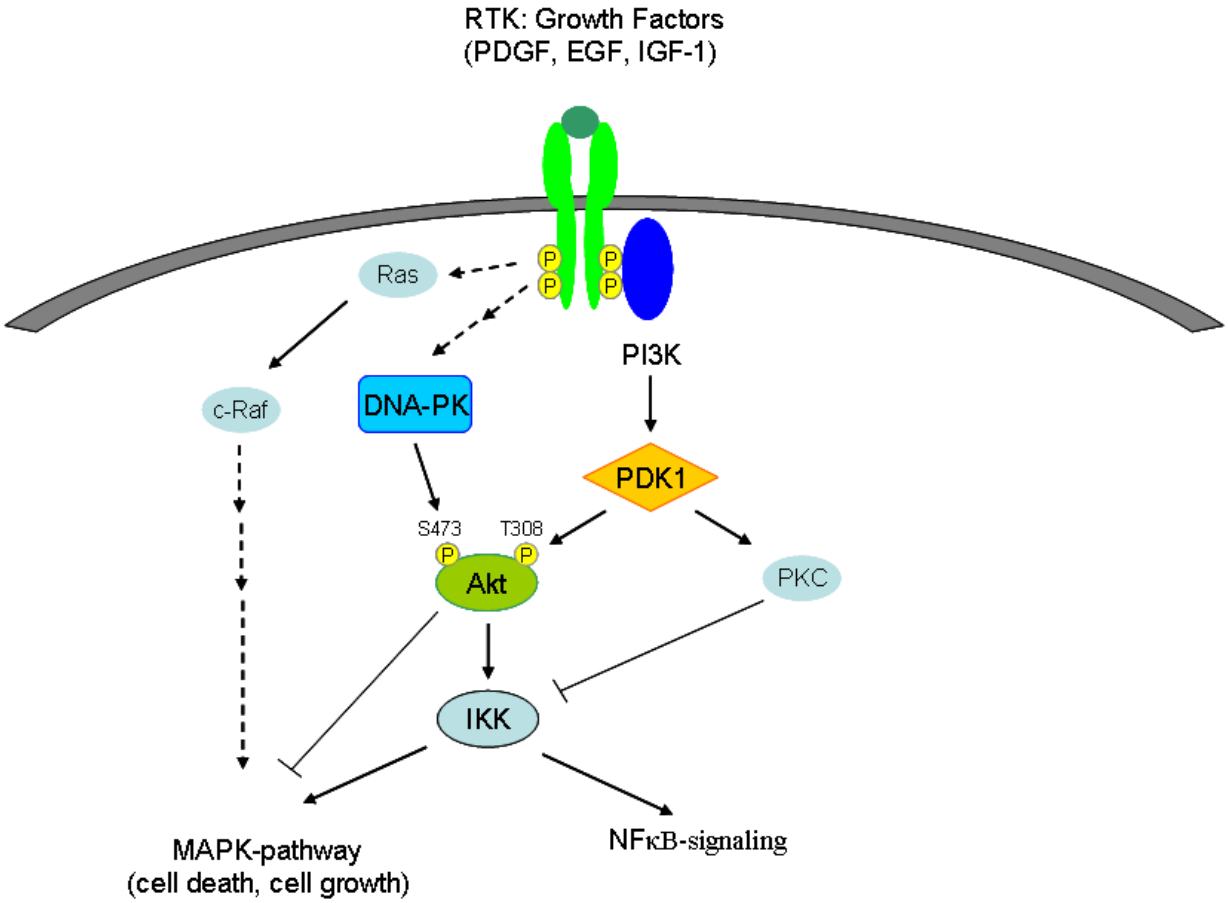

figure 213: Model for Akt (PKB) activation by upstream kinases. Upon stimulation by growth factors, PI3K is activated, which in turn generates the second messenger PIP_3 to recruit Akt and PDK1 to the membrane lipid rafts, where Akt is subsequently phosphorylated on Thr-308 and the hydrophobic motif Ser-473 by PDK1 and DNA-PK, respectively.

It has been shown that efficient DNA repair requires growth factor signalling [56] and that this effect may be due to the physical association of DNA-PK with epidermal growth factor receptor [57]. DNA-PK is activated upon DNA damage by UV irradiation [58] and bacterial products such as lipopolysaccharides (LPS) and CpG-DNA [59], and these signals or factors also activate Akt [59]. Induction of apoptosis by cisplatin was explained by a decrease in DNA-PK activity through proteolytic degradation of DNA-PK [60]; in parallel, Akt activity and Ser-473 phosphorylation are also significantly inhibited by cisplatin treatment [61]. A number of oncogenes and tumour suppressor genes that function upstream of Akt have been found to influence cancer progression by regulating Akt through increasing PI3K activity, including activated Ras and Bcr / Abl [62]. PTEN has also been identified as a human tumour suppressor and loss of PTEN correlates with increased Akt activity [54].

The survival factor Bad is a protein downstream of Akt which regulates (via co-recruitment of other proteins like Bcl-2 or 14-3-3) cell survival or apoptosis [53]. It is possible to determine Akt activity *in vivo* by measuring phosphorylation of Bad at residue Ser-136 **(fig. 214).** The pathways leading to DNA-PK/PI3K-Akt activation by LPS and CpG-DNA still remain poorly defined. Furthermore, DNA-PK and Akt are involved in activation of IKK and NFκB [18, 63], though cancer and inflammation are hardly influenced as well as bacterial infections. In conclusion, Akt is an important key mediator in survival / apoptosis mechanisms.

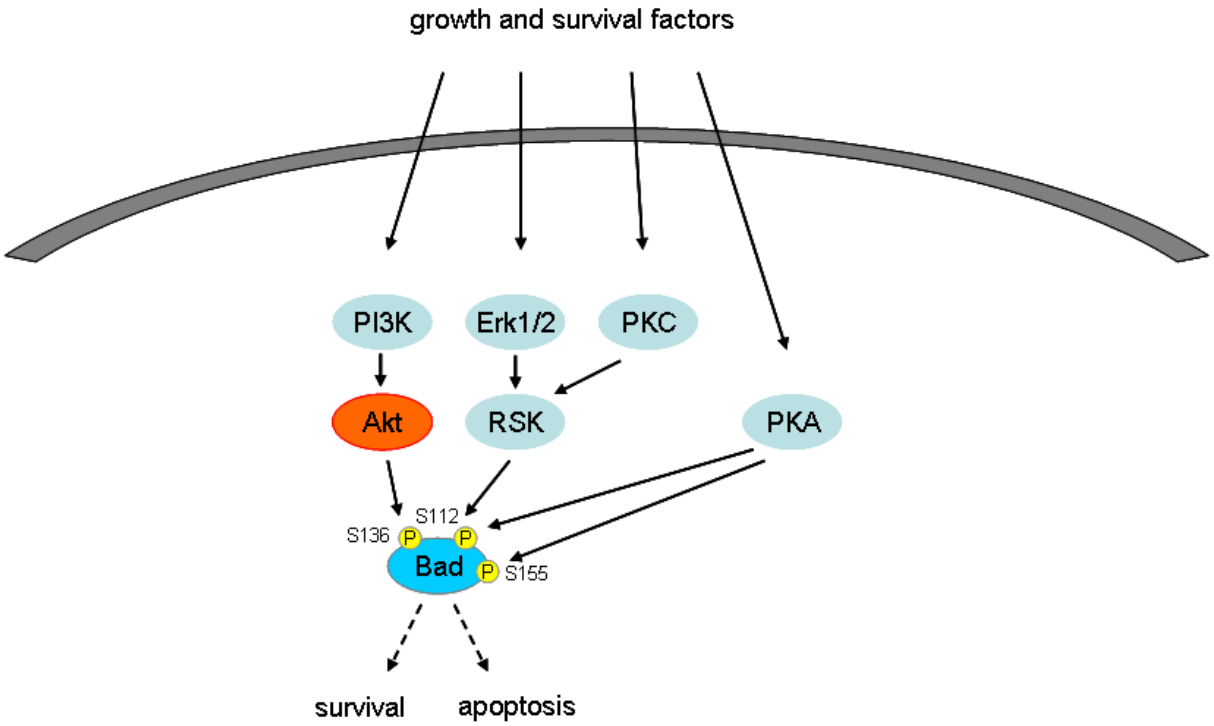

figure 214: **Downstream signalling of Akt**: Bad is phosphorylated by Akt on Ser-136 residue. Co-recruitment of other proteins (14-3-3 or Bcl-xL) is related to cell survival or apoptosis.

2.4 Cellular signalling: Ca^{2+}-homeostasis and MAP kinases

Many cellular processes are mediated by changes in $[Ca^{2+}]_i$. Stimulation of cells causes depolarisation of the plasma membrane and an opening of Ca^{2+} channels. The Ca^{2+} concentration between cytosol (10-100 nM) and extracellular space (1.5 – 2 mM) differs by factor 10^4 to 10^5 [64]. $[Ca^{2+}]_i$ does not only rise by opening plasma membrane channels, intracellular Ca^{2+} stores like sarcoplasmatic reticulum (SR) or endoplasmatic reticulum (ER) may also release Ca^{2+}, contributing to substantial elevations in $[Ca^{2+}]_i$. Rapid influx of Ca^{2+} acts as second messenger and influences important signalling cascades like the MAPK pathway. Because of cytotoxicity of high $[Ca^{2+}]_i$, Ca^{2+} pumps like Ca^{2+}-ATPase rapidly remove Ca^{2+} into intracellular storage sites or export it into extracellular lumen.

BAs influence Ca^{2+}-homeostasis, but the functional properties and the potencies of the BAs depend on their structure (**fig. 212**), in particular on the absence or presence of the 11-keto group. Indeed, 3-*O*-acetyl-11-keto-β-BA (AKBA) is frequently the most effective analogue [4, 9, 65, 66], although in some instances the 11-keto-free BAs possess superior efficacy, depending on the target/effect but also on the respective cell type [11, 13, 17, 67] However, in PMNL, KBA and AKBA elevated $[Ca^{2+}]_i$, whereas the 11-methylene BAs failed in this respect [66]. Finally, in monocytes, AKBA but not 11-methylene BAs suppressed intracellular Ca^{2+} levels [17].

Platelets play a critical role in the homeostasis of the cardiovasculature but also in the inflammatory pathophysiology [68]. Activation of platelets may lead to secretion of granular contents and release of arachidonic acid (AA), shape change, adhesion, and aggregation [69]. Thrombin or collagen are strong agonists of platelets, whereas platelet-activating factor (PAF), adenosine diphosphate (ADP), serotonin, or thromboxane $(TX)A_2$ require autocrine stimulation for the entire platelet response [69]. Soluble platelet agonists, such as thrombin, ADP, PAF, or TXA_2, typically activate specific G protein-coupled receptors (GPCRs), leading to the activation of certain phospholipase (PL)C isoforms that eventually results in elevation of $[Ca^{2+}]_i$ and activation of central signalling protein kinases (PK), including phosphatidylinositol 3-kinase (PI3K)/Akt, PKC isoforms and MAPK [68, 70-72]. Besides these effects in platelets, the four major BAs influence several signalling pathways in other cell types like MonoMac6 or HL-60 cells [17].

MAPK cascades are key signalling pathways involved in the regulation of normal cell proliferation, survival and differentiation. Aberrant regulation of MAPK cascades contributes to cancer and other human diseases. The ERK pathway in particular has been the subject of intense research for inhibitors for the treatment of cancer [73]. ERK is a downstream component of an evolutionary conserved signalling module that is activated by the Raf serine/threonine kinases (**fig. 213**) [73]. Raf, MEK and ERK are downstream effectors of Ras and receptor tyrosine kinases (RTK) like EGFR, which is mutationally activated and / or overexpressed in a wide variety of human cancers. RTK typically regulate cell growth and survival via several pathways, including Ras-Raf-MEK-ERK and PI3K-Akt-IKK cascades[74]. Not only RTK inhibitors are important for the treatment of cancers, modulation and inactivation of downstream targets could also facilitate the cure of many diseases. BAs interact with MAPK, an interesting finding that could possibly lead to new approaches in (cancer) therapy.

2.5 COX and LOs: Key enzymes in eicosanoid biosynthesis

Inflammation is one of the most important processes in host defense; however, it often progresses to painful or chronically harmful diseases that require pharmacological treatment. The inflammatory response involves many effector mechanisms which produce a multiplicity of vascular and cellular reactions. One of the major findings since the discovery of the role of histamine in vascular processes of inflammation at the beginning of the twentieth century, is that many chemical mediators are involved in activating and coordinating various aspects of the inflammatory process [75, 76]. Now we know that vasodilatation, increased microvascular permeability, chemotaxis, cellular activation, pain and finally repair are mediated by the local production and release of several specific mediators. The arachidonic acid (AA) derivatives prostaglandins (PGs), thromboxanes (TXs) and leukotriens (LTs), together with cytokines, oxygen and possibly nitrogen radicals, play a pivotal role. The non-steroidal anti-inflammatory drugs (NSAIDs), mainly the cyclooxygenase (COX) inhibitors, which have been used since the introduction of acetylsalicylic acid in 1899, share many pharmacological properties (and side effects) and are the main drugs used to reduce the unwanted consequences of inflammation [76-78].

As a result of proinflammatory stimuli or injuries, cytosolic phospholipase (cPL) A_2 releases AA from cell membrane phospholipids. AA is the substrate of either lipoxygenases (LOs) or COX. COX-1/2 form the cyclic peroxide PGH_2 as an intermediate product which is further converted to PGs and TXs. In addition to PGs derived from the COX pathways, LTs are formed by LOs from AA that exert pivotal biological functions. For LT biosynthesis, AA is first metabolized by 5-LO to LTA_4 (**fig. 215A**). The unstable LTA_4 is the precursor of the bioactive LTs such as LTB_4 and the cysteinyl-LTs C_4, D_4, and E_4. Interestingly, next to inflammatory and allergic diseases, 5-LO products play a crucial role in cancer development and atherosclerosis [79]. Polymorphonuclear leukocytes (PMNL) and monocytes/macrophages are the major cells capable of synthesizing LTs and express high amounts of 5-LO. These cells are major players in chronic inflammatory diseases. In the treatment of asthma, zileuton is the only 5-LO inhibitor that came into the market (USA). New potent and biocompatible inhibitors would open a new field in therapy of asthma, several cancers and atherosclerosis, because 5-LO is a major target in chronic inflammation. For example, 5-LO is overexpressed in prostate cancer, and other malignant (compared with benign) tumour tissues[80].

The activity of 5-LO in the cell is tightly controlled. The amount of free AA, released by $cPLA_2$, and its accessibility to 5-LO are determinants of LT biosynthesis. Thus, stimuli

capable of inducing leukotriene formation (e.g. fMLP, PAF and Ca^{2+}-ionophores) cause activation of 5-LO[81].

The conversion of endogenously provided AA to LTA_4 occurs at the nuclear membrane, and it seems that leukotriene formation can be particularly prominent at this locus[82]. On cell stimulation, 5-LO migrates from a soluble compartment to the nuclear membrane. Membrane-bound FLAP might facilitate the transfer of AA to 5-LO. In cells lacking FLAP, or where FLAP is pharmacologically inhibited, transformation of endogenous AA by 5-LO is efficiently blocked [82]. 5-LO is phosphorylated *in vitro* by the protein kinases p38 MAPK-regulated MAPKAPK-2/3, ERK1/2, CaMKII and PKA [81]. Phosphorylation does not, however, seem to increase 5-LO activity *in vitro*, but PKA-mediated phosphorylation can inhibit 5-LO activity[83].

Because catalysis by 5-LO requires oxidation of Fe^{2+} to the active Fe^{3+} state by lipid hydroperoxides, the redox tone is an important parameter of cellular 5-LO activity. Conditions that promote lipid peroxidation, such as formation of reactive oxygen species by phorbol 12-myristate 13-acetate, addition of peroxides, inhibition of glutathione perxidase (GPx) enzymes and depletion of glutathione, upregulate 5-LO product synthesis, whereas reduction of peroxides by GPx-1 and GPx-4 suppresses 5-LO product formation[81]. Oxidative stress also activates p38 MAPK; thus, an increase in peroxide tone might activate 5-LO in the cell by promoting phosphorylation of 5-LO [84, 85].

Leukotriene synthesis was first observed after cell stimulation by a Ca^{2+} ionophore [86]. Considerably lower concentrations of Ca^{2+} (~200 nM) seem to be sufficient for substantial activation of 5-LO in intact cells [87], as compared with purified 5-LO (which requires 1–10 μM Ca^{2+}), indicating that cellular events and context modulate the Ca^{2+} requirement. Activation of 5-LO in intact cells, however, might not necessarily involve Ca^{2+}. When exogenous AA was provided to intact human neutrophils, substantial 5-LO product formation occurred even when extra- and intracellular Ca^{2+} had been depleted by chelating agents such as EDTA and BAPTA/AM [79, 88].

A

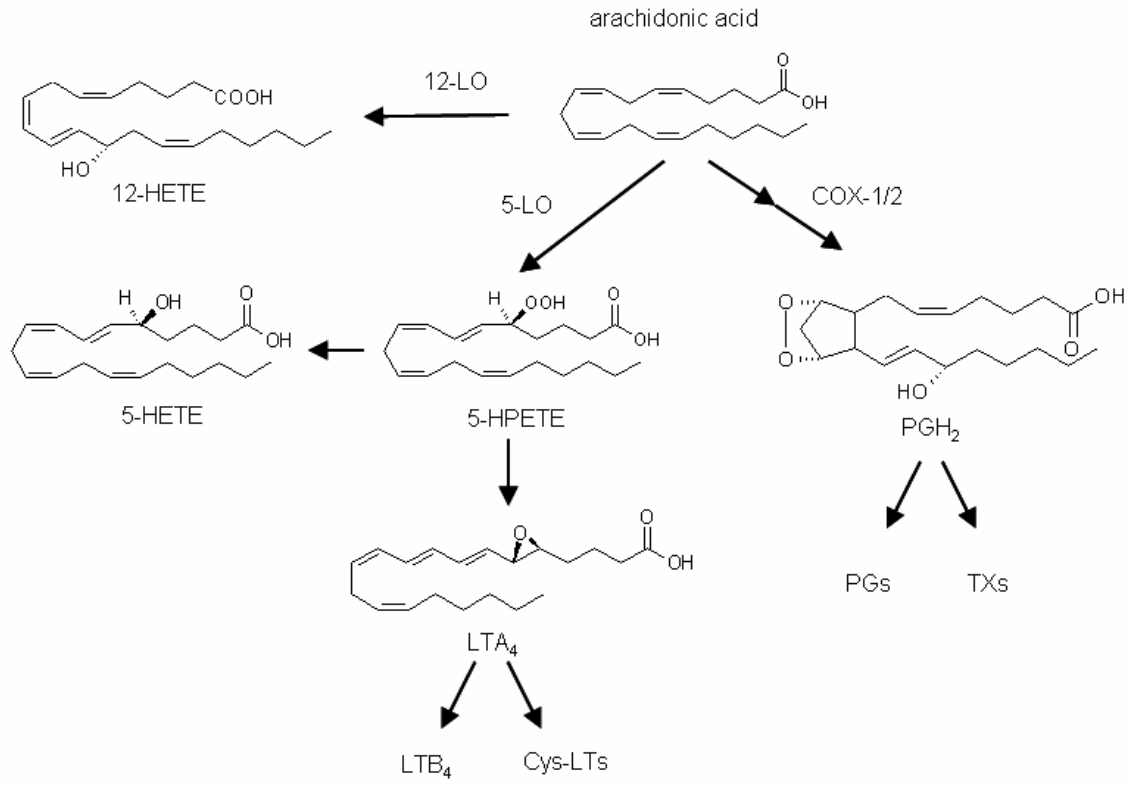

B

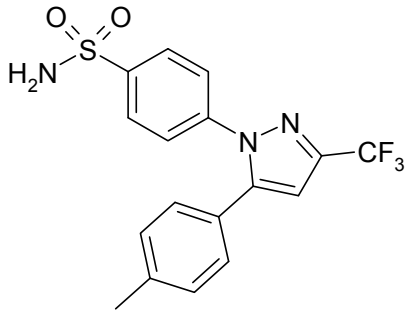

figure: 215: (**A**) **Arachidonic acid metabolism**: Arachidonic acid is released in inflammation and injuries by phospholipases and metabolized by lipoxygenases (5-LO; 12-LO; 15-LO) and cyclooxygenases (COX-1; COX-2) to leukotrienes (LTs) and prostaglandins (PGs), respectively. (**B**) **Structure of celecoxib**

NSAIDs are used for the treatment of pain, fever and inflammation. Traditional NSAIDs inhibit both isoforms of COX which are key enzymes in the conversion of AA to PGs (**fig. 215A**). The housekeeping enzyme COX-1 is primarily responsible for maintenance of homeostasis (gastric and renal protection, platelet function), whereas COX-2 is mainly induced in response to growth factors and various cytokines at sites of inflammation and tumour growth [89, 90]. Thus, COX-2-selective drugs, such as celecoxib, etoricoxib, valdecoxib and rofecoxib, showed anti-inflammatory, analgesic and antipyretic efficacies similar to those of traditional NSAIDs, but displayed a lower incidence of symptomatic ulcers and ulcer complications [91].

Concomitantly with the introduction to the market, the COX-2-selective inhibitor, celecoxib **(fig.215B)** was shown to significantly reduce polyp formation and polyp size in patients with familial adenomatous polyposis at rather high doses (2 x 400 mg/d) [92]. Clear evidence that COX-2-inhibition alone is not responsible for the anticarcinogenic effects of celecoxib has been obtained from cell culture and animal studies showing antiproliferative effects of this drug in human colon carcinoma cells irrespective of COX-2 expression [93, 94]. Several COX-2-independent molecular mechanisms with unclear *in vivo* relevance were identified and assumed to contribute to the anticarcinogenic effects of celecoxib, for instance 3-phosphoinositide-dependent kinase-1 (PDK-1, IC_{50} = 48 μM for celecoxib) and its downstream target Akt kinase. It was also shown that an inhibition of the endoplasmatic reticulum Ca^{2+}-ATPase ($IC_{50} \approx 35$ μM) is associated with the induction of apoptosis [95-98]. However, the impact of these findings was discussed controversially, since a significant discrepancy exists between the concentrations of celecoxib found in the plasma of patients under tumour therapy (3-8 μM) [99] and those concentrations needed to affect intracellular non-COX-2 targets (≥ 30 μM, *in vitro* assays). Hence, the exact molecular mechanisms responsible for the effects of celecoxib at higher doses are still a matter of intensive research.

2.6 Aim of this work

Extracts of B. *spec*. containing bioactive BAs have proven to be effective in the treatment of chronic inflammatory diseases such as rheumatoid arthritis and ulcerative colitis and have been applied in the Indian ayurvedic medicine and traditional Chinese medicine (TCM) for centuries. Due to a growing public interest in Germany in natural (plant-derived) compounds as safe and well-tolerable drugs during the last decades, the scientific community is increasingly focussing on the elucidation of the mechanisms by which these remedies act on the molecular and cellular level. This interest is substantiated by recent clinical trials demonstrating beneficial effects of BS extracts in several inflammatory diseases such as Crohn´s disease, ulcerative colitis and certain types of cancer. However, the utilised extracts consist of a plethora of different compounds. Although BAs represent the largest fraction and are considered to be important pharmacological principles, application of this mixture in cellular experiments for the purpose of identifying molecular targets is not feasible, due to the heterogeneity of the extract and the diversity of the ingredients. Thus, investigations on the cellular level should start with the purified BAs. Research started 15 years ago, and has yielded a number of relevant target proteins, including 5-LO[6]. AKBA was regarded as the most potent BA but the other BAs are also active in several experimental settings. Modulation of LT formation, which are key mediators of inflammation with additional implications in carcinogenesis, was described by a series of studies. Other targets (e.g. HLE, IKK, NFκB), related to cell proliferation and apoptosis, were also identified [18, 100]. None of these findings, however, can presently provide a satisfying explanation for the anti-inflammatory effects of the extracts observed in clinical settings and in traditional folk medicine because of the high effective concentrations required. Hence, this thesis was designed to find pharmacologically relevant targets of BAs. Haematopoietic cells (leukocytes, platelets) and cancer cell lines (MCF-7, LNCaP, MM6, HL-60) were used as model systems. Investigations of the cellular and molecular effects of BAs were started in this group by Oliver Werz [101]. An initial thesis focussing on the effects of BAs on neutrophils was provided by Anja Altmann[102]. Based on these initial findings [66], studies were continued and expanded toward other related cell types (monocytic cells, platelets) in Daniel Poeckel's thesis [103]. He examined a putative correlation of intracellular Ca^{2+} mobilisation and ERK1/2 activation by 11-keto-BAs [66] to the generation of ROS, release of AA and formation of eicosanoids[104].

In this thesis, the antagonistic effects of BAs on Ca^{2+} mobilisation and functional responses in blood cells were investigated. The results with human platelets further underscored the interactions of BAs with platelet-type 12-LO. A construct of immobilised BAs was utilised to identify putative target proteins in cell lysate supernatants via a pulldown approach (protein fishing) and MS analysis. The functional consequences of the interactions of BAs with the identified proteins were studied. The most interesting proteins found were cathepsin G (CatG), DNA–dependend protein kinase (DNA-PK), Akt, PKC and farnesyl pyrophosphate synthase (FPPs).

Celecoxib is a well-known selective COX-2 inhibitor. Celecoxib was introduced to the European market in 1998 as Celebrex® and quickly captured the NSAIDs market. After rofecoxib (Vioxx®) was withdrawn, news surrounding the well-tolerated drug celecoxib quieted down. Several patients with colon carcinoma or strong polyp formation taking celecoxib strongly benefited from it and polyps or tumours regressed, but that occurred independently of COX inhibition [94]. Previous work suspected a role of leukotrienes in the formation of colon carcinoma, and this was the reason to test celecoxib for interference with 5-lipoxygenase *in vitro* and *in vivo* [94].

3 Methods

3.1 Cells and cell culture

3.1.1 Cell culture

All cell lines were cultured in incubators (WTB Binder Labortechnik, Tuttlingen, Germany) at 37°C, 5% CO_2 and saturated humidity. The cultures were seeded at a density of 2 x 10^5 cells per ml. Cells were harvested by centrifugation (200 x g, 10 min at room temperature) and washed once in PBS, pH 7.4. To exclude toxic effects of BAs during various incubation periods, the viability of cells was analysed by means of trypan blue exclusion. Incubation with 30 µM of BAs at 37°C for 30 min caused no significant change in the number of viable cells.

3.1.2 Mono Mac 6 cells

MM6 cells (monocyte like cell line) were obtained from Dr. Ziegler-Heitbrock (Munich, Germany) and maintained in RPMI 1640 medium with glutamine supplemented with 10% fetal calf serum, 100 µg/ml streptomycin, 100 U/ml penicillin, 1 mM sodium pyruvate, 1x nonessential amino acids, 1 mM oxalacetic acid and 10 µg/ml insulin. MM6 cells were treated with 2 ng/ml TGFβ and 50 nM calcitriol for 4 days in order to obtain differentiated cells [105].

3.1.3 LNCaP / HL-60

LNCaP (human prostate cancer cells) and HL-60 (human leukemic cells) were maintained in RPMI 1640 medium with glutamine supplemented with 10% fetal calf serum, 100 µg/ml streptomycin, 100 U/ml penicillin.

3.1.4 MCF-7

MCF-7 (human mamma carcinoma cells) were maintained in DMEM high glucose medium supplemented with 10% fetal calf serum, 100 µg/ml streptomycin, 100 U/ml penicillin and 1 mM sodium pyruvate.

3.1.5 RBL-1

RBL-1 (rat basophilic leukemia cells) were maintained in RPMI 1640 medium with glutamine supplemented with 10% fetal calf serum, 100 µg/ml streptomycin, 100 U/ml penicillin, 1 mM sodium pyruvate, 10 mM HEPES and 1x nonessential amino acids.

3.2 Isolation of human PMNL (polymorphonuclear leukocytes) from venous blood

Human PMNL were freshly isolated from leukocyte concentrates obtained from St. Markus Hospital (Frankfurt, Germany). In brief, venous blood was taken from healthy adult donors and subjected to centrifugation at 4,000 x *g* for 20 min at 20°C for preparation of leukocyte concentrates. PMNL were promptly isolated by dextran sedimentation, centrifugation on Nycoprep cushions (PAA Laboratories, Linz, Austria), and hypotonic lysis of erythrocytes [85, 106, 107]. PMNL (7.5 x 10^6 cells/ml; purity > 96−97 %) were finally resuspended in PBS pH 7.4 plus 1 mg/ml glucose and 1 mM $CaCl_2$ (PGC buffer).

3.3 Isolation of human platelets from venous blood

Platelets were isolated from supernatants (800 x g, 10 min, RT) after centrifugation of leukocyte concentrates on Nycoprep cushions (see above) to obtain platelet rich plasma (PRP). PRP was then mixed with PBS pH 5.9 (3:2, v/v), centrifuged (2,000 x g, 15 min, RT) and the pelleted platelets were resuspended in PBS pH 5.9 / 0.9% NaCl (1:1, v/v), washed by centrifugation (2,000 x g, 10 min, RT) and finally resuspended in PBS pH 5.9. For incubations with solubilized compounds, ethanol or DMSO was used as vehicle, never exceeding 1 % (v/v).

3.4 Human in vitro whole blood assay.

Aliquots of freshly heparinized human blood (450 µl) obtained from healthy male and female informed volunteers were pre-incubated with the drugs or vehicle (DMSO) for 30 min at 37°C. Formation of 5-LO products was initiated by the addition of Ca^{2+}-ionophore dissolved in 50 µl autologous plasma to obtain a final concentration of 20 µM A23187 (final DMSO concentration was < 1 %, final volume 0.5 ml). The reaction was terminated after 15 min by rapid cooling of the plate on ice. Then, the samples were centrifuged at 1000 x g and 4°C for

15 min and eicosanoid concentrations (5-HETE, LTB_4, 12(S)-HETE, 15(S)-HETE and PGE_2) in the plasma supernatant were analyzed using LC/MS-MS. LC-MS/MS analysis was performed on a API 4000 triple quadrupole mass spectrometer (Applied Biosystems, Darmstadt, Germany). Linearity of the calibration curve was proven from 0.5 to 2500 ng/mL for each eicosanoid. Mean accuracy of the assay was found to be 99.9 +- 3.25% for LTB_4, 99.85 +- 4.8% for 5-HETE, 100.2 +- 4.8% for 12-HETE and 99.76 +- 4.4% for 15-HETE. This work was done in collaboration with Dr. TJ Maier and Dr. Geisslinger, Department of Clinical Phamracology, University of Frankfurt

3.5 Expression and purification of 5-LO from Escherichia coli

Human recombinant 5-LO protein was expressed in *E. coli* JM 109 cells, transfected with the plasmid pT3-5LO, and purification of 5-LO was performed via affinity chromatography as described [108]. Cells were grown overnight in LB medium supplemented with 100 µg/ml ampicillin, transferred to M9 minimal medium (48 mM Na_2HPO_4, 22 mM KH_2PO_4, 8.5 mM NaCl, 19 mM NH_4Cl, 6.3 mM NaOH, glycerol 2% and 100 µg/ml ampicillin, pH 7.4 casein 2 g/l) and expression of 5-LO was induced with 200 µM IPTG. Cells were harvested by centrifugation (1,500 x g, 15 min, 4°C) lysed by incubation in 50 mM triethanolamine/HCl pH 8.0, 5 mM EDTA, soybean trypsin inhibitor (60 µg/ml), 1 mM phenylmethylsulfonylfluoride (PMSF), 1 mM DTT, and lysozyme (500 µg/ml), homogenized by sonification (Bandelin, Sonoplus HD 200) (3 x 15 s) on ice and centrifuged at 19,000 x g (Sorvall RC 5B plus) for 15 min at 4°C. The pellet was discarded. After centrifugation of the supernatant at 100,000 x g (Beckman Optima LE-80K) for 70 min at 4°C, the resulting supernatant was applied to an ATP-agarose column (Sigma-Aldrich, Munich, Germany), and the column was eluted with 20 mM ATP in PBS / EDTA [105]. Partially purified 5-LO was used immediately for *in vitro* activity assays.

3.6 Expression and purification of his-tagged platelet-type 12-LO from Escherichia coli

Human recombinant his-tagged platelet-type 12-LO (his12-LO) protein was expressed in *E. coli* JM 109 cells, transfected with the plasmid pT3-his12LO, and purification of 12-LO was performed via ion-metal affinity chromatography (IMAC). Cells were grown overnight in LB medium supplemented with 100 µg/ml ampicillin, transferred to M9 minimal medium (48 mM Na_2HPO_4, 22 mM KH_2PO_4, 8.5 mM NaCl, 19 mM NH_4Cl, 6.3 mM NaOH, glycerol 2% and 100 µg/ml ampicillin, pH 7.4, casein 2 g/l) and expression of his12-LO was induced with 200 µM IPTG. Cells were harvested by centrifugation (1,500 x g, 15 min, 4°C) lysed by incubation in lysis buffer (50 mM NaH_2PO_4, 300 mM NaCl, pH 8.0), 10 mM imidazol, soybean trypsin inhibitor (60 μg/ml), 1 mM phenylmethylsulfonylfluoride (PMSF), and 10 mM β-mercaptoethanol, homogenized by sonification (3 x 15 s) on ice and centrifuged at 19,000 x g for 15 min at 4°C. The pellet was discarded. After centrifugation of the supernatant at 100,000 x g for 70 min at 4°C, the resulting supernatant was applied to a Ni^{2+}-NTA-agarose column (Qiagen, Hilden, Germany), and the column was washed with 4 volumes of lysis buffer plus 20 mM imidazol and eluted with lysis buffer plus 250 mM imidazol (4 ml/l bacteria culture). Partially purified his12-LO was used immediately for *in vitro* activity assays [105].

3.7 Determination of 5-LO product formation in intact cells

For assaying the 5-LO product formation of intact cells, 7.5 x 10^6 freshly isolated PMNL were resuspended in 1 ml PGC buffer. After pre-incubation with the test compounds or vehicle at 37°C for 10 min at the indicated concentrations, 5-LO product formation was started by the addition of the various stimuli (ionophore A23187, NaCl) as indicated. After 10 min at 37°C, the reaction was stopped by addition of 1 ml ice-cold methanol and 30 µl of 1 N HCl, 200 ng PGB_1, and 500 µl of PBS were added. 5-LO metabolites formed were extracted by solid phase extraction and analyzed by C-18 reversed phase HPLC (Waters, Eschborn) as described [109]. Mobile phase was 76% methanol, 24% H_2O and 0.007% trifluoracetic acid with a flow rate of 1.2 ml/min. PGB_1 (internal standard) and 5-LO products were detected and calculated by Empower Pro software (Waters, Eschborn).

3.8 Determination of 5-LO product formation in cell-free systems

For determination of 5-LO activity in cell homogenates, 7.5 x 10^6 freshly isolated PMNL were resuspended in PBS containing 1 mM EDTA, sonicated (3 x 10 s) at 4°C, and 1 mM ATP was added. For determination of the activity of recombinant 5-LO, partially purified 5-LO (0.5 µg in 5 µl PBS) was added to 1 ml of a 5-LO reaction mix (PBS, pH 7.4, 1 mM EDTA, 25 µg/ml phosphatidylcholine, 1 mM ATP, and 20 µg/ml γ-globulin). In some experiments DTT (1 mM) or GSH (5 mM) was added to the reaction mixtures as indicated. After incubation with test compounds or vehicle for 10 min at 4°C, samples were warmed up for 30 s at 37°C and 2 mM $CaCl_2$ and AA at the indicated concentrations were added to start 5-LO product formation. The reaction was stopped after 10 min by the addition of 1 ml ice-cold methanol and 30 µl of 1 N HCl, 200 ng prostaglandin B_1, and 500 µl of PBS were added [108]. Metabolites formed were analyzed by HPLC as described above.

3.9 Determination of 12-LO product formation

To determine p12-LO product formation in intact cells, freshly isolated platelets (10^8 /ml PG buffer) were supplemented with either 1 mM $CaCl_2$, 1 mM EDTA, or 1 mM EDTA plus 30 µM BAPTA/AM. Platelets were preincubated with the indicated agents for 15 min at 37°C. After addition of stimuli and further incubation at 37°C for the times indicated, the reaction was stopped by the addition of 1 ml ice-cold methanol and 30 µl of 1 N HCl, 200 ng prostaglandin B_1, and 500 µl of PBS were added. p12-LO products (12(S)-hydro(pero)xy-6-trans-8,11,14-cis-eicosatetraenoic acid (12-H(P)ETE) were extracted and then analyzed by HPLC [107]. 12-HETE and 12-HPETE elute as one major peak, integration of this peak represents p12-LO product formation, expressed as ng metabolites per 10^8 cells.

For determination of p12-LO product formation in broken cell preparations, platelets (10^8 /ml PG buffer plus 1 mM EDTA and 1 mM PMSF) were sonicated (3 × 10 s) and lysates were centrifuged (100,000 x g / 70 min / 4°C). To the resulting 100,000 x g supernatant or to partially purified his12-LO, BAs were added and samples were pre-warmed at 37°C for 30 sec. $CaCl_2$ (2 mM) was added as indicated and his- or p12-LO product formation was started by addition of AA (10 µM). After 10 min at 37°C, the formation of 12-H(P)ETE was determined as described for intact cells.

3.10 [^{3}H]-Arachidonic acid release

PRP was labeled with 19.2 nM [^{3}H]-AA (1 µCi/ml, specific activity 200 Ci/mmol) for 2 h at 37°C in the presence of 100 µM aspirin to avoid clotting. Then, cells were washed twice with PBS pH 5.9 plus 1 mM $MgCl_2$, 11.5 mM $NaHCO_3$, 1 g/l glucose and 1 mg/ml fatty acid free BSA and finally resuspended in PG buffer (10^8 cells /ml). Preparations of cells at pH 5.9 is thought to minimize temperature-induced activation [110]. After 15 min at room temperature, 1 mM $CaCl_2$ was added 2.5 min prior stimulation with the indicated agents at 37°C. After 5 min, incubations were put on ice for 10 min, followed by centrifugation (5,000 x g, 15 min). Aliquots (300 µl) of the supernatants were measured (Micro Beta Trilux, Perkin Elmer) to detect the amounts of [^{3}H]-labeled AA released into the medium.

3.11 Immobilization of boswellic acids and protein pull-down assays

For immobilization of BAs at EAH Sepharose 4B beads, the free 3-OH group of the BAs was used (manuscript: Kather, N., Tausch, L., Poeckel, D., Werz, O., Herdtweck, E. and Jauch, J. (2008)). In brief, β-BA and KBA were treated with glutaric anhydride to form the half-esters Glut-BA and Glut-KBA, respectively, and analyzed by ^{1}H- and ^{13}C-NMR as well as by MS. These substances were linked to EAH Sepharose 4B by standard amide coupling procedures. The carboxylic acid of the BA-core was unlikely to react under standard conditions due to steric crowding. The success of the coupling reaction was determined by two methods: a) Glut-BAs were used in defined excess (2 µmol of the Glut-BAs per 1 µmol NH_2-groups of the EAH Sepharose 4B). After the coupling reaction, the hypothetical excess of Glut-BAs (1 µmol) could be indeed recovered. b) Treatment of Glut-BAs with KOH in isopropanol under reflux for ca. 3 h cleaved the ester bond and gave BA and KBA respectively, analyzed by thin layer chromatography. Preparation of immobilized BAs was performed by Dr. J. Jauch, Saarbrücken.

For protein pull-down experiments, 3×10^7 PMNL, 5×10^7 RBL-1, 3×10^9 platelets, 1×10^7 MM6, 3×10^7 HL-60, 5×10^7 LNCaP or 8×10^7 MCF-7 were lysed in 1 ml lysis buffer (50 mM HEPES pH 7.4, 200 mM NaCl, 1 mM EDTA, 1% Triton X-100, 2 mM PMSF, 10 µg/ml leupeptin, 120 µg/ml soybean trypsin inhibitor). 50 µl of the sepharose slurries (50%, v/v) were added to the lysates and incubated at 4°C over night under continuous rotation. The Seph-beads were intensively washed 3 times with 5 volumes of binding buffer (HEPES pH

7.4, 200 mM NaCl, 1 mM EDTA) and precipitated proteins were finally separated and denatured by addition of SDS-b (20 mM Tris pH 8.0; 2 mM EDTA; 5% SDS; 10% β-mercaptoethanol). After boiling (95°C, 6 min), beads were removed by centrifugation and the supernatant containing proteins were separated by SDS-PAGE and visualized by WB, coomassie or silver staining, respectively.

3.12 SDS-PAGE

Freshly isolated PMNL, HL-60, or MM6 cells (5 x 10^6 each) were resuspended in PGC buffer; the final volume was 100 µl. After addition of the indicated stimuli (DMSO, final concentration < 1% (v/v)), samples were incubated at 37°C and the reaction was stopped by addition of 100 µl of ice-cold 2 x sodium dodecylsulphate–polyacrylamide gel electrophoresis (SDS–PAGE) sample-loading buffer (SDS-b; 20 mM Tris/HCl, pH 8, 2 mM EDTA, 5% SDS (w/v), 10% β-mercaptoethanol), vortexed and heated for 6 min at 95°C. Total cell lysates (20 µl) were mixed with 4 µl of glycerol/0.1% bromophenolblue (1:1, v/v) and analysed by SDS–PAGE using a Mini Protean III system (Bio-Rad, Hercules, CA, U.S.A.) on a 4-20% gel, unless stated otherwise.

3.13 Western Blot

After electroblot to nitrocellulose membrane (Amersham Pharmacia, Little Chalfont, UK), membranes were blocked with LiCor blocking buffer mixed with 50 mM Tris/HCl, pH 7.4, and 100 mM NaCl (Tris-buffered saline (TBS)) (1:1, v/v) for 1 h at RT. Correct loading of the gel and transfer of proteins to the nitrocellulose membrane was confirmed by Ponceau staining. Membranes were washed and then incubated with primary antibody (AB) overnight at 4°C. Antibodies were diluted 1 : 1000 in LiCor blocking buffer. The membranes were washed and incubated with 1 : 5000 dilution of fluorescence dye-conjugated immunoglobulin G (LiCor, Lincoln, NE, USA) for 45 min at RT. After washing (4 x with TBS plus 0.1% Tween 20 and TBS), visualisation of proteins was performed using a LiCor Odyssey 2-color Western detection system (LiCor, Lincoln, NE, USA), according to the manufacturer's instructions.

3.14 Colloidal Coomassie staining

Washed (in MQ) gels from SDS-PAGE were fixed and stained 6 - 12 h on a shaking table at room temperature in colloidal staining solution (0.08% Coomassie Brilliant Blue G250, 1.6% ortho-phosphoric acid, 8% ammonium sulfate, 20% methanol) and destained in MQ until background was clear. 1% acetic acid (v/v) was added as indicated [111].

3.15 Silver staining

After SDS-PAGE, proteins in the gels were fixed in 5% acetic acid and 10% methanol (v/v, 4x for 30 min), washed in MQ and sensitized 2 min in freshly prepared 0.02% $Na_2S_2O_3$ solution. After washing in MQ and incubation in "silver solution" (0.1% $AgNO_3$) for 30 min the gel was developed several minutes under slow shaking in 2.5% Na_2CO_3 plus 300 µl/l formaline. The developed gel was fixed in 1% acetic acid and scanned in a scanner (AGFA Arcus II).

3.16 In-gel digestion

All gels were subjected to manual gel cutting using a razor blade. Dissected gel pieces were subjected to in-gel digestion protocols [112, 113] which were adapted for use on a Microlab Star digestion robot (Bonaduz, Switzerland) [114]. Samples were reduced, alkylated and subsequently digested over night using bovine trypsin (sequencing grade, Roche, Mannheim, Germany). The gel pieces were extracted and the extracts were dried in a vacuum centrifuge and stored at -20°C until analysis.

3.17 MALDI-TOF-MS

MALDI-TOF-MS experiments were performed on an Ultraflex TOF/TOF mass spectrometer (Bruker Daltonics Inc., Manning Park Billerica, MA) in cooperation with Dr. M. Karas, Institute of Pharmaceutical Chemistry, University of Frankfurt. The samples were dissolved in 5 µL of water/acetonitrile/TFA (29.5/70/0.5, v/v/v). α-cyano-4-hydroxycinnamic acid (3 mg/ml, Bruker Daltonics Inc., Manning Park Billerica, MA) in water/acetontrile/TFA (29.5/70/0.5, v/v/v) was used as matrix. Analyte and matrix were spotted consecutively in a 1:1 ratio on a stainless steel target and dried under ambient conditions. The dried sample was washed with ice-cold 5% formic acid to reduce salt contamination prior to analysis.

Spectra were externally calibrated with a Sequazyme™ Peptide Mass Standard Kit (Applied Biosystems, Foster City, CA) and internally calibrated on a tryptic auto digestion peptide (*m/z* 2163.0564). The spectra were processed in flexAnalysis version 2.2 (Bruker Daltonics Inc., Manning Park Billerica, MA) using the SNAP algorithm (signal to noise threshold: 3, maximal number of peaks: 150, quality factor threshold: 40).
Proteins were identified by Mascot (www.matrixscience.com, Matrix Science, Boston, MA) (peptide mass tolerance: 100 ppm; maximum missed cleavages: 1) using the NCBInr database (2314886 sequences; 1066605192 date 26.01.2005). Proteins with a score of 76 or higher were considered significant ($p < 0.05$).

3.18 In vitro kinase assay for DNA-PK

To determine kinase activity of DNA-PK, 20 U of the kinase were incubated with the BAs for 10 min at 30°C in 50 µl reaction buffer (50 mM HEPES pH 7.5, 100 mM KCl, 10 mM $MgCl_2$, 0.2 mM EGTA, 0.1 mM EDTA, 1 mM DTT) with 10 µg/ml CpG-ODN 1018, 80 µg/ml BSA, 200 µM ATP, 3 µCi [^{32}P]-ATP and 100 µg DNA-PK peptide substrate or 600 ng Akt-1 as substrate. Reaction was stopped by adding 20 µl of 30% acetic acid, samples were separated by SDS-PAGE and bands were visualized by Coomassie-staining. The dried gel was exposed to a radioactivity sensitive-film and [^{32}P] incorporation was measured with a FLA-3000 reader (Fuji Film)[63].

3.19 In vivo phosphorylation

LNCaP or MCF-7 cells were cultured overnight in a 24-well cell culture plate (8 x 10^4, 7 x 10^4 per well, respectively), and cells were starved in serum-free media for 24 h. After preincubation with the BAs for 1 h, cell activity was stimulated with 10 µg/ml CpG-ODN 1018 for 20 min. Cells were lysed with icecold lysis buffer (160 mM NaCl, 20 mM Tris pH 7.4, Tx-100 0.1%, NP-40 0.1%, 1 mM EDTA) and phosphorylation of Akt was detected by Western Blot using a phospho-specific antibody.

3.20 Akt activity assay

Active recombinant Akt-1 (50 ng) was incubated with eNOS (Ser-1177) biotinylated peptide in 50 µl assay buffer (25 mM Tris pH 7.5, 10 mM $MgCl_2$, 5 mM β-glycerolphosphate, 0.1 mM Na_3VO_4, 2 mM DTT, 200 µM ATP, 1.5 mM peptide) for 30 min at room temperature. Reaction was stopped with 50 mM EDTA, pH 8.0, and an aliquot was transferred to a streptavidin coated 96-well plate. After incubation with phospho-eNOS (Ser-1177) antibody and a fluorescence dye-conjugated secondary antibody, visualisation was performed using a LiCor Odyssey 2-color Western detection system (LiCor, Lincoln, NE, USA), according to the manufacturer's instructions. The amount of phosphorylated peptide is given as percent of maximum fluorescence[115].

3.21 In vitro kinase assay of PKC

To preparate crude PKC containing samples, 6 x 10^7 HL-60 cells were harvested, washed and sonicated (5 x 10 s on ice) in 1 ml sample preparation buffer (50 mM Tris, 50 mM β-mercaptoethanol, 10 mM EGTA, 5 mM EDTA, 1 mM PMSF, 10 mM benzamidine, pH 7.5) and centrifuged (100,000 x g, 60 min, 4°C). Protein concentration was determined by Bradford-assay.

4.5 – 5.0 µg of the protein mixture were incubated (25 mM Tris, pH 7.0, 3 mM $MgCl_2$, 0.1 mM ATP, 2 mM $CaCl_2$, 50 µg/ml phosphatidylserine, 0.5 mM EDTA, 1 mM EGTA, 5 mM β-mercaptoethanol) for 15 min at 25°C in a 96-well plate, coated with a PKC-pseudosubstrate (--RFARKGSLRQKNV). The reaction was stopped with 20% H_3PO_4 , the wells were washed and treated with a biotinylated antibody against the pseudosubstrate. After incubation with a streptavidin-coated peroxidase and development with *o*-phenylenediamine, the OD 492 nm was measured in a plate reader.

3.22 Farnesyl pyrophosphate synthase activity assay

Farnesyl pyrophosphate synthase activity was determined in vitro. 100 mio HL-60 cells were homogenized in 5 ml ice-cold homogenisation buffer (0.3 M sucrose, 10 mM EDTA, 1.2 mM β-mercaptoethanol, pH 7.4) by sonication (3 x 8 s) on ice and centrifuged (900 x g, 5 min, 4°C) to remove cell debris. To obtain the peroxisomal fraction, the supernatant was centrifuged twice (8,700 x g, 10 min, 4°C and 10,000 x g, 10 min, 4°C). The resulting pellet was resuspended in ice-cold resuspension buffer (20 mM imidazol, 5 mM DTT, pH 7.4).

Protein concentration was measured by Lowry-assay. The reaction was started by addition of 100 µg of total protein in 150 µl assay buffer (25 mM HEPES pH 7.4, 2 mM $MgCl_2$, 1 mM DTT, 5 mM KF, 1% n-octyl-β-glucopyranoside, 20 µM geranylpyrophosphate, 13.3 µM [^{14}C]-IPP (55 mCi/mmol)) with the indicated BAs or alendronate. After 45 min at 37°C the reaction was stopped by addition of 150 µl stop buffer (2.5 N HCl in 80% ethanol, 100 µg/ml farnesol), the mixture was hydrolysed (30 min, 37°C) and pH normalized with 150 µl NaOH 10%. The farnesyl pyrophosphate was extracted with 1 ml n-hexane and 200 µl of the organic phase was pipetted into 3 ml scintillation liquid to measure (Micro Beta Trilux, Perkin Elmer) the produced [^{14}C]-FPP .

3.23 Release of TNFα in MM6

Differentiated MM6 cells (10^6 / well) were preincubated in a 24-well plate for 30 min with the indicated compounds. After incubation with stimuli for 4 h, 50 µl of cell supernatants were transferred together with a biotinylated TNFα antibody (source: rabbit) into a 96-well plate (coated with an anti-rabbit antibody). After washing and incubation with a streptavidin-peroxidase, colour development of the ELISA-substrate was determined within 30 min at 450 nm.

3.24 Protease activity assays

Inhibition of the enzymatic activity of all proteases was determined in a 96-well plate format by mixing the protease with the test compounds or DMSO as vehicle (never exceeding 0.5%) as control in the respective assay buffer in a total volume of 200 µl and subsequent incubation for 20 min at 25°C. The reaction was then started by addition of the respective chromogenic protease substrate and the proteolysis was monitored at 410 nm by spectrophotometrical measurement using a Victor^2 plate reader (PerkinElmer). Inhibition of the protease is given as the percentage of control without inhibitor (DMSO as vehicle).

For analysis of crude CatG, the enzyme was freshly prepared from PMNL (2.5×10^7 /ml PGC buffer) that were stimulated with 10 µM cytochalasin B and 2.5 µM fMLP for 5 min at 37°C [116]. After centrifugation at 1,200 x g for 5 min at 4°C the resulting supernatant (containing approx. 10 µg CatG/ml) was immediately used for CatG activity assays. For analysis of isolated CatG, the enzyme was purified from PMNL as described below. The assay was composed of 100 ng crude CatG (approx. 10 µl supernatant) or alternatively 200 ng of

purified enzyme, diluted in 180 µl HEPES 0.1 M, NaCl 0.5 M, pH 7.4. As substrate for CatG, N-Suc-Ala-Ala-Pro-Phe-pNA (Suc-AAPF-pNA) (1 mM final concentration) was used and the absorbance was measured at 410 nm at 25 or 37°C. Kinetic studies were performed with substrate concentrations from 0.1 to 4 mM and the K_m was determined from initial rate of hydrolysis by the Lineweaver-Burk method [117].

Inhibition of related proteases was performed in analogy to CatG adjusting the amount of protease, the assay buffer and the substrate individually to each type of protease as follows: Tryptase, 0.5 µg purified enzyme, Tris-HCl 0.1 M, pH 8.3 as assay buffer, and N-α-benzoyl-DL-arginine-pNA (1 mM) as substrate. Chymase, 0.1 µg purified enzyme, Tris-HCl 0.45 M, NaCl 1.8 M, pH 8.0, and 0.5 mM Suc-AAPF-pNA as substrate. Chymotrypsin, 0.1 µg purified enzyme, Tris-HCl 0.1 M, $CaCl_2$ 25 mM, pH 8.3 and 0.2 mM Suc-AAPF-pNA as substrate. Elastase, 0.15 µg purified enzyme, HEPES 0.1 M, NaCl 0.5 M, pH 7.4 and 0.2 mM N-methoxysuccinyl-Ala-Ala-Pro-Val-pNA as substrate. Proteinase 3, 0.5 µg purified enzyme, MOPS 0.1 M, NaCl 0.5 M, 5,5´-dithiobis-(2-nitro-benzoic acid) 0.1 mM, pH 7.5, and 1 mM Boc-Ala-Ala-Nva-SBzl as substrate.

3.25 Docking experiments

Rigid automated molecular docking was performed in collaboration with Dr. G. Schneider, Institute of Organic Chemistry and Chemical Biology, University of Frankfurt, using GOLD 3.01. (Cambridge Crystallographic Data Centre, Cambridge, UK, http://www.ccdc.cam.uk) which relies on a genetic algorithm [118]. We used the known crystal structure of CatG (1T32) from the database PDB. Hydrogens were added, and then energy minimized using the AMBER99 force field within the software MOE [119]. For the co-crystallized inhibitor (2-[3-{methyl[1-(2-naphthoyl)piperidin-4-yl]amino}carbonyl)-2-naphthyl]-1-(1-naphthyl)- 2-oxoethylphosphonic acid) hydrogen atoms were added, and energy minimization was performed using the MMFF94x force field [120]. The 3D structure of AKBA was recently determined (manuscript: Kather, N., Tausch, L., Poeckel, D., Werz, O., Herdtweck, E. and Jauch, J. (2008)). GOLD parameter settings for the genetic algorithm were: number of generations = 100000, population size = 100, selection pressure = 1.1, number of islands = 5, niche size = 2, migrate = 10, mutate = 95, crossover = 95. A 20 Å radius around the active site defined the binding pocket. The default Goldscore function [118] was employed for scoring the predicted receptor-ligand complexes. Larger positive score values indicate more favourable receptor-ligand complexes, negative values indicate unfavourable binding modes (non-

binding). Each docking run was repeated ten times to obtain average score values with standard deviations. The same method was used for the redocking of the co-crystallized inhibitor. RMSD values between the coordinates determent via x-ray crystallography and the docking solutions were computed, and a mean value with standard deviation was calculated. PyMOL was used for visualization of docking poses [121]. This work was almost completely done by Lutz Franke, Dr. G. Schneider, Institute of Organic Chemistry and Chemical Biology, University of Frankfurt.

3.26 Measurement of platelet aggregation (turbidimetric)

Aggregation of platelets in (PRP or diluted PRP) washed platelets was determined using a turbidimetric light-transmittance device (ChronoLog 490 2D, Haverton, PA, USA). 30 ml whole blood was centrifuged (200 x g, 15 min, without brake) and 500 µl of ACD (85 mM trisodium citrat, 65 mM citric acid, 100 mM dextrose) were added to 6 ml of PRP. After centrifugation for 10 min at 800 x g the pellet was resuspended carefully in Tyrode´s buffer (129 mM NaCl, 8.9 mM $NaHCO_3$, 0.8 mM KH_2PO_4, 0.8 mM $MgCl_2$, 5.6 mM glucose, 10 mM HEPES, pH 7.4) without Ca^{2+} and 500 µl of the suspension was gently prewarmed in temperated aggregation cuvettes for 2 min and 15 min incubated at 37°C with the indicated substances or DMSO as control, solvent concentration never exceeded 0.5%.

For aggregation, the response is given as percent of the maximal light transmission Amax. In Ca^{2+}-containing samples, 1 mM $CaCl_2$ was added right before the start of the measurement. Aggregation was recorded for 7 min.

3.27 Measurement of platelet activation markers CD62 and PAC-1 by flow cytometry

Whole blood samples (containing 3.13% sodium citrate), recalcified PRP, or washed platelets resuspended in PGC were incubated with β-BA, AKBA, thrombin receptor-activating peptide (TRAP), or vehicle (DMSO, control) for 2 or 15 min at RT. To measure CD62 and PAC-1, samples were diluted 1 : 1 in 20 mM HEPES, 137 mM NaCl, 2.7 mM KCl, 1 mM $MgCl_2$, 5.6 mM glucose, 1 mg/ml BSA, pH 7.4, and aliquots of 5 ml were incubated with saturating concentrations of CD41-PC7, CD62-PE, and PAC1-FITC at RT for 15 min in the dark. Samples were fixed with formaldehyde 1% (in PBS), washed twice (CellWash, Becton-Dickinson, Heidelberg, Germany), and resuspended in 300 µl PBS. Isotype-matched IgG and

IgM antibodies were used to correct for the nonspecific binding of the specific antibodies. P-selectin (represented by CD62) and PAC-1 antigen expression were quantified. Three-color flow cytometric analysis was used with logarithmic modes set for all channels. A gate was set around the platelet population (CD41), and 5000 events were acquired from each probe. The percentage of CD62- positive cells (%) as well as their mean channel fluorescence intensity (MFI) was determined at a level which yields a value of 1% for mouse IgG1-PE labelled sample. A histogram of PAC1-FITC against cell events was generated and MFI of the total platelet population was recorded. Acquisition of data was carried out using a FACSCalibur flow cytometer with CELLQuest software (Becton-Dickinson). The instrument calibration and compensation was assured daily with calibration beads (CaliBRITE Beads, Becton-Dickinson) and FACSCompt. Fluorescence-conjugated antibodies CD41-PC7, CD62-PE, and PE-labelled isotype IgG1 control were obtained from Beckman Coulter (Krefeld, Germany), PAC1-FITC and FITC-isotype IgM were from Becton- Dickinson.

3.28 Endogenous thrombin potential

Thrombin generation was assessed by using a fluorometric assay, based on the cleavage of a thrombin-specific fluorogenic substrate resulting from stimulation of recalcified or citrate-chelated PRP, yielding the so-called endogenous thrombin potential (ETP) [122]. 80 µl of PRP and 20 µl of buffer containing the thrombin generation trigger were added to each well of a 96-well microtitre plate. The Fluoroskan Ascent Type 374 plate fluorometer (Labsystems; Finland) was used with excitation wavelength of 390 nm, emission wavelength of 460 nm, and a measurement integration time per well of 20 ms. The first derivative of the fluorescence–time curve reflects the course of thrombin activity in the sample. The parameter of interest in the samples using recalcified PRP was the maximal generation rate, which is the peak of the first derivative (ETP peak velocity, relative fluorescence units (RFU) per min) of the thrombin generation curve, or, due to low peak values in Ca^{2+}-free samples, the ETP–area under the curve (AUC).

3.29 Intracellular Ca^{2+} measurement

Platelets (5×10^9 /ml PBS plus 1 mg/ml glucose) were incubated with 2 µM Fura-2/AM for 30 min at 37°C. After washing, 10^9 platelets were resuspended in 1 ml PBS plus 1 mg/ml glucose and 1 mM EDTA and incubated in a thermally controlled (37°C) fluorimeter cuvette in a spectrofluorometer (Aminco-Bowman series 2, Thermo Spectronic, Rochester, NY) with continuous stirring. After preincubation with the indicated inhibitors, stimuli and Ca^{2+} (2mM) were added and the fluorescence was measured, $[Ca^{2+}]_i$ was calculated according to Grynkiewicz et al. [123]. F*max* (maximal fluorescence) was obtained by lysing the cells with 1% Triton-X 100 and F*min* by chelating Ca^{2+} with 10 mM EDTA.

3.30 PMNL chemoinvasion assay

Freshly isolated PMNL (2×10^6) were resuspended in 1 ml HEPES-buffered RPMI 1640 medium with 10% (v/v) fetal calf serum (FCS) and preincubated with test compounds or with vehicle (DMSO, never exceeding 0.5% DMSO). 150 µl of the cell suspension were then placed on the upper chamber of two compartment Boyden chamber (8 µm pore-size filters) in a 24-well format. Cells were allowed to migrate through matrigel-coated pore-size filters for 40 minutes in the lower chamber containing buffer (negative control) or buffer plus fMLP (0.1 µM) as chemoattractant. Cells on the bottom of the wells were fixed with 3.7% formaldehyde, stained with grams violet, washed and the stain was solubilized using acetic acid. The absorption of the eluted stain was measured at 570 nm / 620 nm, respectively.

3.31 Purification of CatG from PMNL

CatG was purified as previously described [124] with slight modifications. All purification steps were performed at 4°C. Human isolated PMNL (10^{10}) were suspended in ice-cold 0.15 M NaCl and sonicated (5 × 30 s, 65%). Remaining nuclei and cell debris were removed by centrifugation (600 x g, 10 min). The supernatant was again centrifuged (16,000 x g, 30 min) to separate the granular fraction (pellet) from the post-granular supernatant fraction. The granular fraction was resuspended in 1 M NaCl plus 0.05% Triton X-100, and stored for 36 h for protease extraction. The suspension was centrifuged at 16,000 x g for 30 min, and four volumes of water added to restore isotonicity. Proteins were precipitated by ammonium sulfate (60% saturation) and the pellet was resuspended in 40 ml 0.05 M Tris-HCl, pH 8.0. After centrifugation (16,000 x g, 30 min), the supernatant was subjected to elastin-Sepharose

affinity chromatography column (2.5 × 20 cm) equilibrated with 0.05 M Tris buffer, pH 8.0 (ÄKTA explore, GE Healthcare, Freiburg, Germany). The protein was loaded and the column was eluted with the equilibration buffer until the OD_{280} returned to baseline. The column was then washed with two volumes of 0.05 M Na-acetate, 1 M NaCl, pH 5.0, and fractions containing CatG activity were eluted with 0.05 M Na-acetate, 1 M NaCl, 20% DMSO, pH 5.0. Active fractions were pooled, dialyzed in vivaspin cut-off columns (5,000 MWCO) versus 20 mM Na-acetate, 0.15 M NaCl, pH 5.5, and subjected to ion-exchange chromatography (CM Sephadex C-50) column, equilibrated in the same buffer. The sample was applied, washed with equilibration buffer and bound material was eluted by a linear NaCl gradient from 0.15 M to 1 M. The total elution volume was 300 ml and fractions of 6 ml were collected at a flow rate of 30 ml/h. The homogeneity of the purified material was checked by SDS-PAGE and CatG activity assays.

3.32 Determination of protein concentration

3.32.1 Lowry

BSA was diluted in Tris buffer (5 mM, pH 7.4) in the range 0.1 to 1 mg/ml. 25 µl of Biorad Lowry reagent A (alk. coppertartrate) were mixed with 5 µl standard or protein sample in triplicates in a 96-well plate. Under slow agitation, 200 µl of Biorad Lowry reagent B (Folin-ciocalteau) was added and incubated for 15 min. The OD was determined at 620 nm in a microplate photometer (Digiscan, High Tech)[125, 126].

3.32.2 Bradford

Standard (BSA or γ-globulin) and protein of interest was diluted in appropriate buffer and pipetted in triplicates, 80 µl per well in a 96-well plate. After addition of 5x Biorad Protein assay Bradford reagent (20 µl) the plate was agitated for 15 min and measured in a microplate reader (Dynatech MR5000) at 620 nm[127, 128].

3.33 Crystallography and X-ray determination

Purified CatG from granules of human PMNL were used (see above). We screened for crystallization conditions with Sigma screen kits I and II (Sigma-Aldrich) and grew diffraction quality crystals by the hanging drop vapour diffusion method and at 20°C over 28 days. CatG (10 mg/ml) and Aβ-BA were mixed in a 1:2 molar ratio, and the crystals were grown from 30% poly(ethylene glycol) 4000, 0.2 M lithium sulfate, 20 mM zinc sulfate, and 0.1 M Tris, pH 8.5 [129, 130]. A second screen with Structure screen I & II HT 96 (Molecular Dimensions Limited, Suffolk, UK) with the sitting drop vapour diffusion method in a 96 well plate and CatG mixed with AKBA in a 1:2 molar ratio related to crystals grewing in 0.2 M sodium chloride, 0.1 M Na acetate pH 4.6, 30% (v/v) MPD and in 0.1 M Na citrate pH 5.6, 20% (v/v) 2-propanol, 20% (w/v) PEG 4000.

Crystals grew as long needles or cubes. For cryoprotection crystals were transferred into mother liquor containing 10% glycerol (v/v) and immediately frozen in liquid nitrogen. Data were collected at beamline ID23-1 at ESRF, in one degree oscillations. Diffraction was observed to a useable resolution of 2.7 Å processing and scaling were performed with HKL-2000. Crystallography and x-ray measurement was done in collaboration with Dr. J. Chen, Institute for Biophysical Chemistry, University Frankfurt.

3.34 Statistics

All data are presented as mean + s.e.m (standard error of the mean). For statistical analysis GraphPad Prism version 4.00 (GraphPad Software, San Diego, California, USA) was used. Data were subjected to Kolmogorov-Smirnov test to confirm Gaussian distribution followed by one-way ANOVA coupled with Bonferroni post hoc test for multiple comparisons (in celecoxib assays, ex vivo data were subjected by one-way ANOVA coupled with Dunnett´s post t-test for multiple comparisons). All other data were subjected to paired, 2-sided t-tests. The IC_{50} and ID_{50} values were analysed using GraphPad Prism version 4.00 and a sigmoid curve fitting model.

4 Results

4.1 Target identification of BAs using a protein-fishing strategy

4.1.1 Pulldown experiments

An elegant technique for the identification of a high-affinity small molecule (ligand) - protein (target) interaction is the protein-fishing approach using an affinity matrix composed of the small molecule linked covalently to an insoluble resin [131]. Prominent examples for a successful application of this strategy are the identification of human histone deacetylase as target for trapoxin [132] or of rapamycin binding protein (FKBP) as the target of the immunosuppressant FK-506 (rapamycin) [133]. A protein fishing strategy for the identification of molecular targets of BAs was developed in collaboration with Dr. J. Jauch, University of Saarland. Thus, KBA was linked at the C3-OH moiety to glutaric acid forming the half ester 3-*O*-glutaroyl-KBA (glut-KBA). The remaining free carboxylic group of glut-KBA was amide-coupled with the primary amine of EAH Sepharose 4B yielding KBA-Seph as an affinity resin (**fig. 411**). Freshly prepared lysates of Triton X-100 (1 %)-treated cells were incubated with KBA-Seph, EAH Sepharose 4B without glut-KBA (Seph) was used as negative control to exclude unspecific protein binding. The precipitates were intensely washed; proteins were detached from the resin using SDS-b.

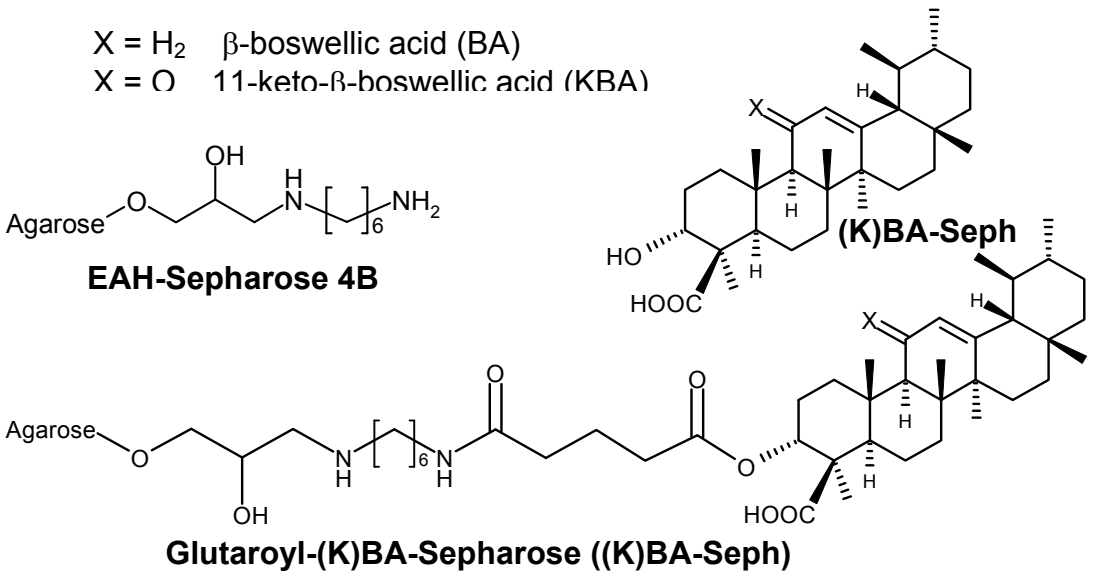

figure 411: **Chemical structure of the KBA-Seph affinity matrix.** KBA is linked to glutaric acid by esterification of the C3-OH group of KBA to EAH Sepharose 4B (Seph) via amide coupling, yielding the KBA-Seph affinity matrix.

4.1.2 Separation of precipitated proteins by SDS-PAGE

Proteins from pulldown experiments were separated by SDS-PAGE. The absolute amounts of precipitated proteins were comparable in pull-downs obtained with Seph and KBA-Seph. Proteins were visualized by Coomassie- and silver-staining (**fig. 412A-C**).

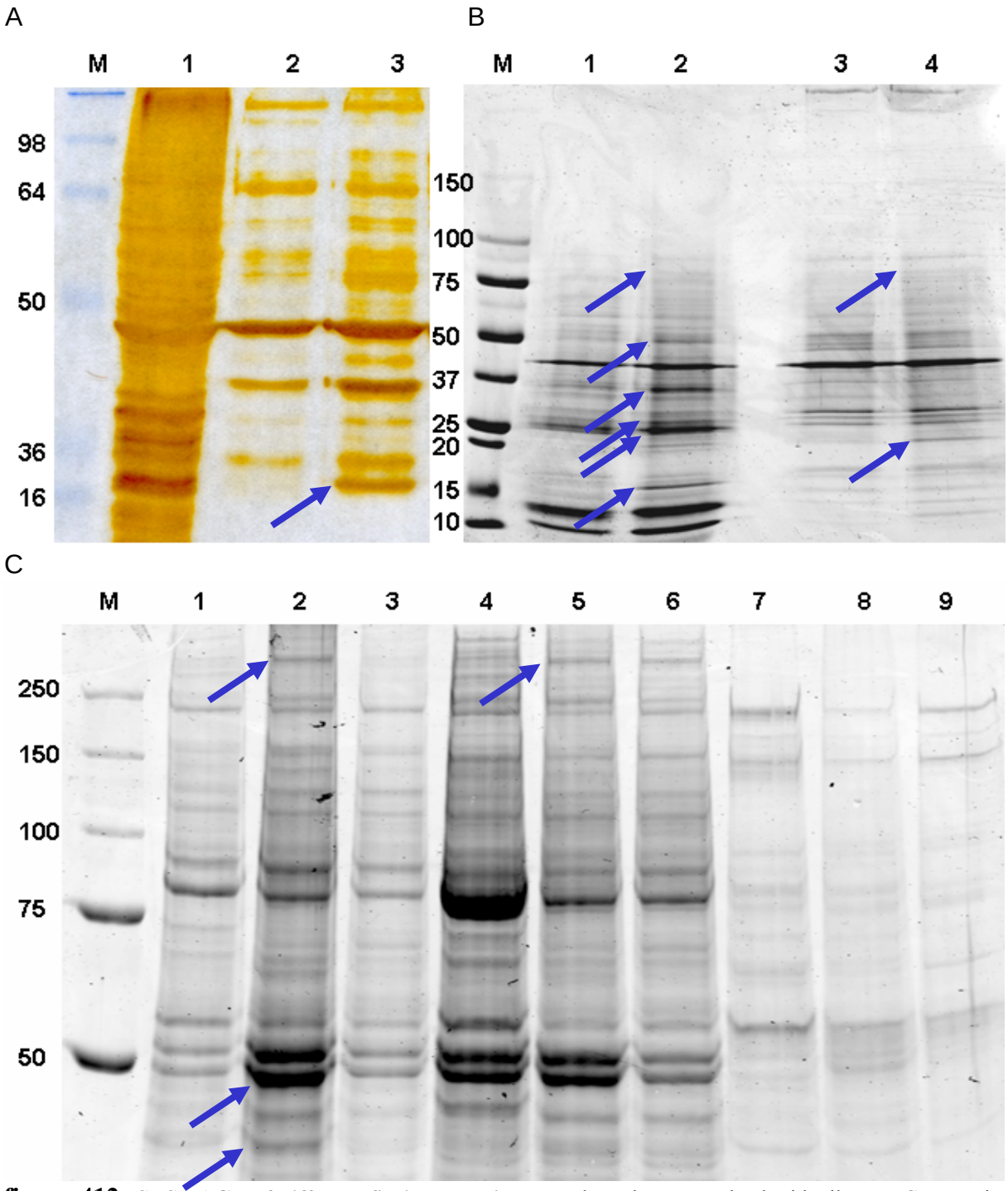

figure 412: SDS-PAGE of different fishing experiments. The gels were stained with silver or Coomassie, Biorad. All-blue protein marker (M) was used for estimation of the protein-size. Differential bands in KBA-Sepharose and Sepharose lanes were marked by arrows, results are given in table 411: (**A**) SDS-PAGE 10%, silver stain, PMNL-lysate, 1: lysate as control, 2: PMNL + Sepharose (Seph), 3: PMNL + KBA-Sepharose (KBA-Seph); (**B**) SDS-PAGE 4-20%, Coomassie, 1: PMNL + Seph, 2: PMNL + KBA-Seph, 3: platelets + Seph, 4: platelets + KBA-Seph; (**C**) SDS-PAGE 8%, Coomassie, 1-3: LNCaP-lysate (Seph, KBA-Seph, β-BA-Seph), 4-6: MCF-7-lysate, 7-9: PMNL-lysate

Control-lanes with samples of Seph-precipitated protein were compared with lanes of KBA-Seph-precipitated samples and bands visible in both lanes were excluded. Bands only existent in the KBA- or β-BA-Seph lane (arrows in **fig. 412A-C)** were analysed by mass spectrometry. These proteins bind specifically to KBA-Sepharose and could be a target for BAs.

4.1.3 Analysis of proteins by mass spectrometry

The protein bands of KBA-Seph pulldowns indicated by the arrows (**fig. 412)** were excised from the gel. Parallel to that, a corresponding piece of gel was excised from the neighboring lane, where proteins of the Seph-precipitates were separated. Proteins were in-gel-digested by trypsin and subjected to MALDI-TOF-MS in cooperation with Dr. M. Karas, Institute of Pharmaceutical Chemistry, University of Frankfurt. Analysis of the obtained peptide fragments using the peptide sequence data base www.matrixscience.com clearly indicated that the major proteins were significantly identified and could not be detected in the control sample (selection in **table 411)**. Some proteins listed in **table 411** were further analysed by Western blot. An example of database searching of protein fragments identified by MS is given in **fig. 413**. With a threshold of $p<0.01$, the analysed protein in the gel-band is considered as CatG.

MS data cell type	species	size [kDa]	found protein (statistically significant)
PMNL	homo sapiens	19.5	**cathelicidin antimicrobial peptide CAP18**
platelets	homo sapiens	21.2	**Ras-related protein Rap-1b** MS/MS: O-Krev precursor; Complexed With Gppnhp And The Ras-Binding-Domain Of Human C-Raf1, Residues 51-131
PMNL	homo sapiens	25.8	**Cathepsin G**
PMNL	homo sapiens	26.1	**proteinase 3**
LNCaP	homo sapiens	29.8	**prohibitin**
RBL-1	Rattus norvegicus	41.1	**Farnesyl pyrophosphate synthetase (FPP synthetase)**
PMNL	homo sapiens	41.6	**vesicle amine transport protein 1 VAT1**
LNCaP	homo sapiens	51.1	**ATP synthase beta subunit**
PMNL	homo sapiens	60	**ATP synthase, H+ transporting**
PMNL	homo sapiens	76.4	**UNC-112 related protein 2**
platelets	homo sapiens	76.5	**UNC-112 related protein 2**
LNCaP	homo sapiens	470.1	**DNA dependent protein kinase**

table 411: MS data pulldown experiments. KBA-Seph bound significant proteins in four different cell types. Proteins are assorted by size.

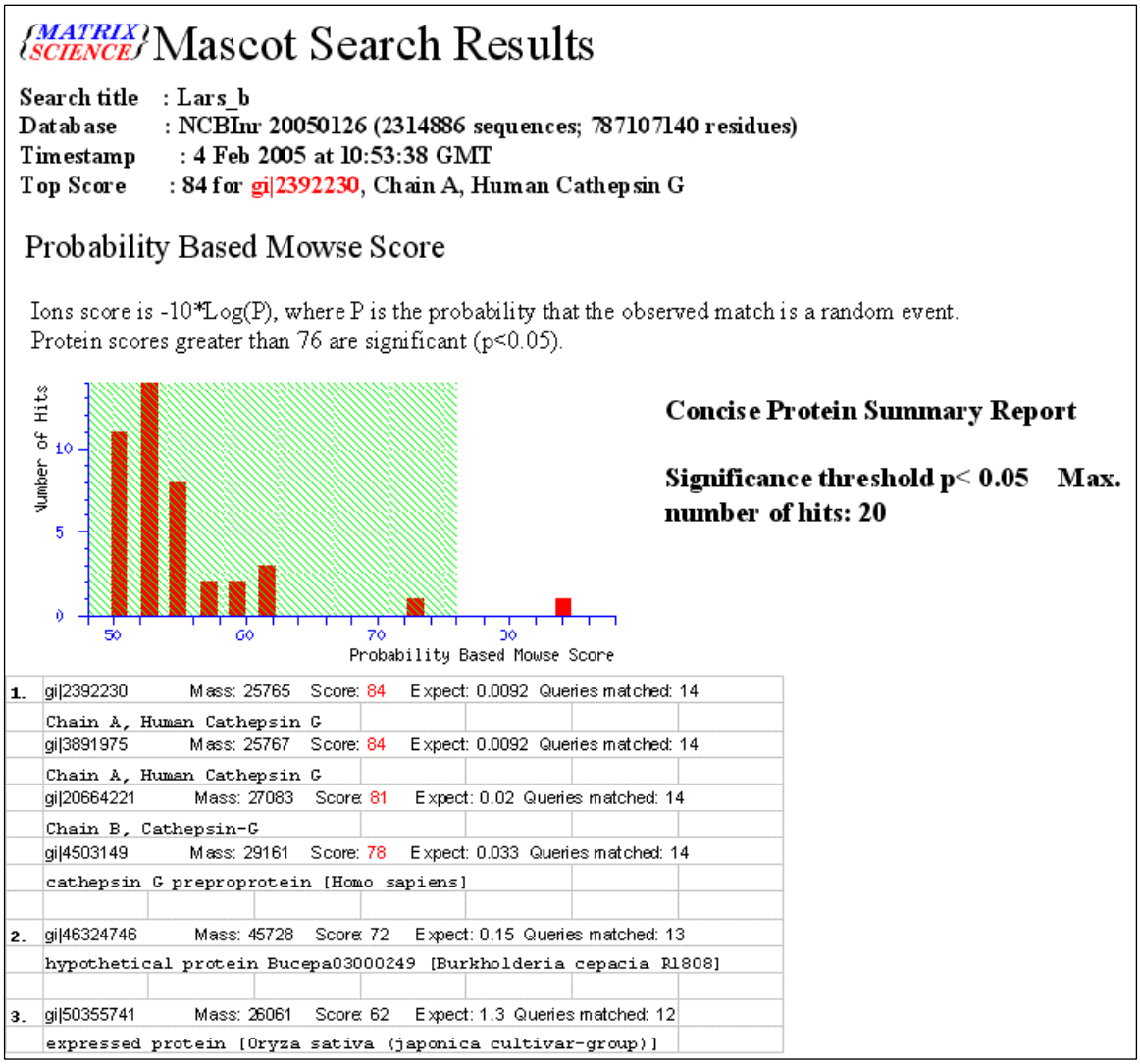

MATRIX SCIENCE Mascot Search Results

Search title : Lars_b
Database : NCBInr 20050126 (2314886 sequences; 787107140 residues)
Timestamp : 4 Feb 2005 at 10:53:38 GMT
Top Score : 84 for gi|2392230, Chain A, Human Cathepsin G

Probability Based Mowse Score

Ions score is -10*Log(P), where P is the probability that the observed match is a random event.
Protein scores greater than 76 are significant (p<0.05).

Concise Protein Summary Report

Significance threshold p< 0.05 Max. number of hits: 20

1.	gi|2392230	Mass: 25765	Score: 84	Expect: 0.0092	Queries matched: 14	
	Chain A, Human Cathepsin G					
	gi|3891975	Mass: 25767	Score: 84	Expect: 0.0092	Queries matched: 14	
	Chain A, Human Cathepsin G					
	gi|20664221	Mass: 27083	Score: 81	Expect: 0.02	Queries matched: 14	
	Chain B, Cathepsin-G					
	gi|4503149	Mass: 29161	Score: 78	Expect: 0.033	Queries matched: 14	
	cathepsin G preproprotein [Homo sapiens]					
2.	gi|46324746	Mass: 45728	Score: 72	Expect: 0.15	Queries matched: 13	
	hypothetical protein Bucepa03000249 [Burkholderia cepacia R1808]					
3.	gi|50355741	Mass: 26061	Score: 62	Expect: 1.3	Queries matched: 12	
	expressed protein [Oryza sativa (japonica cultivar-group)]					

figure 413: Identification of CatG by MS and data base search

4.1.4 Immunodetection of proteins

The identity of selected proteins was analysed further by Western blot. A part of the results is shown in **fig. 414.** KBA-Sepharose significantly binds Ras, protein kinase C (cPKCβ), platelet 12-LO, Akt, and several tyrosine-phosphorylated proteins with approximate sizes of 50, 60 and 80 kDa, whereas Seph as negative control does not bind these proteins. Because of unspecific protein-binding at the same size, proteins in **fig. 414** could not be detected selectively by MALDI-MS.

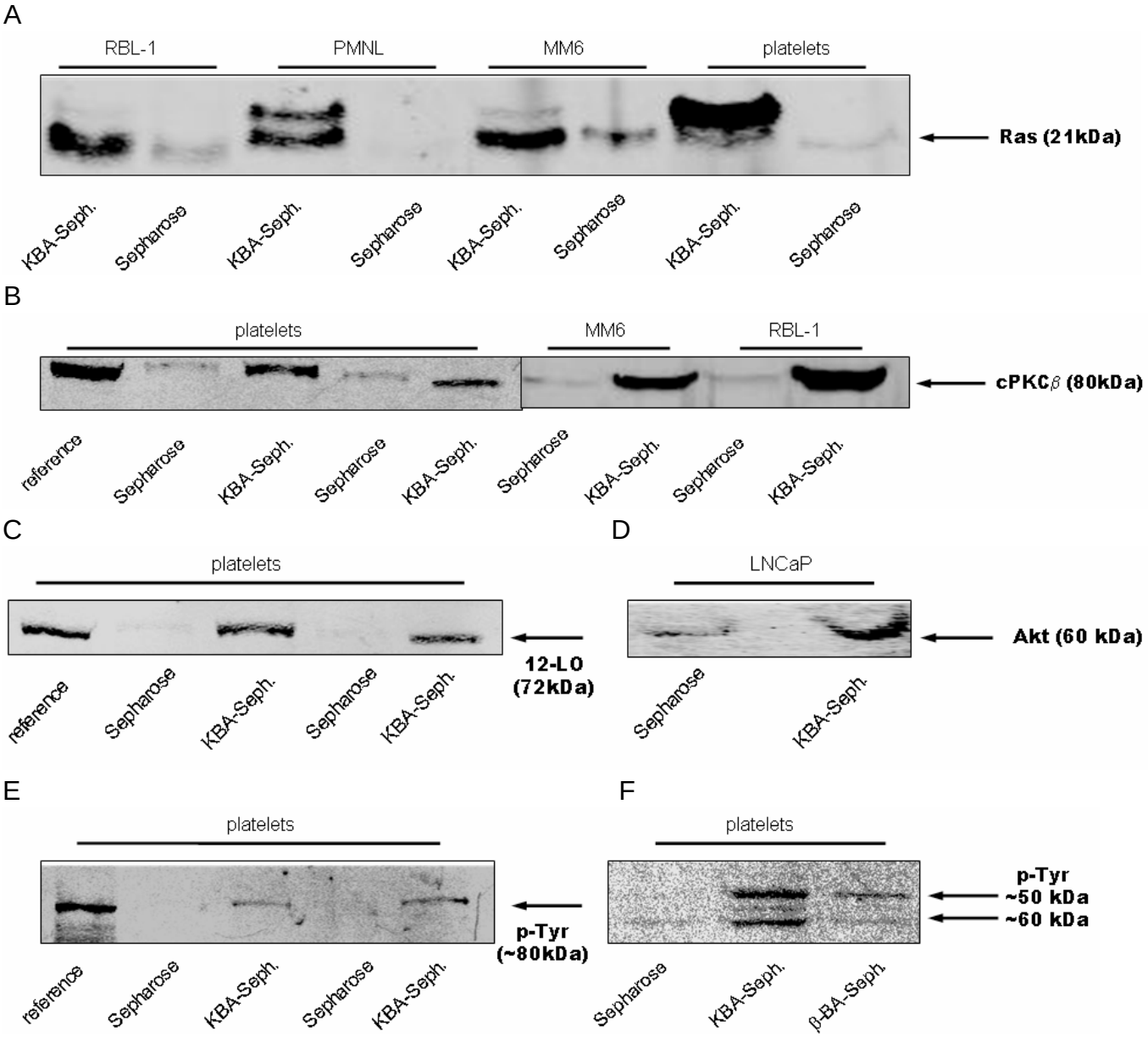

figure 414: Western blot analysis of selected proteins. Pulldowns of cell lysates (from 5 x 10^7 RBL-1, 3 x 10^7 PMNL, 1 x 10^7 MM6, 3 x 10^9 platelets or 5 x 10^7 LNCaP) were separated by SDS-PAGE, blotted and immunostained with the indicated antibody. Visualization was performed with an Odyssey reader. Reference = cell lysate (**A**) Ras (21kDa); (**B**) cPKC (80kDa); (**C**) 12-LO (72kDa); (**D**) Akt (60kDa); (**E**) pTyr (band at appr. 80kDa); (**F**) pTyr (bands at appr. 50/60kDa). Each blot is representative for at least three independent experiments.

4.1.5 FPPs activity

One of the identified proteins was farnesyl pyrophosphate synthase (FPPs). FPPs is one of the major proteins for terpene synthesis in humans and the target for bisphosphonates (like alendronate) in osteoporosis. As shown in table 411, it binds selectively to KBA-Sepharose but is not inhibited in vitro by BAs up to 30 µM (**fig. 416**).

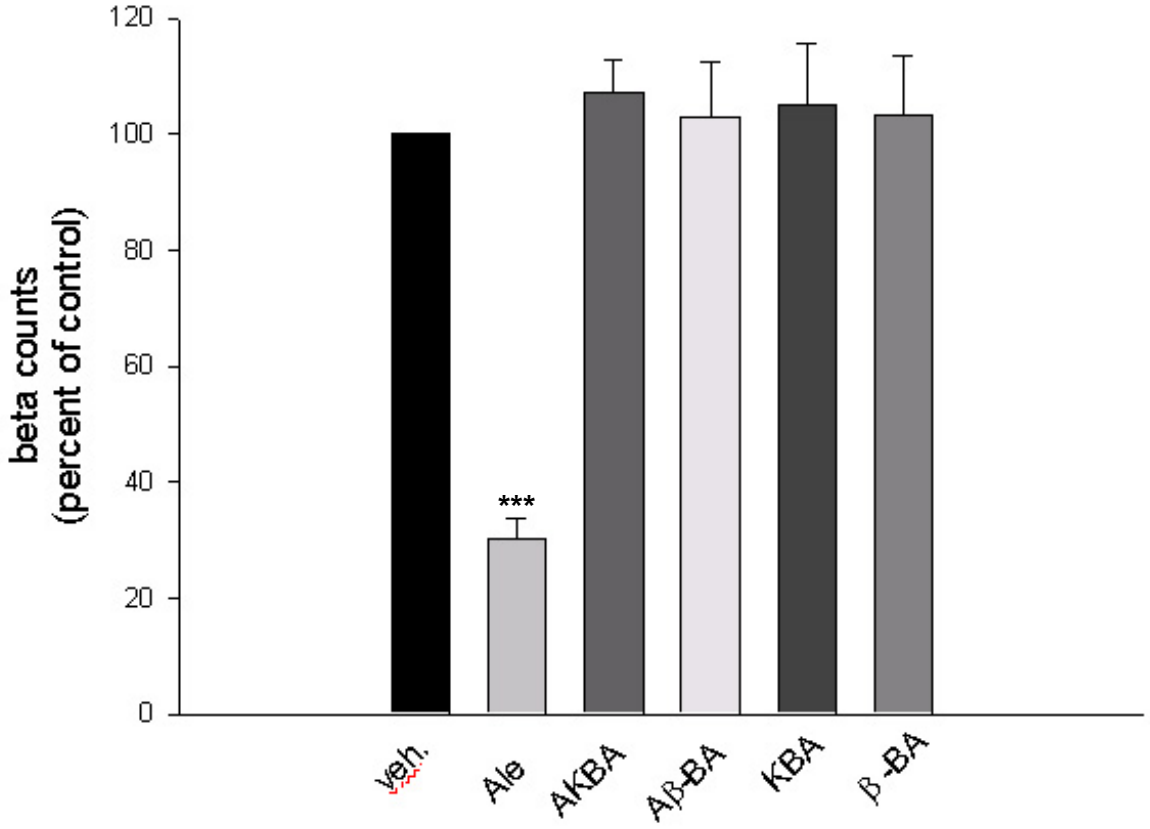

figure 415: Radioactive test system for FPPs activity in vitro. FPPs from the peroxisomal fraction of HL-60 cells was incubated with [^{14}C]-isopentenylpyrophosphate and geranylpyrophosphate to form [^{14}C]-FPP. Product was extracted and measured in a beta counter. DMSO was used as vehicle (veh.), alendronate 3 µM (Ale) as positive control and BAs were used in concentrations of 30 µM. Results are given as mean + s.e.m., n = 4-6, and analysed by one-way ANOVA followed by a Bonferroni post-hoc test: ***$p<0.001$.

4.1.6 PKC activity

Protein kinase C is involved in several diseases like cancer and diabetes via diverse signal cascades (see fig. 213). As shown in **fig. 414B**, PKC is bound to immobilized BAs whereas Sepharose as negative control does not bind PKC. The inhibition of the enzyme by BAs was tested in an activity assay in vitro (**fig. 417**). Only β-BA inhibits moderately at a concentration of 30 µM, but is not statistically significant.

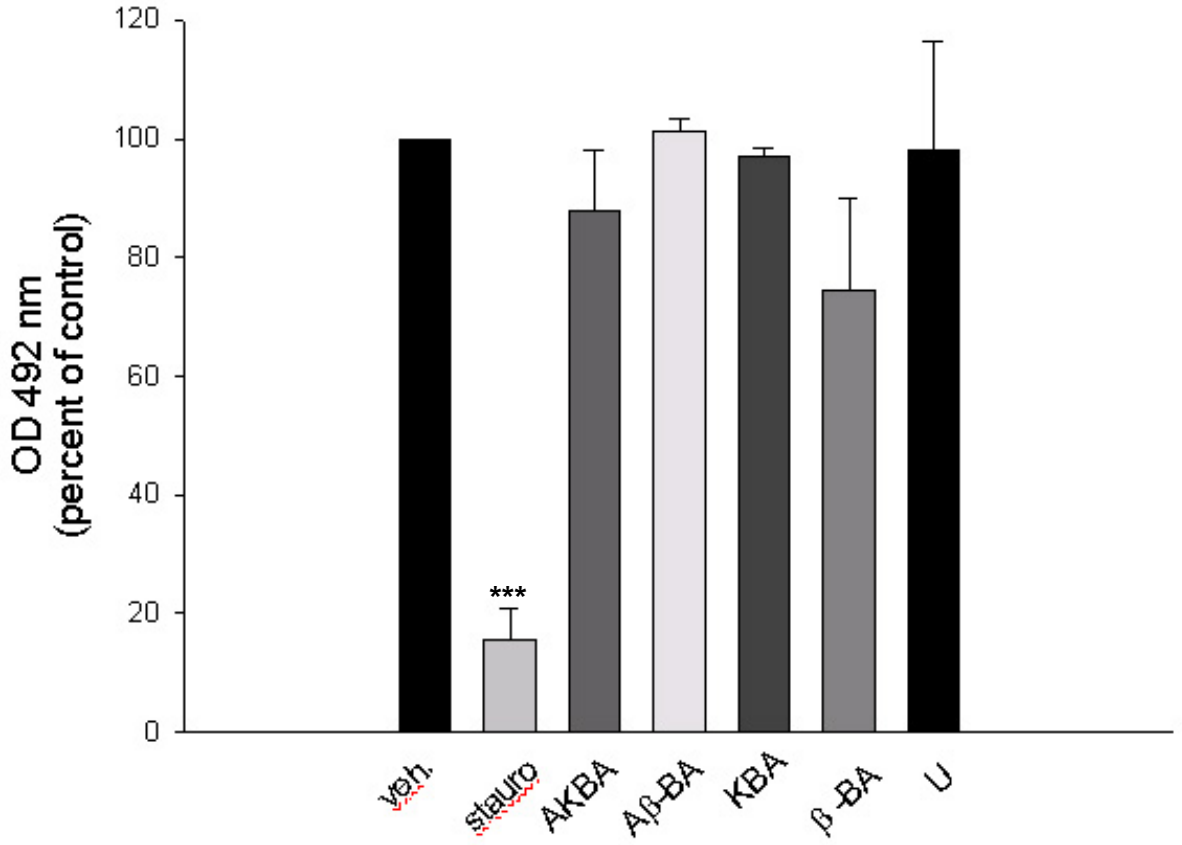

figure 416: PKC activity in vitro. In a 96-well plate, HL-60 lysate, preincubated with the indicated test compounds (U-73122 (U), BAs at 10 µM, staurosporine (stauro) = 1 µM) or vehicle (veh., DMSO) for 2 min at 25°C, converted a PKC-pseudo substrate and product was detected by ELISA as described in the *Methods* section. Data is given as mean + s.e.m., n = 3 and analysed by one-way ANOVA followed by a Bonferroni post-hoc test: ***p<0.001.

4.1.7 Rap1b

The small guanine-nucleotide-binding protein Ras-related protein Rap1b is involved in signal transduction of apoptosis and cell survival in nearly all cells, but is essential for normal function of human platelets [134]. Rap1b efficiently activates various integrins including the platelet integrin $\alpha_{IIb}\beta_3$, which mediates fibrinogen binding required for platelet aggregation [135]. Rap1b is a common target of many different activation pathways in platelets. ADP, thrombin, collagen, epinephrine and platelet-activating factor induce Rap1-GTP formation. The pathways leading to Rap1 activation in platelets are not clearly defined [136]. For example, ADP has been suggested to activate Rap1 by Ca^{2+}-dependent as well as Ca^{2+}-independent mechanisms involving the $G\alpha_i$ -coupled P_2Y_{12} receptor [137, 138]. Recently, phosphatidylinositol 3-kinase (PI3K) was reported to mediate Rap1b activation by different platelet agonists [139]. Rap1b is a key mediator in the development of several cancers and atherosclerosis.

Rap1b was precipitated with KBA-Seph, therefore it was plausible to investigate the influence of BAs on Rap1b activity. AKBA but not β-BA inhibits ADP-induced Rap1 activation in human platelets (**fig 417**). This work was done in collaboration with Dr. Albert Smolenski, Institute of Biochemistry II, University of Frankfurt and will be continued in the thesis of Ulf Siemoneit, University of Tübingen.

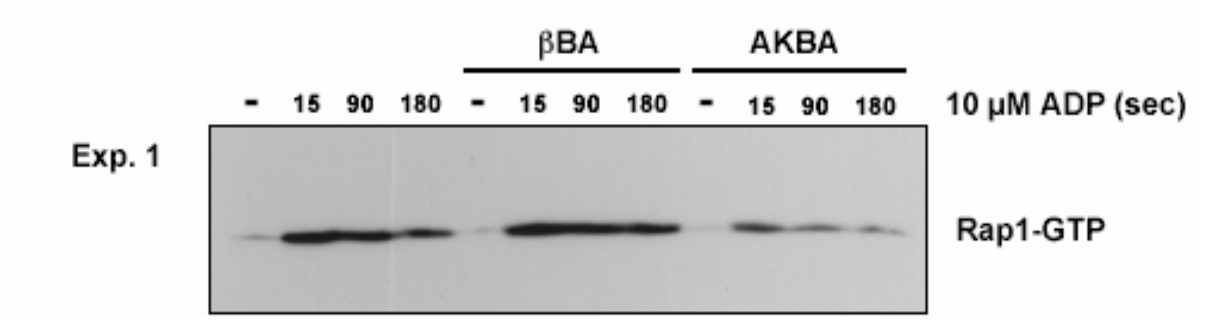

figure 417: Inhibition of ADP-induced Rap1 activation. ADP 10µM, various time points, β-BA/AKBA 10µM, preincubation 10 min. The blot is representative of at least three independent experiments.

4.2 Cathepsin G

4.2.1 Protein fishing with immobilized boswellic acids selectively precipitates cathepsin G

As shown in **fig. 421**, a number of proteins from PMNL were bound to the EAH-Sepharose 4B material and thus were detectable in both pull-downs. However, a 25.8 kDa protein was significantly enriched in KBA-Seph precipitates as compared to Seph lacking the ligand. No other protein selectively present in KBA-Seph but not in Seph precipitates was readily detectable. The sequence coverage using MALDI-TOF-MS was about 63% (**fig. 422A**). In order to confirm the identity of CatG as the select protein precipitated by KBA-Seph, the Seph and KBA-Seph pulldowns were subjected to SDS-PAGE and analysed by WB using CatG antibodies. Whereas no CatG was detected in the sample derived from the negative control (Seph precipitates), a strong immunoreactive band was apparent in the sample of KBA-Seph (**fig. 422B**). Moreover, purified CatG from human leukocytes was bound to KBA-Seph as detected by WB, but not to Seph, implying a specific and direct interaction with the BA (**fig. 422C**).

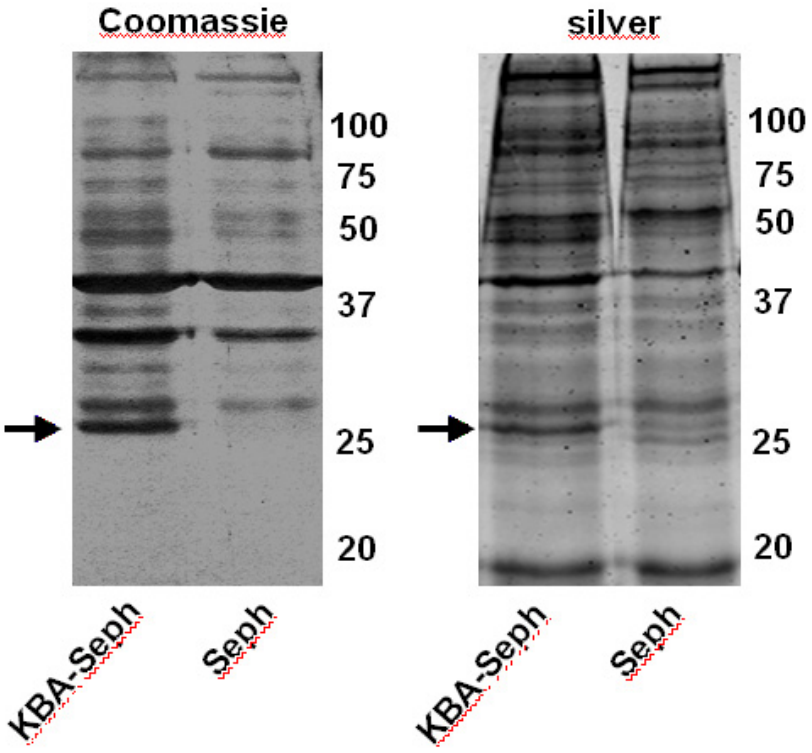

figure 421: 12,000 x g supernatants of PMNL lysates were incubated over night at 4°C with either KBA-Seph or crude Seph. Precipitates separated by SDS-PAGE and proteins were visualized by Coomassie- and by silver-staining. The band of interest at 25.8 kDa for KBA-Seph and a corresponding piece of gel from the Seph sample were excised, in-gel digested and analysed by MALDI-TOF-MS.

A

```
  1 IIGGRESRPH SRPYMAYLQI QSPAGQSRCG GFLVREDFVL TAAHCWGSNI
 51 NVTLGAHNIQ RRENTQQHIT ARRAIRHPQY NQRTIQNDIM LLQLSRRVRR
101 NRNVNPVALP RAQEGLRPGT LCTVAGWGRV SMRRGTDTLR EVQLRVQRDR
151 QCLRIFGSYD PRRQICVGDR RERKAAFKGD SGGPLLCNNV AHGIVSYGKS
201 SGVPPEVFTR VSSFLPWIRT TMRS
```

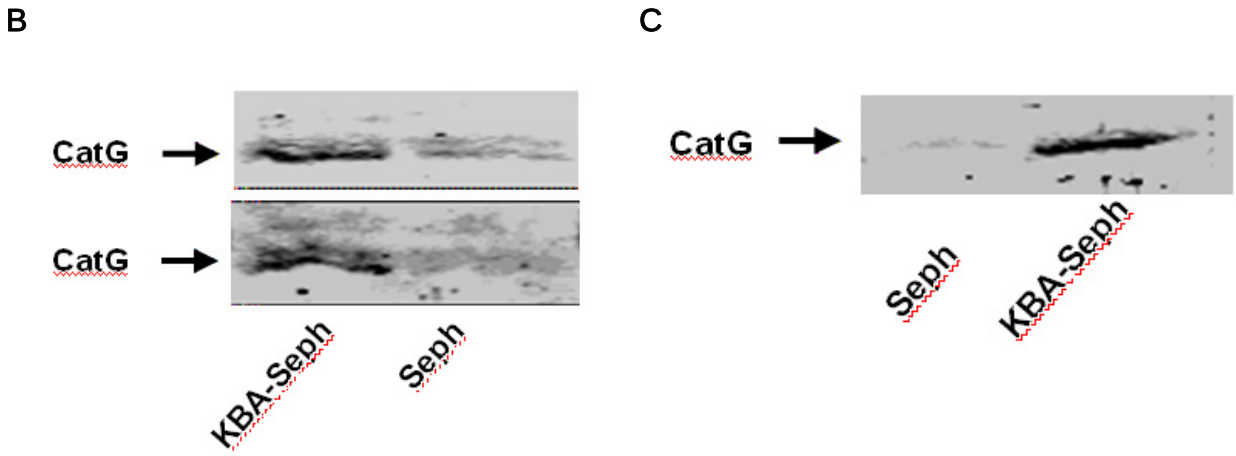

figure 422: (**A**) MALDI-TOF-MS data: Peptides matched to the protein sequence of human cathepsin G (chain A) (sequence coverage: 63%). The matched peptides are shown in bold (red) letters. Similar results were obtained in at least three additional experiments. (**B**) PMNL-lysate precipitates and (**C**) purified enzyme precipitates (Seph and KBA-Seph) analysed by SDS-PAGE and Western-blotting using specific antibodies against CatG.

4.2.2 Boswellic acids inhibit the proteolytic activity of cathepsin G

In order to investigate whether or not the interaction of BAs with CatG may alter its enzymatic activity, the proteolytic activity of CatG, secreted from cytochalsin B/fMLP-stimulated human PMNL, was analyzed in the presence of structurally different BAs and the related triterpenes α-amyrin and ursolic acid (10 μM each) [116]. As can be seen from **fig. 423A**, all BAs potently inhibited CatG activity, comparable to a synthetic CatG inhibitor (0.5 μM, used as a reference compound) [129], whereas α-amyrin and ursolic acid caused no significant inhibition. Note that also the glutaroyl-linked-KBA (glut-KBA) was an effective inhibitor. Concentration-response curves (**fig. 423B**) for the BAs demonstrate concentration-dependent inhibition of CatG with IC_{50} values of 0.6 μM for AKBA, 0.8 μM for β-BA, 1.1 μM for Aβ-BA and 3.7 μM for KBA. Variation of the peptide substrate concentration reduced the potency of BAs, and Lineweaver-Burke plots indicate a competitive inhibition of CatG (**fig. 423C**). Potent inhibition of 10 μg CatG by 10 μM AKBA (final concentration) obtained after incubation for 20 min at 37°C was reversed upon 50-fold dilution (**fig. 423D**), suggesting a reversible inhibition mode of CatG by BAs.

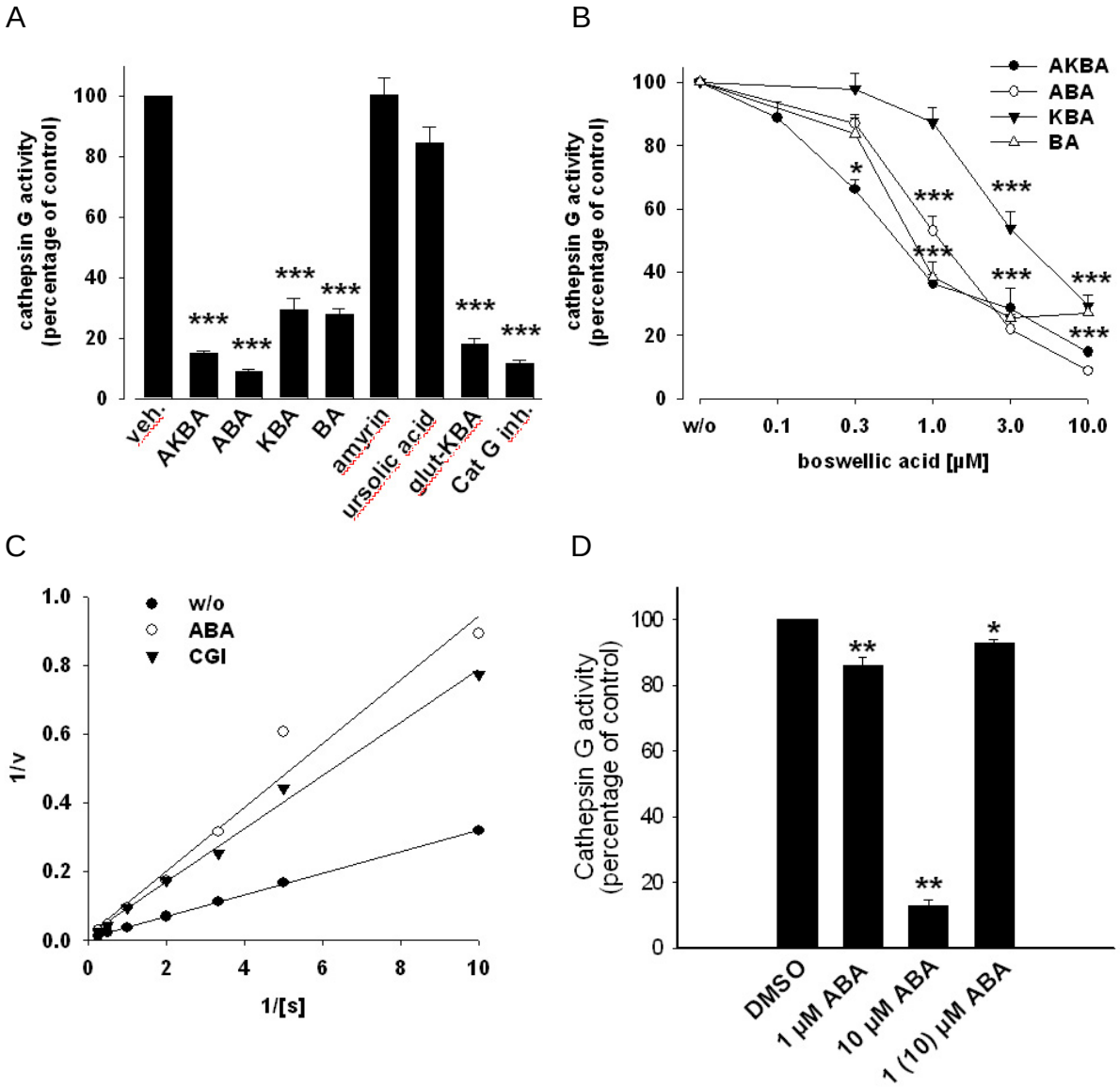

figure 423: BAs inhibit the proteolytic activity of CatG (**A**) Isolated CatG (200 ng) from PMNL was diluted in 180 µl HEPES 0.1 M, NaCl 0.5 M, pH 7.4 and preincubated with the indicated test compounds (all at 10 µM, except CGI = 0.5 µM) or vehicle (veh., DMSO) for 20 min at 25°C. Then, Suc-AAPF-pNA (1 mM final concentration in 200 µl final volume) was added to start the reaction and the absorbance was measured at 410 nm. The enzyme activity was determined by the progress curve method. Results are presented as percentage of control (veh.) and data are given mean + s.e.m., n = 4-6. (**B**) Concentration-response curves of BAs on CatG activity. Inhibition of the activity of CatG (200 ng isolated enzyme from PMNL) by BAs was determined as described above. Data are given as mean + s.e.m., n = 4. (**C**) Kinetic analysis of CatG inhibition by 10 µM Aβ-BA and 0.1 µM CGI. Data are given as mean of three independent experiments and results are presented as Lineweaver-Burke plots. The CatG substrate concentrations were 0.1, 0.2, 0.3, 0.5, 1, 2, and 4 mM. (**D**) Reversibility analysis of Cat G inhibition by Aβ-BA. Cat G is preincubated with 10 µM Aβ-BA for 5 min. After 1:10 dilution with incubation buffer, Cat G activity was determined as described above. Data are given as mean + s.e.m., n = 3. Data was further analysed by one-way ANOVA followed by a Bonferroni post-hoc (A, B) test or by a Dunnett post-hoc test (D): *p<0.05; **p<0.01, ***p<0.001.

4.2.3 Effects of boswellic acids on related serine proteases

In order to assess the selectivity of BAs for inhibition of CatG, the effects of BAs on the activity of the closely related serine proteases chymase, tryptase, HLE, proteinase-3 and chymotrypsin were determined under individually optimized, yet comparable experimental conditions. As shown in **fig. 424**, AKBA and Aβ-BA (10 µM, each) failed to significantly inhibit chymase and tryptase. However, both BAs suppressed proteinase-3, and Aβ-BA (but not AKBA) also inhibited HLE and chymotrypsin, although less efficient as compared to CatG. Concentration response studies showed that for HLE and for proteinase-3 the IC_{50} values of AKBA and Aβ-BA were ≥ 30 µM, whereas for chymotrypsin an IC_{50} = 4.8 µM for Aβ-BA was apparent. Together, AKBA and Aβ-BA are potent inhibitors of CatG, and apart from the inhibitory effect of Aβ-BA on chymotrypsin, these BAs are rather selective for CatG.

A

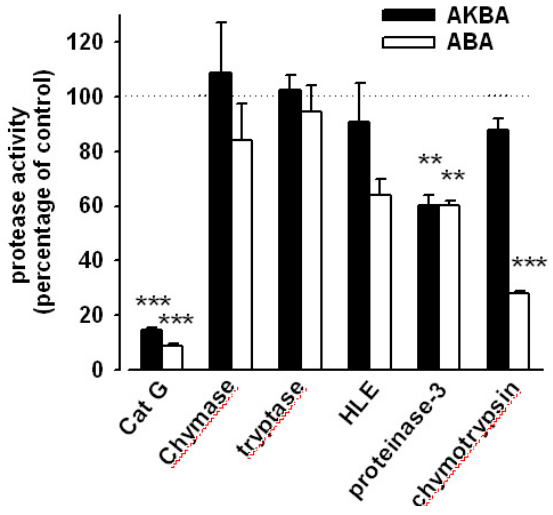

figure 424: Effects of Aβ-BA and AKBA on the activity of various serine proteases. (**A**) Aβ-BA and AKBA (10 µM, each) or vehicle (DMSO) were preincubated with the serine proteases for 20 min at 25°C and the activities of the respective proteases were assayed under standard conditions as described in the *Methods* section. Results are presented as percentage of control (vehicle) and data are given as mean + s.e.m., n = 4-5. (**B**) Concentration-response curves of Aβ-BA and AKBA on the activities of HLE, proteinase-3 and chymotrypsin. Inhibition of the activity of the proteases by the BAs was determined as described above. Data are given as mean + s.e.m., n = 3-4 and analysed by one-way ANOVA followed by a Bonferroni post-hoc test: **p<0.01, ***p<0.001.

B

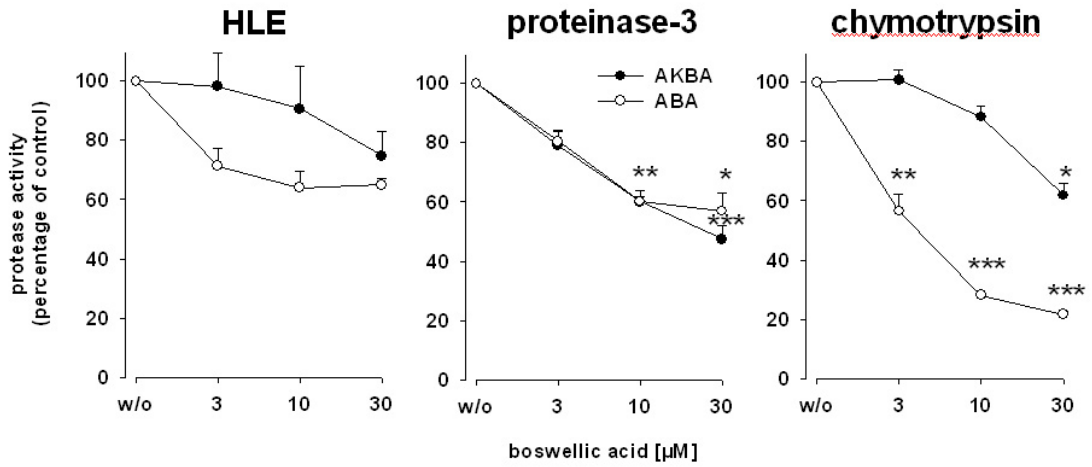

4.2.4 Docking of boswellic acids to cathepsin G

Automated molecular docking of AKBA in collaboration with Dr. G. Schneider, Institute for Biophysical Chemistry, University of Frankfurt using the protein data base (PDB) structure 1T32 as a reference for CatG, was performed for the purpose of finding a potential binding mode within the active site. To verify the validity of the GOLD software, we successfully re-docked the 1T32 co-crystallized inhibitor (2-[3-{methyl[1-(2-naphthoyl)piperidin-4-yl]amino}carbonyl)-2-naphthyl]-1-(1-naphthyl)- 2-oxoethylphosphonic acid) [129], with an RMSD of 0.4 ± 0.06. The acquired binding mode was identical to the X-ray structure and yielded a Goldscore of 102.6 ± 2.5. Docking of AKBA into the same docking box resulted in an average docking score of 44.1 ± 1. Both inhibitors partially occupy the same part of the active center (**fig. 425**).

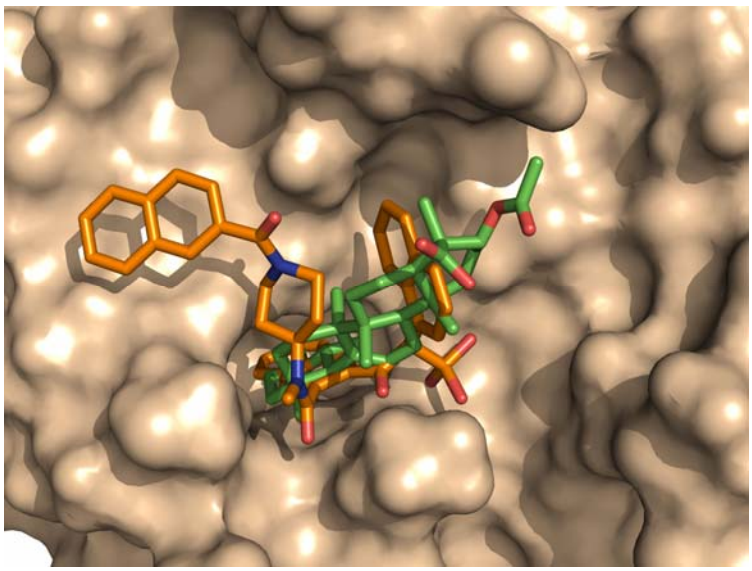

figure 425: Rigid automated molecular docking of AKBA into CatG. Active site of CatG (PDB: 1T32) together with the co-crystallized CGI displayed in orange. The orientation of AKBA in an overlapping binding mode is shown in green.

4.2.5 Boswellic acids inhibit (cathepsin G-mediated) PMNL chemoinvasion

Since CatG is assumed to contribute to invasion and migration of PMNL along chemoattractant gradients by degrading extracellular matrix proteins [36], we determined the effects of AKBA and Aβ-BA on PMNL migration through matrigel towards the chemoattractant fMLP in a modified Boyden chamber assay. fMLP caused a 4.2-fold increase in the numbers of migrated cells and this was efficiently blocked by AKBA and Aβ-BA (IC_{50} approx. 2.7 and 2.9 µM, respectively). Comparison of the effect of CGI at 0.1 µM demonstrated that AKBA and Aβ-BA at 8 to 9 µM cause quantitatively the same inhibitory effect (approx. 75 % inhibition) on chemoinvasion of PMNL (**fig. 426**).

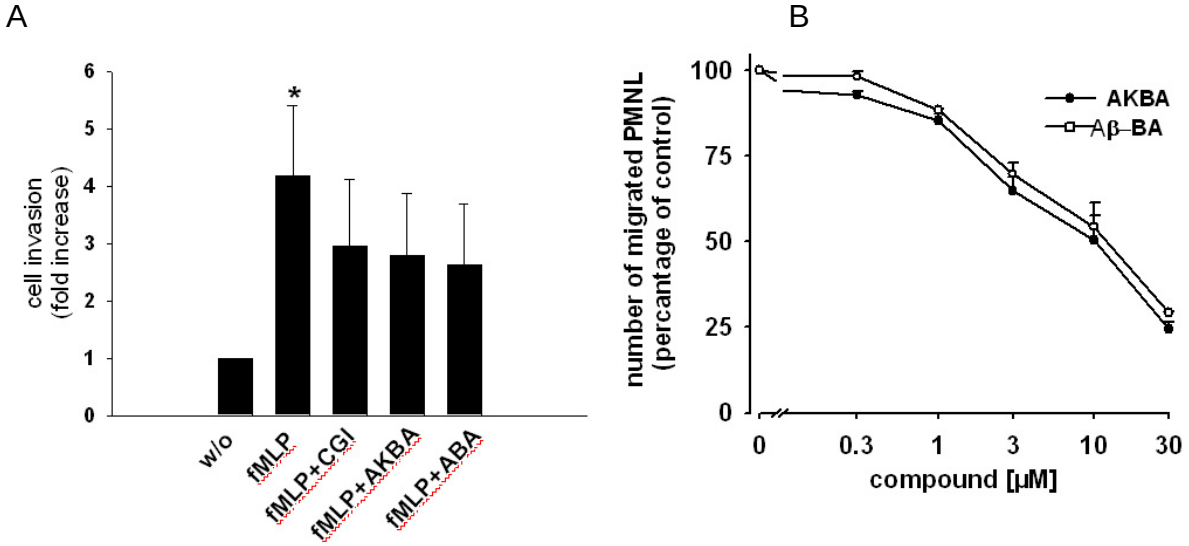

figure 426: BAs suppress CatG-mediated functional cellular responses. (**A**) Aβ-BA and AKBA inhibit PMNL chemoinvasion. PMNL were pretreated with the test compounds or with vehicle (DMSO) and placed on the upper chamber of a two compartment Boyden chamber. Cells that migrate through matrigel-coated pore-size filters in the lower chamber containing buffer (control; DMSO) or 0.1 µM fMLP (positive control) within 40 minutes were fixed, stained with grams violet, and after washing the absorption of the solubilized stain was measured at 570 nm / 620 nm, respectively. CatG inhibitor 0.1 µM (CGI) and AKBA 10 µM were used as invasion inhibitors. Results are presented as fold-increase of the number of migrated cells where vehicle-treated cells were set to 1. (**B**) Concentration-response curves of β-BA and AKBA on the invasion inhibition of PMNL. Cells migrating toward the chemoattractant fMLP were set as 100% Data are given as mean + s.e.m., n = 5 and analysed by one-way ANOVA followed by a Bonferroni post-hoc test: *$p<0.05$.

.

4.2.6 Boswellic acids inhibit cathepsin G-mediated Ca^{2+} mobilisation in human platelets

CatG released from fMLP-stimulated PMNL can cleave the PAR-4 on platelets resulting in the mobilisation of Ca^{2+}, suggesting that PAR-4 mediates platelet responses to CatG [45]. Accordingly, BAs should be able to block Ca^{2+} mobilisation in platelets evoked by fMLP-activated PMNL. Addition of fMLP to Fura-2-loaded platelets caused no Ca^{2+} mobilisation (not shown), but when PMNL were co-incubated then addition of fMLP resulted in a transient elevation of $[Ca^{2+}]_i$ in platelets (**fig. 427B**). In the presence of 3 µM AKBA or 0.1 µM CGI, this elevation of $[Ca^{2+}]_i$ was strongly suppressed. These data suggest that AKBA is able to block Ca^{2+} mobilisation in platelets due to inhibition of CatG (**fig. 427A**).

A

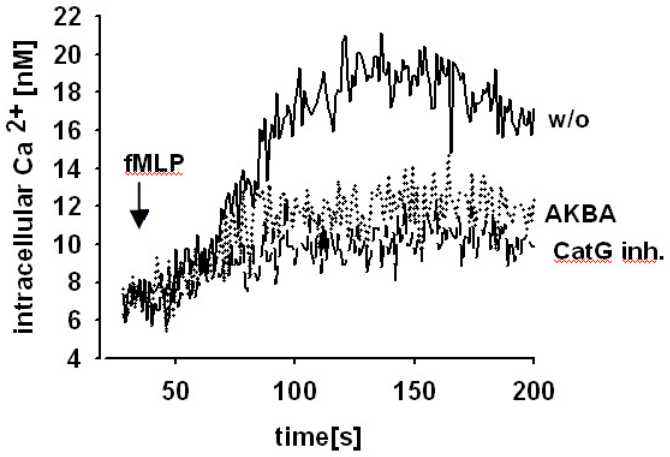

figure 427: (**A**) AKBA inhibits Ca^{2+} mobilisation in platelets induced by fMLP-stimulated PMNL. Fura-2-loaded platelets (10^8 cells) were mixed with 10^7 unloaded PMNL in 1 ml PG buffer containing 0.1 mM EDTA and incubated with AKBA (3 µM), CGI (0.1 µM) or vehicle (DMSO). After 5 min the measurement of $[Ca^{2+}]_i$ was started. After 30 sec, 100 nM fMLP was added and the fluorescence was recorded for another 100 sec. Curves are representative of at least 4 experiments. (**B**) Molecular mechanism of calcium influx in platelets via CatG-PAR4-receptor interaction

B

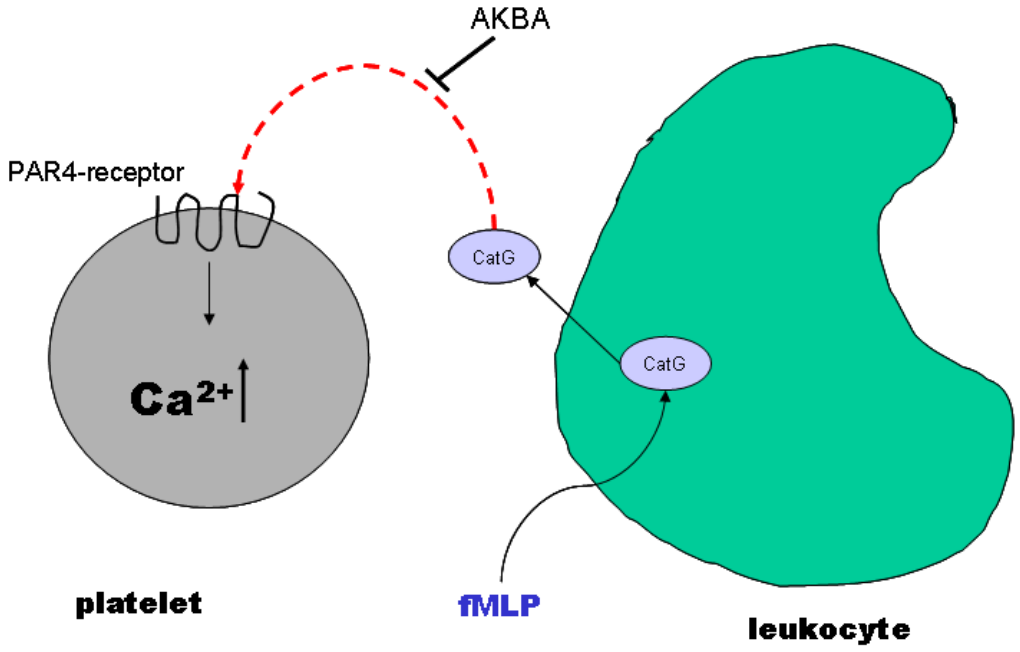

4.2.7 Inhibition of cathepsin G by Boswellia serrata extracts ex vivo

A multicentered, double-blind, randomized and placebo-controlled clinical trial aiming to protract an acute attack in patients with Crohn´s disease was conducted by Pharmasan GmbH. Patients were in remission and use of aspirin, nonsteroidal anti-inflammatory drugs and glucocorticoids were not allowed in the 3 weeks before enrollment. The orally administered BS extract (Pharmasan GmbH, PS0201Bo, 400 mg) was taken twice daily in the morning/evening over a 12-month period and endpoint was an acute attack. Between October 2006 and October 2007, 13 healthy subjects were enrolled and randomization was computer-generated by using block randomization in two groups, but only one patient did not drop out until December 2007.

The effectiveness on CatG inhibition in plasma *ex vivo* was measured as part of this study. After screening and randomization, venous blood was first taken prior to medication (verum or placebo) and again after 4 weeks of treatment with 2 x 400 mg extracts/d (steady state). Citrated blood was stimulated with 10 µM cytochalasin B and 2.5 µM fMLP for 5 min and plasma was prepared for determination of CatG activity. As shown in **fig. 428A**, a mean reduction (47 ± 18 %) of CatG activity in the plasma of patients was measured after treatment as compared to plasma prior treatment. After partial deblinding in December 2007, data of seven patients could be analysed. CatG activity in patients who had taken verum (n=2) was reduced by 64 % ± 23 % and in patients who had taken placebo (n=5) by 15 % ± 25 % (**fig. 428B)**. Plasma levels of BAs were 3380 / 2470 ng/ml (6.4 ± 1 µM) for β-BA, 2190 / 2670 ng/ml (4.9 ± 1 µM) for Aβ-BA, 188 / 135 ng/ml (0.34 ± 0.05 µM) for KBA and 21.8 / 22.5 ng/ml (0.04 ± 0.01 µM) for AKBA.

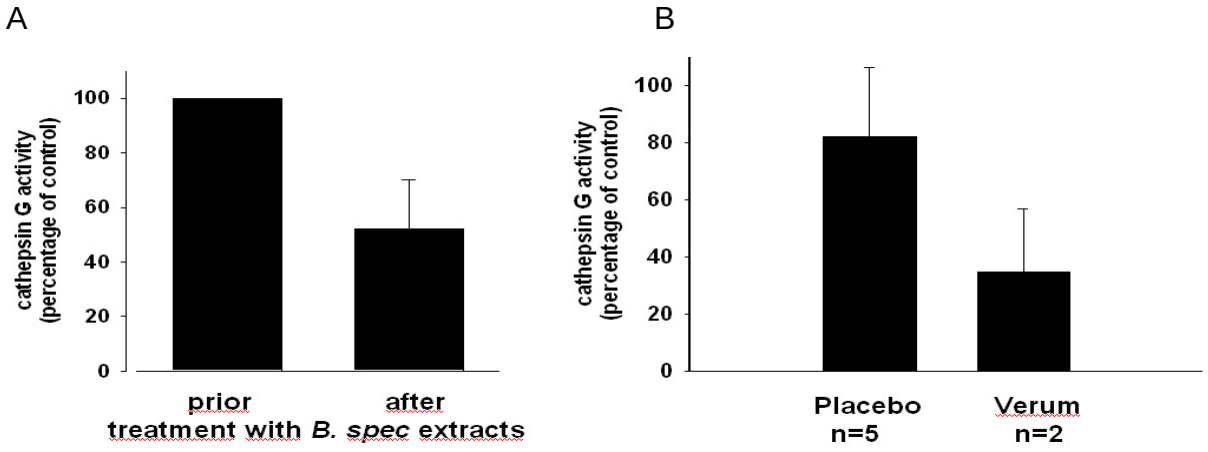

figure 428: BS extracts lower the CatG levels in human subjects *ex vivo*. Blood was taken from subjects prior medication as well as after four weeks of continuous administration of 2 x 400 mg/d BS extracts. After venipuncture, the blood was promptly stimulated with 10 µM cytochalasin B and 2.5 µM fMLP for 5 min, and plasma was prepared. Aliquots (20 µl) of the plasma were immediately used for determination of CatG as described in the *Methods* section. (**A**) CatG activity prior and after treatment with BS extracts, n = 7. (**B**) CatG activity after 4 weeks treatment (steady state). Data are shown as mean + s.e.m.

In a second trial, an adult healthy male volunteer (28 years old) took three times a day three capsules with 400 mg BS extract (BS extract, acid fraction;Ch.B.: 2605010, BAs 91.37%; Euro OTC Pharma GmbH, Bönen; in total 3.6 g/d) over four weeks to demonstrate safety, tolerability, pharmacokinetics of BS extracts and to determine plasma levels of BAs in steady state. Co-medication was not allowed three weeks before and during the treatment. Blood was taken three times before treatment and three times during the fourth week under therapy and stimulated as described above to determine CatG activity *ex vivo*. CatG activity was reduced by intake of BS extract significantly by 24 +/- 1.5% **(fig. 429)**.

Plasma levels of BAs were 8013 ± 479 ng/ml (17.6 ± 1 µM) for β-BA, 6612 ± 82 ng/ml (13.3 ± 0.2 µM) for Aβ-BA, 355 ± 83 ng/ml (0.76 ± 0.2 µM) for KBA and 37 ± 6 ng/ml (0.07 ± 0.01 µM) for AKBA. BA plasma levels were determined by LC-MS/MS analysis [140] in collaboration with Dr. Geisslinger, Clinical Pharmacology, University of Frankfurt. No side-effects appeared during intake, thus the BS extract was safe and tolerable.

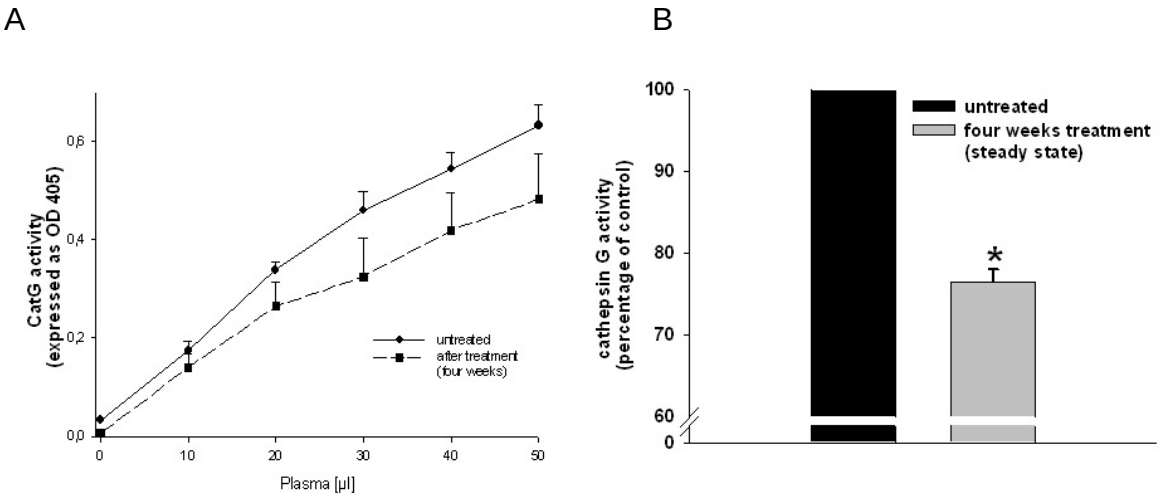

figure 429: CatG activity in human plasma before and after continuous treatment with 3.6 g extract per day. Blood was promptly stimulated with 10 µM cytochalasin B and 2.5 µM fMLP for 5 min, and plasma was prepared. Aliquots (20 µl) of the plasma were immediately used for determination of CatG as described in the *Methods* section. (**A**) Dose response of treatment of the volunteer on CatG activity in plasma. (**B**) Activity of endogenous CatG ex-vivo before and after treatment with extract (3 x 1200 mg/d). Data are shown as mean + s.e.m, n = 3 and analysed by ANOVA followed by Bonferroni post-hoc test, *p<0.05.

In experiments with rats, animals were fed with gelatinous slurry as negative control or with three different extract slurries, containing BS extract, *Boswellia carterii* extract or BS solubilisate. Four hours after feeding, rats were sacrified; whole blood was prepared and stimulated with 10 µM cytochalasin B and 2.5 µM fMLP for 5 min. Then plasma was prepared for determination of CatG activity. Absolute activity measured in OD at 405 nm is shown in **fig. 4210A**. Only blood of rats treated with BS extract exhibited lower activity of CatG *ex vivo* as control (w/o), but not significantly because of high variations between individuals as well as the low number (n = 5). When exogenous Aβ-BA (10 µM) was accessorily added to the plasma samples, CatG activity was only lowered in untreated animals and animals treated with the solubilisate (**fig. 4210B**), while CatG activity was already fully inhibited in extract-treated rats.

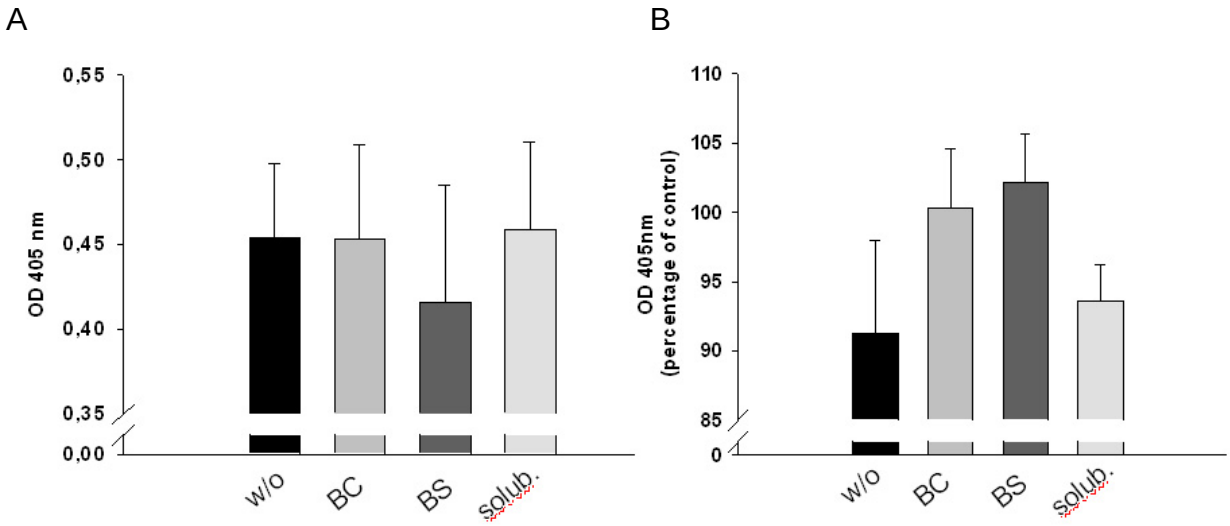

figure 4210: Cathepsin G activity *ex vivo* in rat plasma. Four hours after feeding with gelatinous slurry (w/o), BS extract (BS), *Boswellia carterii* extract (BC) or BS solubilisate (solub.), whole blood was prepared and stimulated with CytB and fMLP as described in the *Methods* section. Stimulated plasma was divided in two parts and CatG activity was measured with 1 µl DMSO as vehicle (**A**) or with 10 µM exogenous Aβ-BA (**B**). Results are shown as mean + s.e.m, n = 5 and analysed by ANOVA followed by Bonferroni post-hoc test.

4.2.8 Crystallography of CatG and Aβ-BA

CatG was purified as described in *Methods* (3.30). Concentrated protein (10 mg/ml) was mixed with Aβ-BA (1:2 molar ratio) and incubated at 22 °C for 15 min prior to crystallization trials [129, 141]. Crystals were grown by using the hanging drop method at 22 °C, with 0.2 M lithium sulfate, 20 mM zinc sulfate, 0.1 M Tris pH 7.4 and 30% (w/v) PEG 4000, as the precipitant. Crystals grew as long needles (**fig. 4210**) within 2 weeks to a maximum size. For cryoprotection, crystals were transferred into mother liquor containing 10% glycerol (v/v) and immediately frozen in liquid nitrogen. Data were collected at beamline ID23-1 at the European Synchrotron Radiation Facility in 1° oscillations. Diffraction was observed to a resolution of 3.0 Å. Aβ-BA was expected as inhibitor in the catalytic center. The crystals grew in space group P6(3), with a = 73.4 and b = 70.2. Because of the weak diffraction pattern and strong ice rings at 3 Å, indexing was only done to 3.5 Å. Solving the structure by molecular replacement appeared very problematic and no inhibitor could be observed at this resolution. Further condition screening and modifications in the freezing procedure should solve the problems.

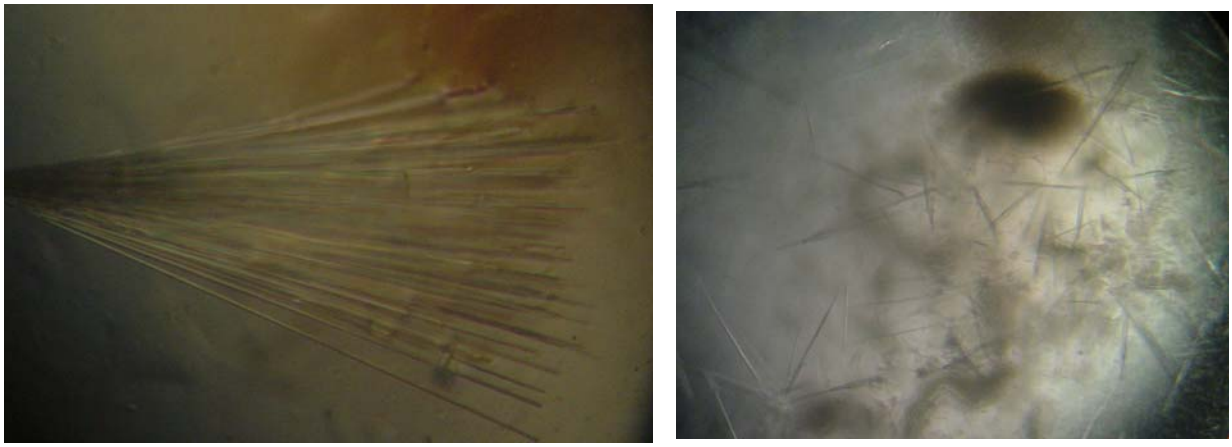

figure 4211: CatG crystals under microscope. Crystals grew as long needles or in the form of a brush.

4.3 DNA-PK and Akt are influenced by boswellic acids

4.3.1 Akt phosphorylation is inhibited by BAs in vivo and in vitro

Downstream of receptor tyrosine kinases (RTK) (**fig. 213**), DNA-PK and Akt play critical roles in cell growth, apoptosis and the immune response [50, 51]. LNCaP were incubated for 1 hour with the indicated test compounds (AKBA, Aβ-BA, DNA-PK-inhibitor (DNA-PKI) or wortmannin), and then stimulated with CpG-ODNs for 20 min to activate DNA-PK [52]. As shown in **fig. 431 and 432**, AKBA significantly inhibits phosphorylation of Akt at position Ser-473 in prostate cancer cells (LNCaP), acts synergistically with the PI3K-inhibitor wortmannin, and inhibition is concentration-dependent (**fig. 431B**). Bad is a downstream target of Akt, therefore, phosphorylation of Bad at residue Ser-136 is an indicator for the activity of Akt [53]. Beside Akt phosphorylation, Bad phosphorylation is also potently inhibited by AKBA (20 µM) and the combinations of wortmannin (200 nM) and DNA-PKI (600 nM; **fig. 432**), but not by wortmannin or by DNA-PKI alone.

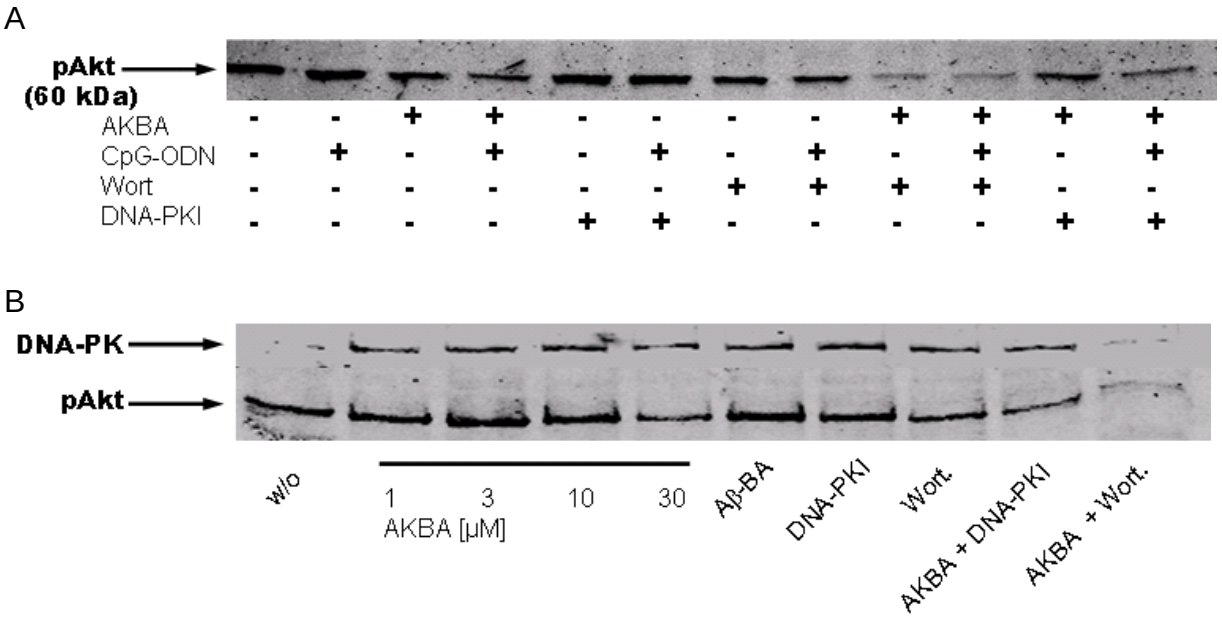

figure 431: Inhibition of Akt-phosphorylation in LNCaP cells by BAs. LNCaP were incubated for 1 hour with the test compounds prior to stimulation with CpG-ODNs (10 µg/ml). Cells were lysed and immunoblotted against pAkt or pBad. (**A**) Akt-phosphorylation is inhibited by AKBA (20 µM) and the control inhibitors wortmannin (200 nM) and DNA-PKI (600 nM); unstimulated or stimulated with CpG-ODNs. (**B**) Concentration-response of AKBA in Akt-phosphorylation, Aβ-BA 10µM, wortmannin 200 nM and DNA-PKI 600 nM and the combinations were used as controls. Blots are representative of at least four experiments.

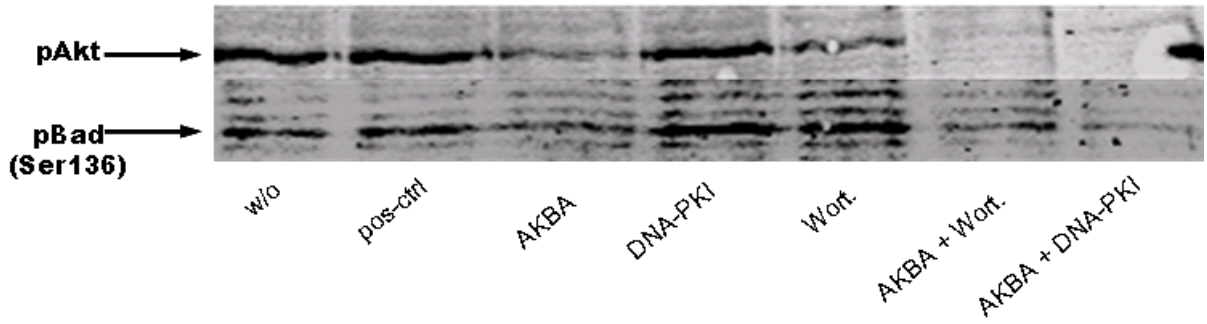

figure 432: Correlation of Akt- and Bad-phosphorylation. Bad is a downstream-target of Akt and an indicator of active Akt (used concentrations: AKBA 20 µM, wortmannin 200 nM and DNA-PKI 600 nM). Blots are representative of at least four experiments.

Akt phosphorylation by DNA-PK was tested in a radioactive ([^{32}P]-ATP) in-vitro-kinase assay. Active DNA-PK (20 U) was incubated for 10 min at 30°C with BAs, CpG-ODNs (10 µg/ml), [^{32}P]-ATP (3 µCi) and 100 µg DNA-PK peptide-substrate or 600 ng Akt-1 as substrate. After separation, the [^{32}P]-phosphorylated proteins were exposed to a radioactivity-sensitive film. Phosphorylation of Akt (**fig. 433A**) and the DNA-PK peptide-substrate (**fig. 433B**) by DNA-PK is inhibited concentration-dependently by BAs.

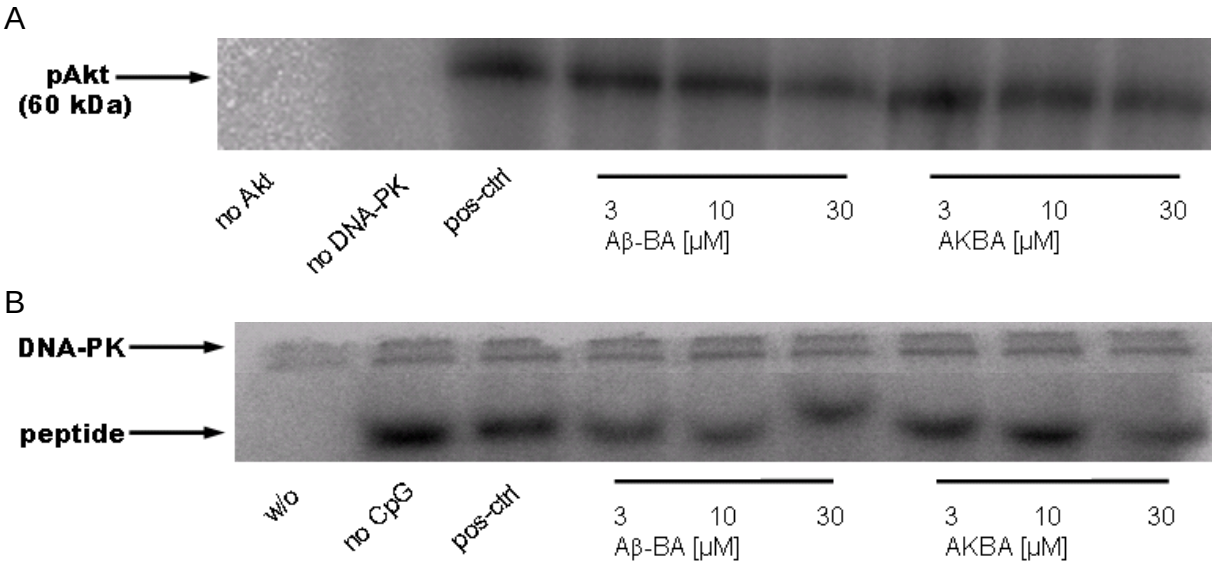

figure 433: Akt-phosphorylation is inhibited in-vitro. DNA-PK (20 U) was incubated for 10 min at 30°C with BAs, CpG-ODN (10 µg/ml), [^{32}P]-ATP (3 µCi) and 100 µg DNA-PK peptide substrate or 600 ng Akt-1 as substrate. Samples were separated as described in the *Methods* section and [^{32}P]-phosphorylated proteins were detected with a radioactivity-sensitive film. (**A**) In-vitro-kinase assay with recombinant Akt-1 and DNA-PK, (**B**) In-vitro-kinase assay with DNA-PK-peptide-substrate (1.75 kDa) and DNA-PK. Gel-loading was controlled with DNA-PK (upper band). Similar results were obtained in at least three additional experiments.

4.3.2 Akt-activity is directly inhibited by boswellic acids

In pulldown experiments with KBA-Seph and isolated recombinant DNA-PK and Akt, only Akt but not DNA-PK was detectable by immunoblotting in the precipitates (**fig. 434**). No Akt was detected in the sample derived from the negative control (Seph precipitates).

To determine the activity of Akt *in vitro*, purified enzyme was incubated with the test compounds and the specific substrate as described in the *Methods* section and fluorescence was quantified. BAs and ursolic acid (10 µM each) potently inhibit Akt-activity. Staurosporine (1 µM) was used as positive control; it inhibits the phosphorylation of substrate in an effective manner (**fig. 435A**). The 11-me-BAs are very potent inhibitors of Akt with an IC_{50} of 300 nM for Aβ-BA and 1 µM for β-BA whereas the 11-keto-BAs are less effective (AKBA 5 µM; KBA 10 µM). Akt inhibition by BAs is concentration-dependent (**fig. 435B**).

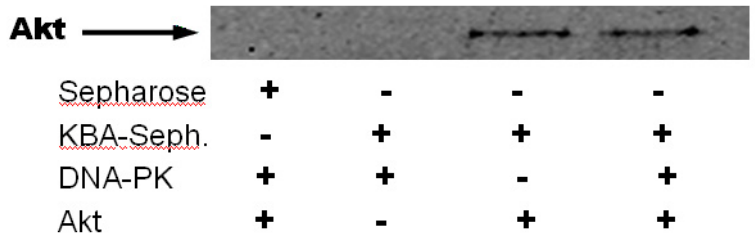

figure 434: Purified enzyme precipitates (Seph and KBA-Seph) analysed by SDS-PAGE and Western-blotting using specific antibodies against Akt (60 kDa). Similar results were obtained in at least three additional experiments.

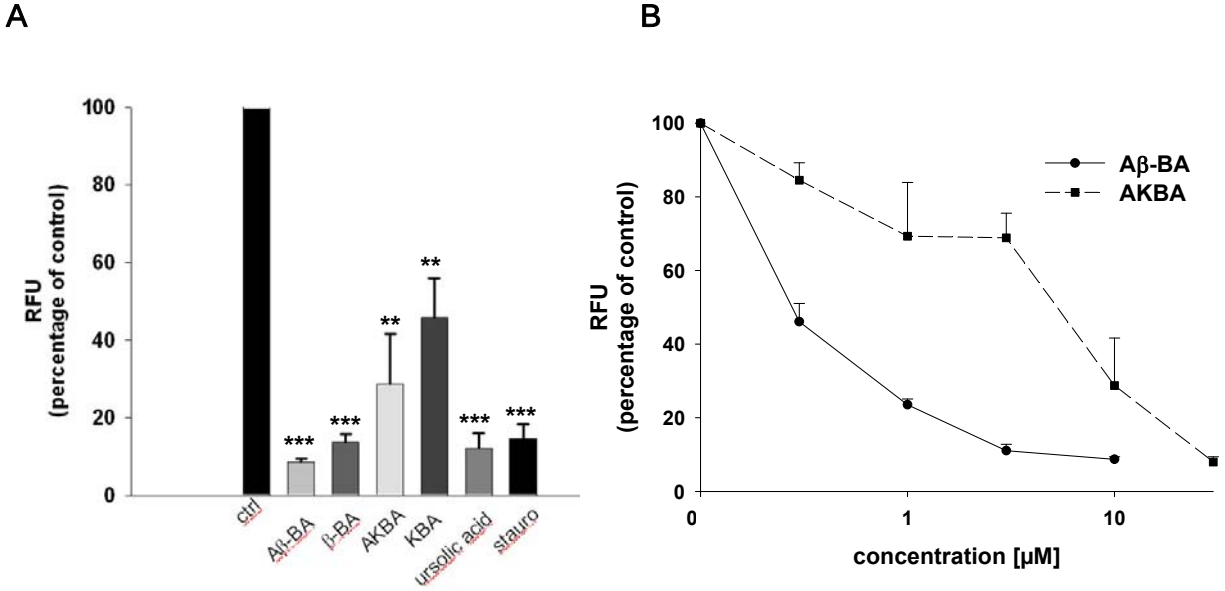

figure 435: BAs inhibit Akt activity in vitro. Purified active Akt enzyme was incubated with the test compounds at RT. After 15 min, eNOS was added as described in *Methods* section and fluorescence of secondary antibodies were detected and quantified with the Odyssey-system. (**A**) Akt inhibition by BAs, ursolic acid (each 10 µM) and staurosporine (stauro 1 µM) as positive control; (**B**) concentration-response curves of Akt inhibition by AKBA and Aβ-BA. Results are shown as mean + s.e.m, n = 5 and analysed by a one-way ANOVA followed by Bonferroni post-hoc test, **p<0.01, ***p<0.001.

4.4 Modulation of signal transduction and functionality of platelets and monocytes by boswellic acids

4.4.1 Modulation of Ca^{2+} mobilization in washed human platelets by boswellic acids.

This study investigates, whether or not BAs, in particular the 11-keto-BAs, may have detrimental actions on agonist-evoked mobilization of intracellular free Ca^{2+}. Thus, thrombin, collagen, platelet-activating factor (PAF) and the stable synthetic thromboxane analogue U-46619 were chosen as relevant platelet agonists [69]. Concentration-response studies in Fura-2-loaded washed human platelets revealed approximate EC_{50} values of these agonists for Ca^{2+} mobilization as follows: 0.5 U/ml thrombin, 8 µg/ml collagen, 100 nM PAF, and 1 µM U-46619 (not shown). These concentrations were used for subsequent analysis of BA effects. Although ADP is known as potent physiological stimulus, it failed to mobilize Ca^{2+} in platelets under our assay conditions.

In the presence of extracellular Ca^{2+} (1 mM), BAs lacking the 11-keto moiety (Aβ-BA and β-BA, 10 mM each) induced a transient but robust elevation of $[Ca^{2+}]_i$ in washed platelets that peaked 18–30 s following exposure, whereas KBA was ineffective and AKBA caused only a weak and rather slow Ca^{2+} mobilization (fig. **441A** and **B**). β-BA was effective already at 3 µM, though not yet significant (**fig. 441A**). At 10 µM, the maximum elicited increase in $[Ca^{2+}]_i$ (381 ± 28 nM) was comparable to that obtained by thrombin (0.5 U/ml; 364 ± 34 nM), and exceeded the signal obtained by PAF (100 nM; 62 ± 5 nM, **fig. 441C**). However, thrombin- and PAF-induced Ca^{2+} mobilization was more rapid, peaking 5–10 s after exposure and (for thrombin) was more sustained. Collagen (8 µg/ml) caused a slow and only moderate elevation of $[Ca^{2+}]_i$ (78 ± 7 nM, after 90 s).

$[Ca^{2+}]_i$ was also measured in the absence of extracellular Ca^{2+} (not shown). BAs as well as thrombin evoked an internal Ca^{2+} release (no extracellular Ca^{2+}) with similar kinetics observed for the total Ca^{2+} response in the presence of extracellular Ca^{2+}, respectively. Nevertheless, in the absence of extracellular Ca^{2+}, elevation of $[Ca^{2+}]_i$ was reduced to about 37 ± 14% for thrombin and 28 ± 17% for β-BA, as compared to the total Ca^{2+} response.

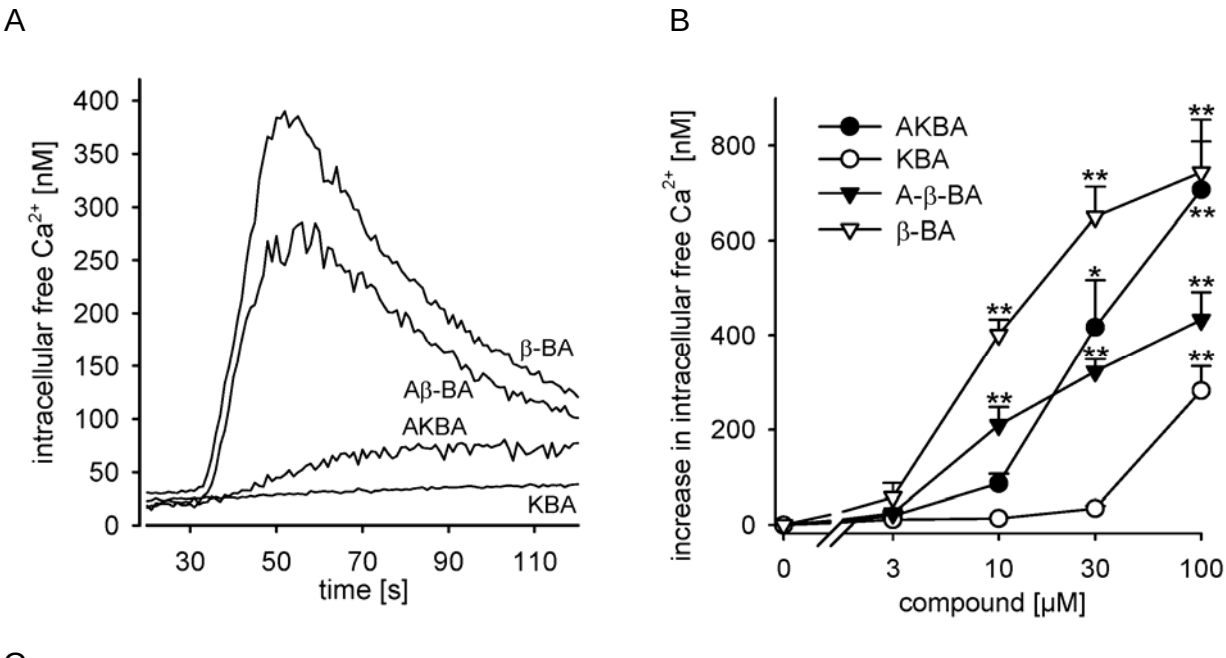

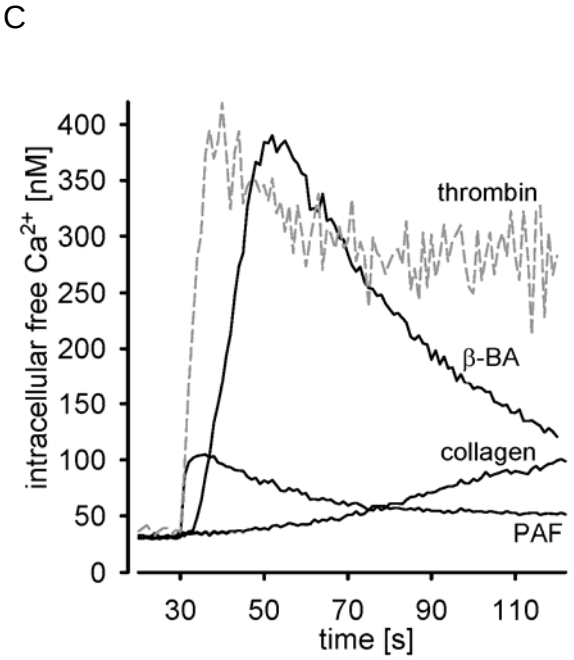

figure 441: BAs induce intracellular Ca^{2+} mobilization. To Fura-2-loaded platelets (10^8 /ml PG buffer), 1 mM $CaCl_2$ was added 2 min prior stimulation, and $[Ca^{2+}]_i$ was determined. (**A**) Ca^{2+} mobilization in the presence of extracellular Ca^{2+}. BAs (10 mM, each) were added 30 s after the measurement was started. (**B**) Concentration–response curves of BAs in the presence of extracellular Ca^{2+}. The maximal increase in $[Ca^{2+}]_i$ obtained within 100 s of measurement is given. (**C**) Ca^{2+} mobilization induced by various agonists. The following agonists were used: β-BA (10 µM), thrombin (0.5 U/ml), collagen (8 µg/ml), and PAF (100 nM). Values are given as mean + s.e.m., n = 5; curves are representative of at least five experiments. One-way ANOVAs followed by Tukey HSD tests were applied to data related to unstimulated controls in (B), *p<0.05 or **p<0.01.

In agreement with previous studies, at a concentration of 10 µM, AKBA (or KBA, not shown) caused only a slight and delayed (and transient) elevation of $[Ca^{2+}]_i$, whereas β-BA and Aβ-BA (10 µM, each) led to substantial Ca^{2+} mobilization (**fig. 441A)**. At higher concentrations (≥ 30 µM), AKBA caused a slow yet continuous increase of $[Ca^{2+}]_i$ (not shown). Interestingly, pre-incubation of platelets for 15 min with AKBA (10 µM) reduced Ca^{2+} mobilization induced by U-46619, PAF and collagen, but not when thrombin was used as agonist (**fig. 442A-D**).

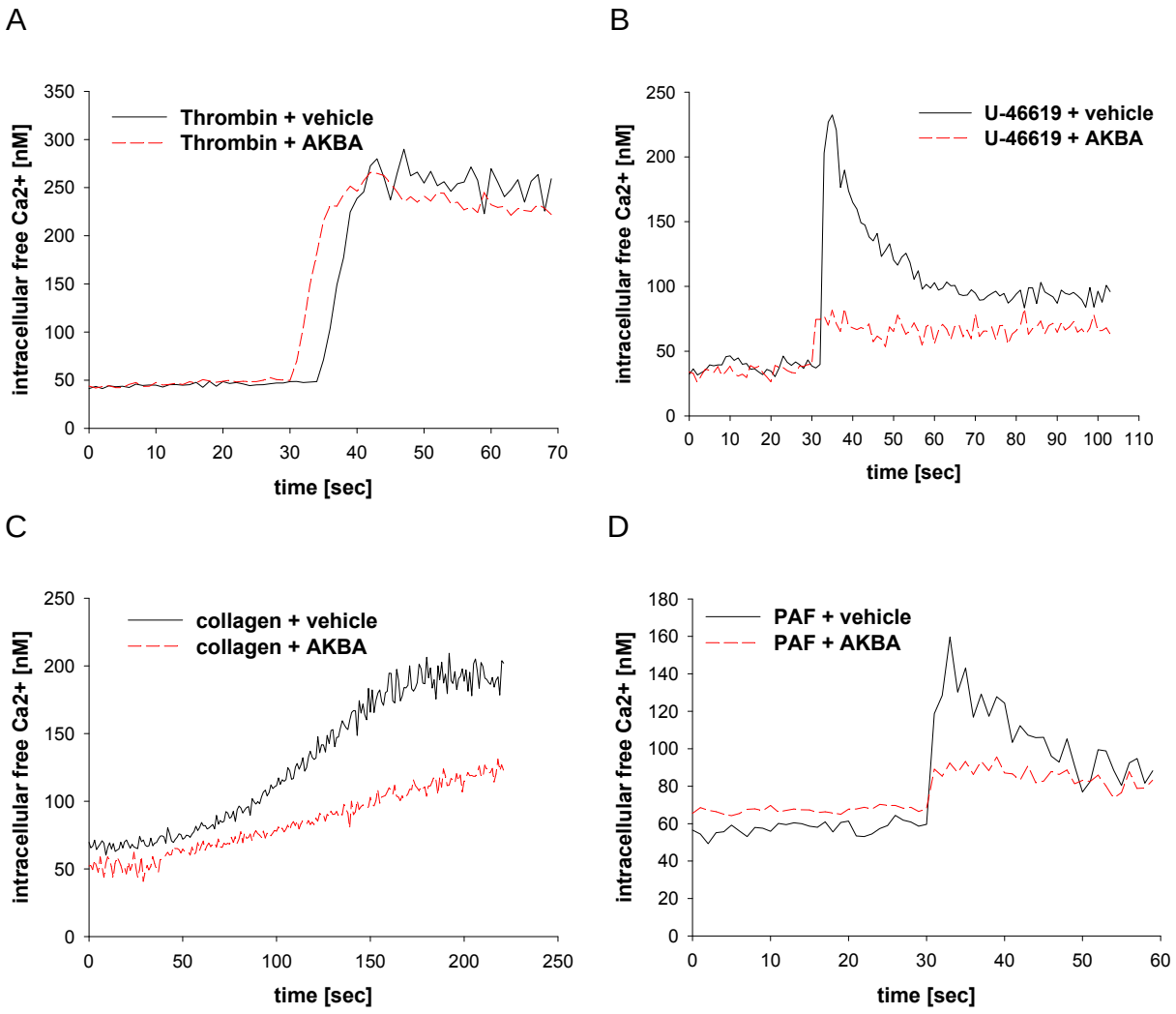

figure 442: Differential effects of boswellic acids on $[Ca^{2+}]_i$ in human washed platelets. Fura-2 loaded platelets (10^8/ml PG buffer) were preincubated with 10 µM AKBA or with vehicle (DMSO) as indicated. After 15 min at 37°C the suspension was supplemented with $CaCl_2$ (1 mM) and the measurement of $[Ca^{2+}]_i$ was started. After 30 s, (**A**) 0.5 U/ml thrombin, (**B**) 1 µM U-46619, (**C**) 8 µg/ml collagen, or (**D**) 100 nM PAF were added. Curves are representative of at least four experiments.

Next, the efficacy of BAs (10 µM, each) to prevent agonist-induced Ca^{2+} mobilization was compared. As shown in **fig. 443**, for platelets stimulated with collagen, PAF or U-46619, AKBA was most efficient to inhibit Ca^{2+} mobilization, followed by β-BA. Aβ-BA was somewhat less potent, whereas KBA even enhanced Ca^{2+} mobilization when compared to AKBA. Notably, all BAs essentially failed to prevent Ca^{2+} mobilization induced by thrombin **(fig. 443A)**. IC_{50} values of AKBA and β-BA for collagen-induced Ca^{2+} mobilization were 3 and 7 µM, respectively, for PAF-induced Ca^{2+} mobilization 2 and 7 µM and for U-46619-induced Ca^{2+} mobilization 5 and 8 µM, respectively (**fig. 444A-D**). When thrombin was used as agonist, the IC_{50} values for AKBA and β-BA were > 30 µM. Pretreatment of platelets with AKBA also prevented the elevation of $[Ca^{2+}]_i$ induced by β-BA similar to that observed for collagen or U-46619.

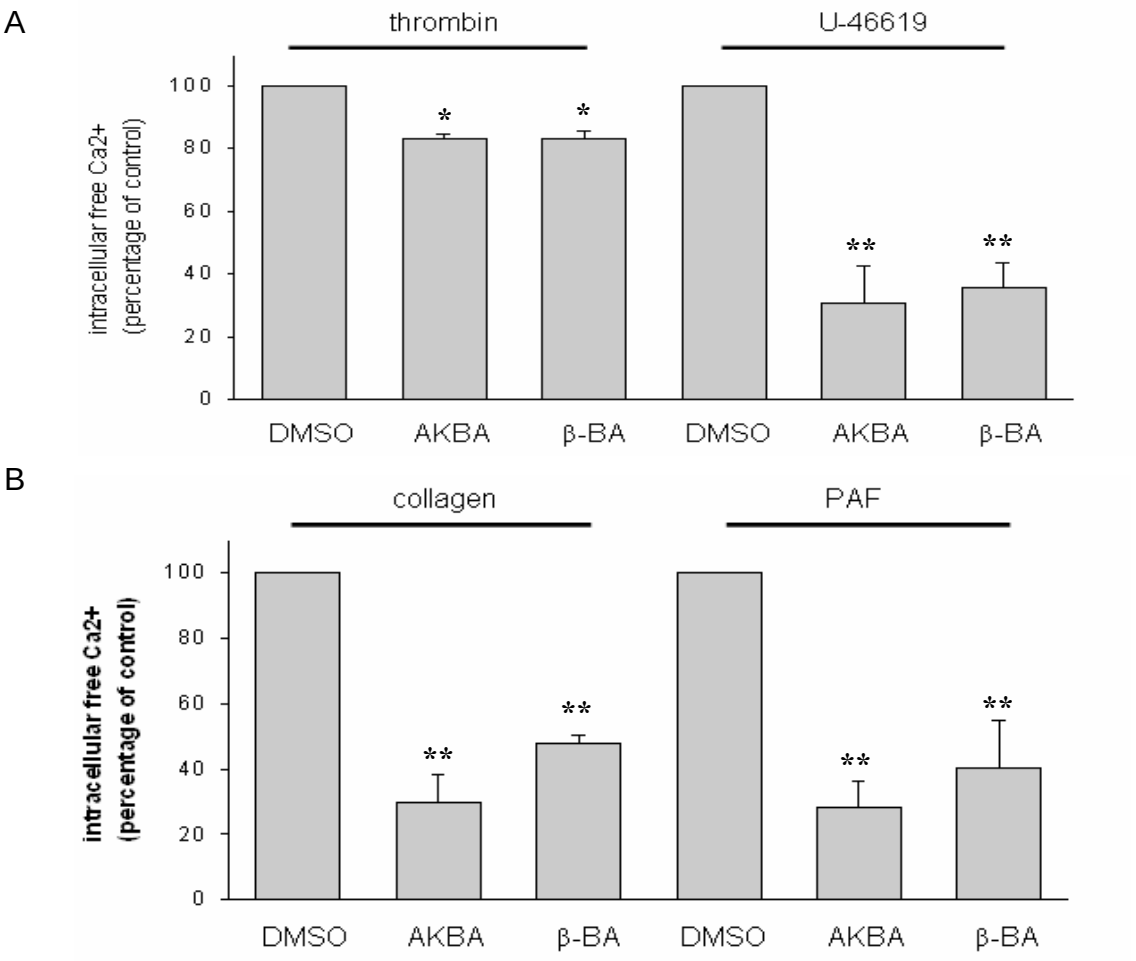

figure 443: Boswellic acids selectively suppress agonist-induced Ca^{2+} mobilization in human washed platelets. Fura-2 loaded platelets (10^8/ml PG buffer) were supplemented with $CaCl_2$ (1 mM) and preincubated with the indicated BAs (10 µM, each) or with vehicle (DMSO, negative control) as indicated. After 15 min at 37°C, the measurement of $[Ca^{2+}]_i$ was started and after another 30 sec, (**A**) 0.5 U/ml thrombin, 1 µM U-46619, (**B**) 8 µg/ml collagen, or 100 nM PAF, were added. The maximal increase in $[Ca^{2+}]_i$ determined within 100 sec of measurement is expressed as percentage of control (DMSO). Values are given as mean + s.e.m., n = 4-6 One-way ANOVAs followed by Tukey HSD tests were applied to data related to unstimulated controls in figs A to D, $p<0.05$ (*) or <0.01 (**)

Since β-BA (≥ 3 µM), and to a minor degree also AKBA (≥ 10 µM), caused a transient elevation of $[Ca^{2+}]_i$ returning to baseline after about 5 to 7 min [67], it appeared possible that such an unspecific increase in $[Ca^{2+}]_i$ leading to desensitized platelets could be the reason for the subsequent failure of Ca^{2+} mobilization upon addition of other agonists. Accordingly, U-46619 which causes a transient Ca^{2+} mobilization similar to that observed for 11-methylene-BAs, was first added to platelets and after 15 min, platelets were stimulated with either collagen or thrombin. In contrast to 11-methylene-BAs, preincubation with U-46619 failed to substantially suppress elevation of $[Ca^{2+}]_i$ evoked by either collagen or thrombin, although a slight reduction of the signals was detected. Taken together, depending on the structure (e.g. the presence of the 11-keto- and 3-O-acetyl group), BAs differentially modulate Ca^{2+} mobilization in platelets which is further influenced by the nature of the platelet agonist.

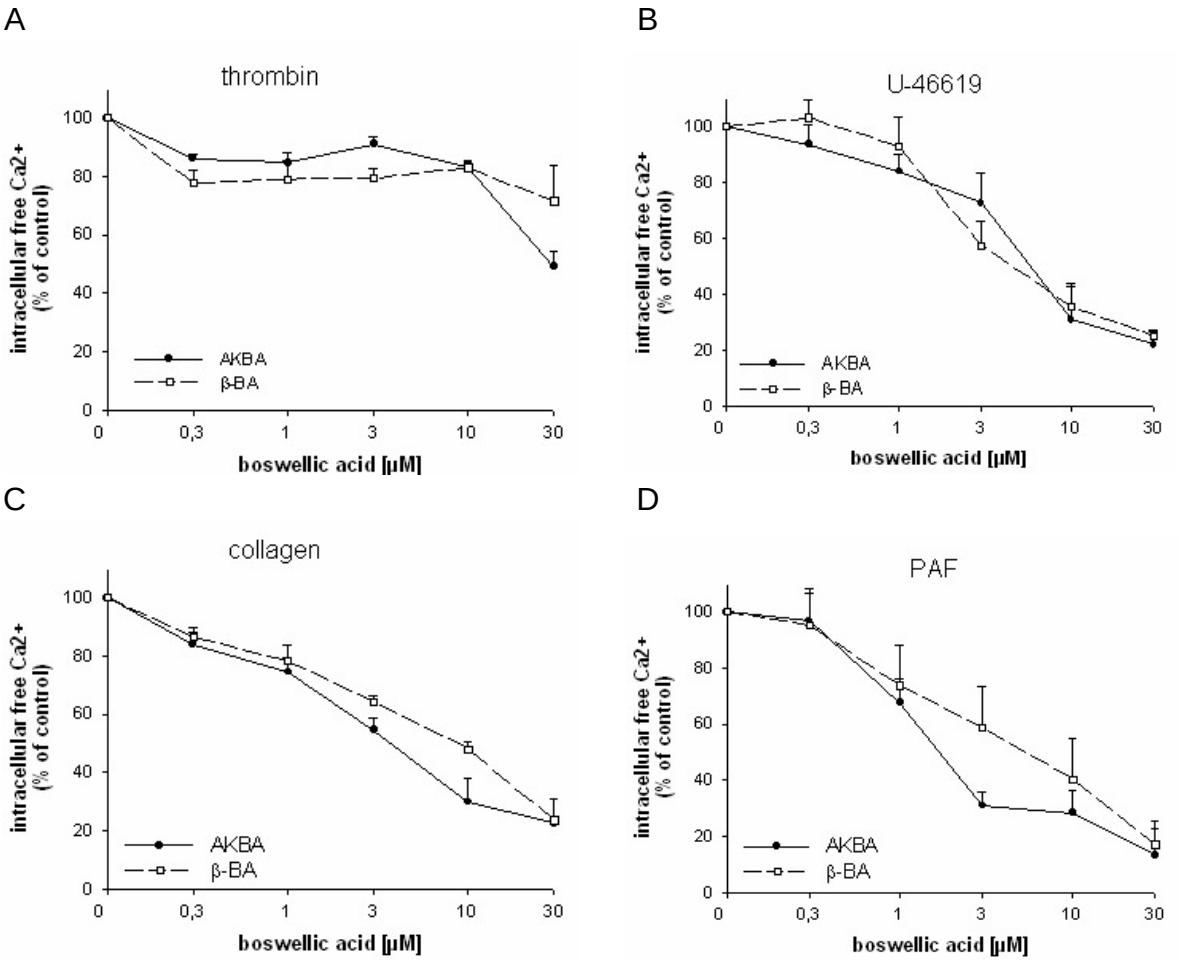

figure 444: Concentration-response curves for AKBA and β-BA. Fura-2 loaded platelets (10^8/ml PG buffer, supplemented with 1 mM $CaCl_2$) were preincubated with the indicated concentrations of AKBA or β-BA and after 15 min at 37°C, the measurement of $[Ca^{2+}]_i$ was started. After 30 s, (**A**) 0.5 U/ml thrombin, (**B**) 1 µM U-46619, (**C**) 8 µg/ml collagen, or (**D**) 100nM PAF were added and the maximal increase in $[Ca^{2+}]_i$ was determined within 100 s, expressed as percentage of control (DMSO). Values are given as mean + s.e.m., n = 4-5.

4.4.2 Src family kinases are involved in β-BA-induced Ca^{2+} mobilization

The role of Src family kinases in β-BA-induced Ca^{2+} mobilization was assessed using the selective Src family kinase inhibitors PP2 (and its inactive analogue PP3) [142] and SU6656 [143]. PP2 (3 μM) blunted the Ca^{2+} response initiated by β-BA (92 ± 2% inhibition, n = 7, **fig. 445**), whereas the inactive analogue PP3 (3 μM) was hardly effective (89 ± 8% residual activity, n = 4, **fig. 445**). In addition, the structurally unrelated Src kinase inhibitor SU6656 (10 μM) also abolished the β-BA signal (93 ± 1% inhibition, n=4, **fig. 445**). In sharp contrast, no such inhibitory effects of PP2 on Ca^{2+} signals induced by thrombin, PAF, or AKBA were apparent (not shown).

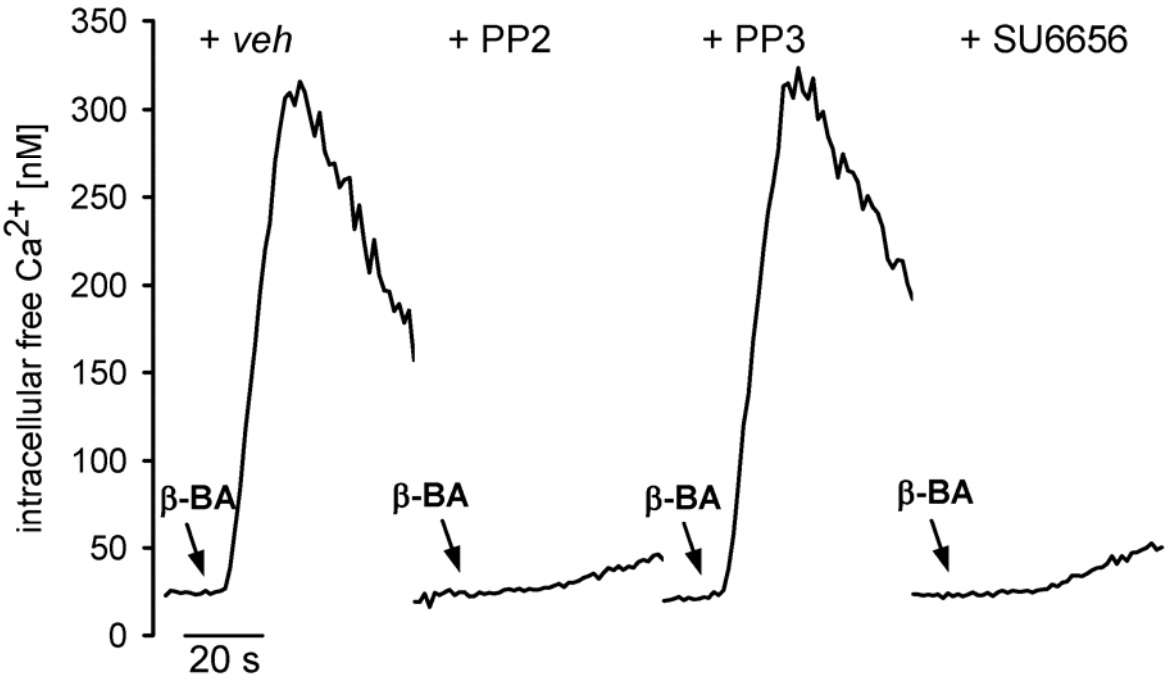

figure 445: Effects of Src family kinase inhibitors. Fura-2-loaded platelets (10^8 /ml PG buffer) were preincubated with PP2 (3 μM), PP3 (3 μM), SU6656 (10 μM), or vehicle (DMSO) for 15 min. $CaCl_2$ (1mM) and β-BA (10 μM) were added, and $[Ca^{2+}]_i$ was determined. Curves are representative of at least four experiments.

4.4.3 BAs and modulation of thrombin generation and expression of activation markers

β-BA was tested for its ability to generate thrombin from PRP, expressed as the endogen thrombin potential (ETP). β-BA (10 μM) potently stimulated thrombin generation, whereas AKBA (10 μM) was inactive (**fig. 446A**, **left panel**). Although collagen was only moderately superior to β-BA in the peak thrombin generation velocity, there was again a delayed onset of the β-BA effect, visualized by the kinetic progression of the ETP (**fig. 446B**). In the absence of Ca^{2+}, neither stimulus induced a marked increase in the ETP over time although analysis of the ETP-AUCs revealed a slight stimulatory effect of β-BA (10 μM) as compared to DMSO and collagen that both were inactive (**fig. 446A, right panel**).

Finally, the expression of the activation markers PAC-1 (the activated GPIIb/IIIa-receptor for fibrinogen) and CD62, which indicates the release of platelet alpha-granules, were assessed. Incubations were carried out in (I) whole blood (containing 3.13% citrate), (II) recalcified PRP, and (III) washed platelets in Ca^{2+}-containing PGC buffer, for 2 or 15 min. Neither β-BA (30 or 100μM) nor AKBA (30 μM) led to a significant expression of CD62 and PAC-1 under all experimental settings (I–III), whereas TRAP (used as positive control) was a strong activator (**fig. 446C**).

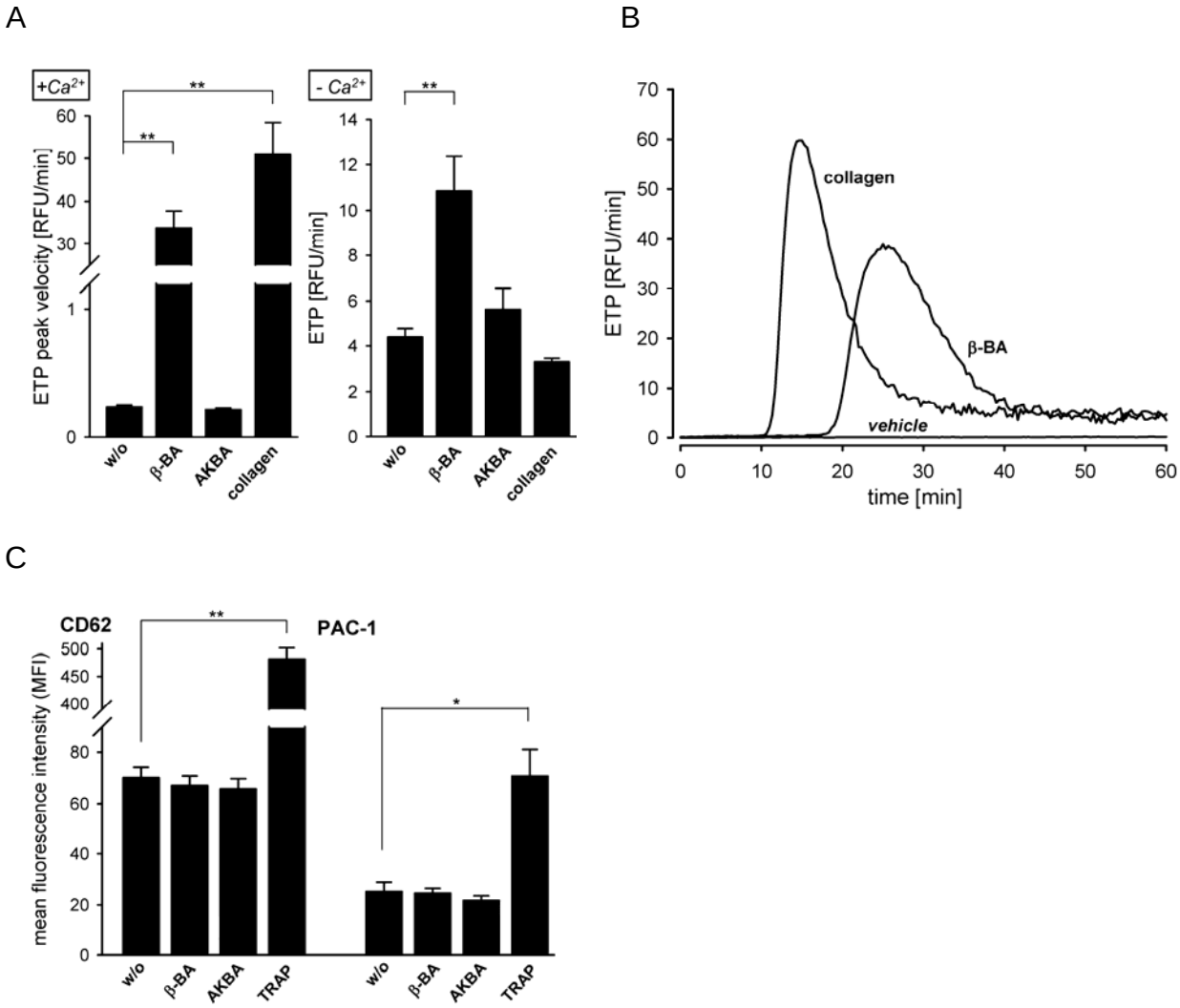

figure 446:Thrombin generation and activation marker expression. (**A**) Thrombin generation was assessed in recalcified PRP (given as ETP peak velocity, left bar chart), or citrate-chelated PRP (given as ETP-AUC, right bar chart). PRP and buffer containing the indicated stimuli were added to each well of a 96-well microtitre plate. β-BA (10 µM), AKBA (10 µM), collagen (2 µg/ml, final concentrations each), and vehicle (DMSO) were tested for their ability to induce thrombin generation. Data are expressed as mean + s.e.m., n = 4 (β-BA, AKBA, collagen) or n=8 (vehicle). One-way ANOVA and Tukey HSD tests were performed, **p<0.01. (**B**) Representative original traces of the ETP kinetic progression. Cells in recalcified PRP were stimulated as described above. (**C**) Expression of the platelet activation markers CD62 and PAC-1. Flow cytometry in recalcified PRP was performed as described in the *Methods* section. Expression of CD62 (left bar chart) and PAC-1 (right bar chart) after stimulation with vehicle (DMSO), β-BA (30 µM), AKBA (30 µM), or TRAP (10 µM) is given. The percentage of CD62-positive cells (%) as well as their mean channel fluorescence intensity (MFI) was determined (left diagram). Right, a histogram of PAC1-FITC against cell events was generated and MFI of total platelet population was recorded, n = 4. One-way ANOVA and Tukey HSD tests were performed, *p<0.05 or **p<0.01.

4.4.4 β-BA induces aracidonic acid release in human platelets

An elevation of $[Ca^{2+}]_i$ and/or activation of members of the MAPK family are considered important for the liberation of AA by the $cPLA_2$ [144]. In platelets AA is the substrate of COX 1 and platelet-type 12-LO. AA-metabolism by COX and 12-LO leads to prostaglandins, 12-HETE and other signal molecules in atherosclerosis and inflammation. On the other hand, AA is an important component of the lipid bilayer responsible for the fluidity of the cell membrane. Incubation of [^{3}H]-AA-labelled platelets with β-BA caused a concentration-dependent increase in the amounts of [^{3}H]-AA released into the medium. At about 50 µM, β-BA was equipotent to 2 U/ml thrombin (**fig.447**).

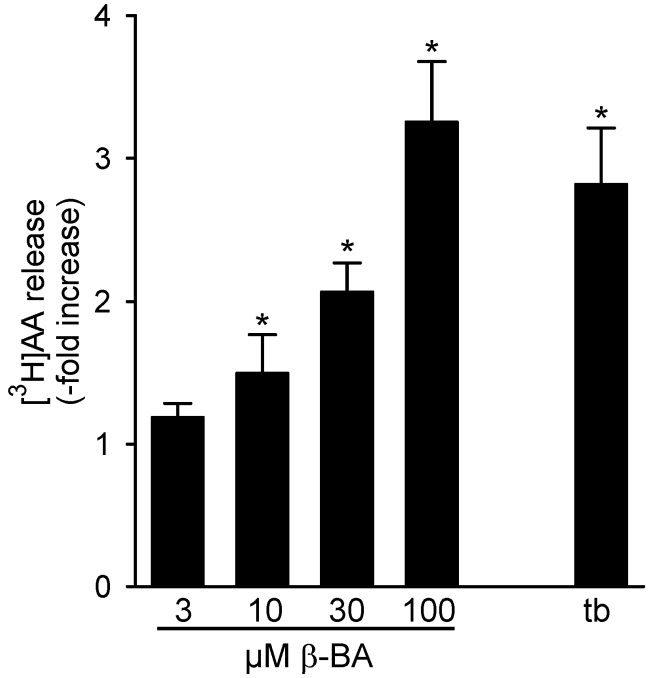

figure 447: β-BA induces the release of AA. Platelets were labelled with [^{3}H]-AA for 2 h. $CaCl_2$ (1 mM) was added to the cells (10^8 in 1ml PG buffer), and after 2.5 min, cells were stimulated with the indicated concentrations of β-BA or 2 U/ml thrombin (tb). [^{3}H]-AA released into the medium was measured after 5 min at 37°C. Data are expressed as increase over unstimulated cells, values are given as mean + s.e.m., n = 5. Statistical analysis (directed t-tests for correlated samples) was applied to original data prior to normalisation, *$p<0.05$.

4.4.5 AKBA attenuates agonist-induced elevation of $[Ca^{2+}]_i$ in MM6

The attempt was made to investigate whether or not AKBA could also prevent agonist-induced elevations of $[Ca^{2+}]_i$ in monocytes. Agents that elevate $[Ca^{2+}]_i$ involving PLC/IP3 signalling (e.g. PAF, fMLP and *m*-3M3FBS) but also stimuli that raise $[Ca^{2+}]_i$ independent of the PLC/IP3 pathway like ionomycin were added to MM6 cells that received BAs, 20 s prior to agonist addition. As shown in **fig. 448**, AKBA, but not Aβ–BA, potently inhibited the subsequent Ca^{2+} mobilization induced by PAF or fMLP as well as by the direct PLC activator *m*-3M3FBS [145]. The IC_{50} value for AKBA was in the range of 10 – 30 µM, depending on the stimulus. In contrast, initial elevation of $[Ca^{2+}]_i$ induced by the ER/SR Ca^{2+}- ATPase inhibitor thapsigargin (TG) or by the Ca^{2+}-ionophore ionomycin were not affected (not shown).

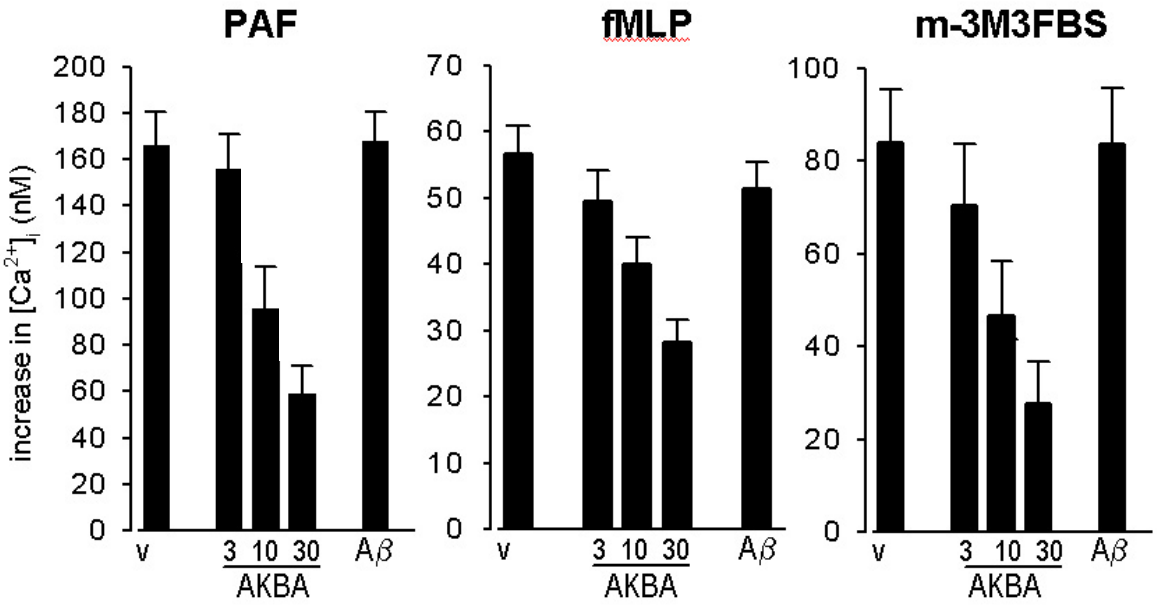

figure 448: AKBA antagonizes agonist-induced Ca^{2+} mobilization. Fura-2 loaded MM6 cells ($3x10^6$/ml PG buffer, supplemented with 1 mM $CaCl_2$) were treated with vehicle (v), AKBA (3, 10, 30 µM), or Aβ-BA (Aβ, 30 µM) followed by the addition of PAF (0.1 µM), fMLP (0.1 µM), or *m*-3M3FBS (50 µM) after 20 s as indicated. The amplitude of the agonist-induced elevation of $[Ca^{2+}]_i$ was determined. Values are given as mean + s.e.m., n = 4 - 5, and compared to the positive controls.

4.4.6 AKBA attenuates Ca^{2+} mobilization from intracellular stores in monocytic cells.

Next, the test was carried out to investigate wether or not AKBA may also affect the PAF-induced release of Ca^{2+} from intracellular stores, a process that is typically PLC/IP3-dependent. MM6 cells were resuspended in Ca^{2+}-free buffer containing 1 mM EDTA and treated with AKBA or Aβ-BA, followed by the addition of PAF after another 20 s. Neither AKBA nor Aβ–BA exhibited an effect on basal $[Ca^{2+}]_i$ in resting cells under these conditions. However, AKBA reduced the release of Ca^{2+} from internal stores elicited by PAF (**fig. 449B** left panel), although slightly higher concentrations of AKBA were required as compared to those needed to suppress total Ca^{2+} mobilization in the presence of extracellular Ca^2panel) was also partially antagonised by AKBA, implying that PLC inhibition may not be the sole mechanism by which AKBA affects $[Ca^{2+}]_i$, since TG-mediated Ca^{2+} mobilization circumvents the PLC/IP3 route.

A

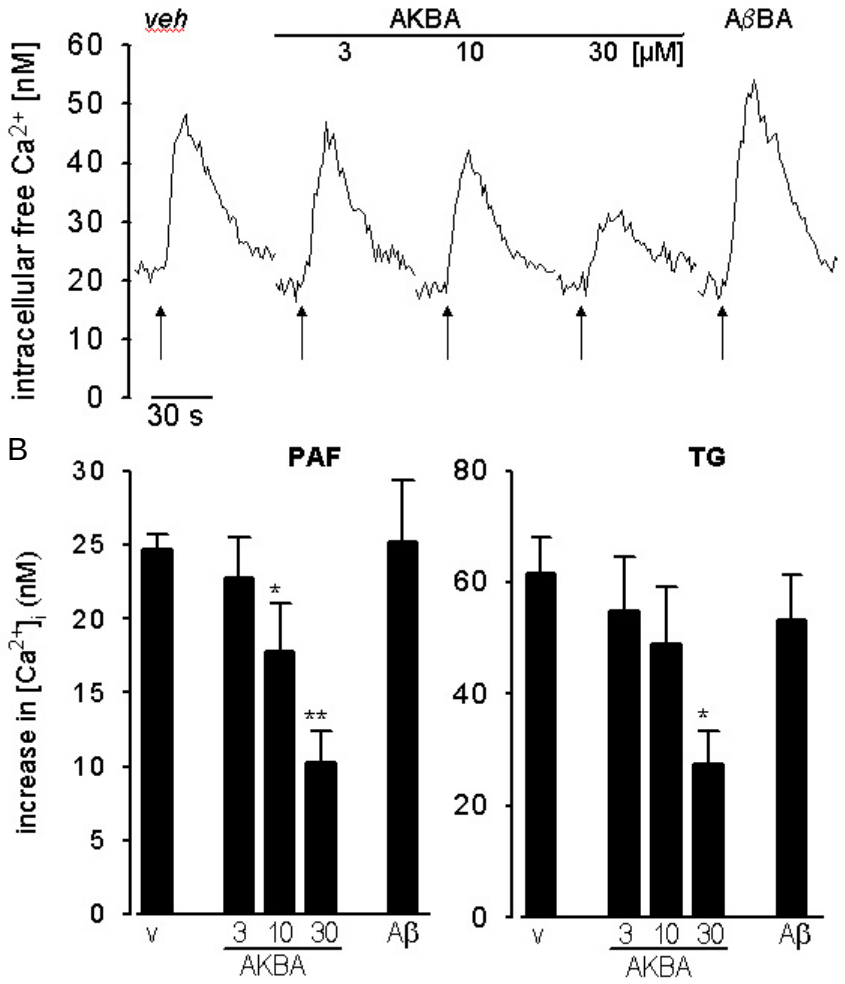

figure 449: Effects of BAs on Ca^{2+} release from internal stores. MM6 cells were prepared as described in fig. 448, except that 1 mM EDTA was added instead of 1 mM Ca^{2+}. (**A**) Original $[Ca^{2+}]_i$ recordings of samples stimulated by PAF (0.1 µM) after preincubation with vehicle (veh), AKBA (3, 10, 30 µM), or Aβ-BA (30 µM) for 20 s. Curves are representative of 3 - 4 independent determinations. (**B**) Cells were treated with vehicle (v), AKBA (3, 10, 30 µM), or Aβ-BA (Aβ, 30 µM) followed by the addition of PAF (0.1 µM, left panel), or thapsigargin (TG, 0.1 µM, right panel). The amplitude of the stimulus-induced elevation of $[Ca^{2+}]_i$ was determined. Values are given as mean + s.e.m., n = 4, $p<0.05$ (*) or <0.01 (**).

4.4.7 Effects of boswellic acids on TNFα-release in MM6 cells

Macrophages and monocytes are considered to be the main source of TNFα [146], which as a prototypical proinflammatory cytokine, plays a key role not only in chronic inflammatory diseases but also in innate immunity [147]. To investigate whether Aβ-BA or AKBA are able to affect the TNFα generation in fMLP- and in LPS-stimulated MM6 cells (**fig. 4410**). TNFα is synthesized as a precursor, which is processed and released from the membrane [148], implying that regulation can occur at any of those steps. Unstimulated cells did not release detectable amounts of TNFα. AKBA and Aβ-BA (10 µM each) slightly inhibit fMLP- or LPS-induced TNFα-release.

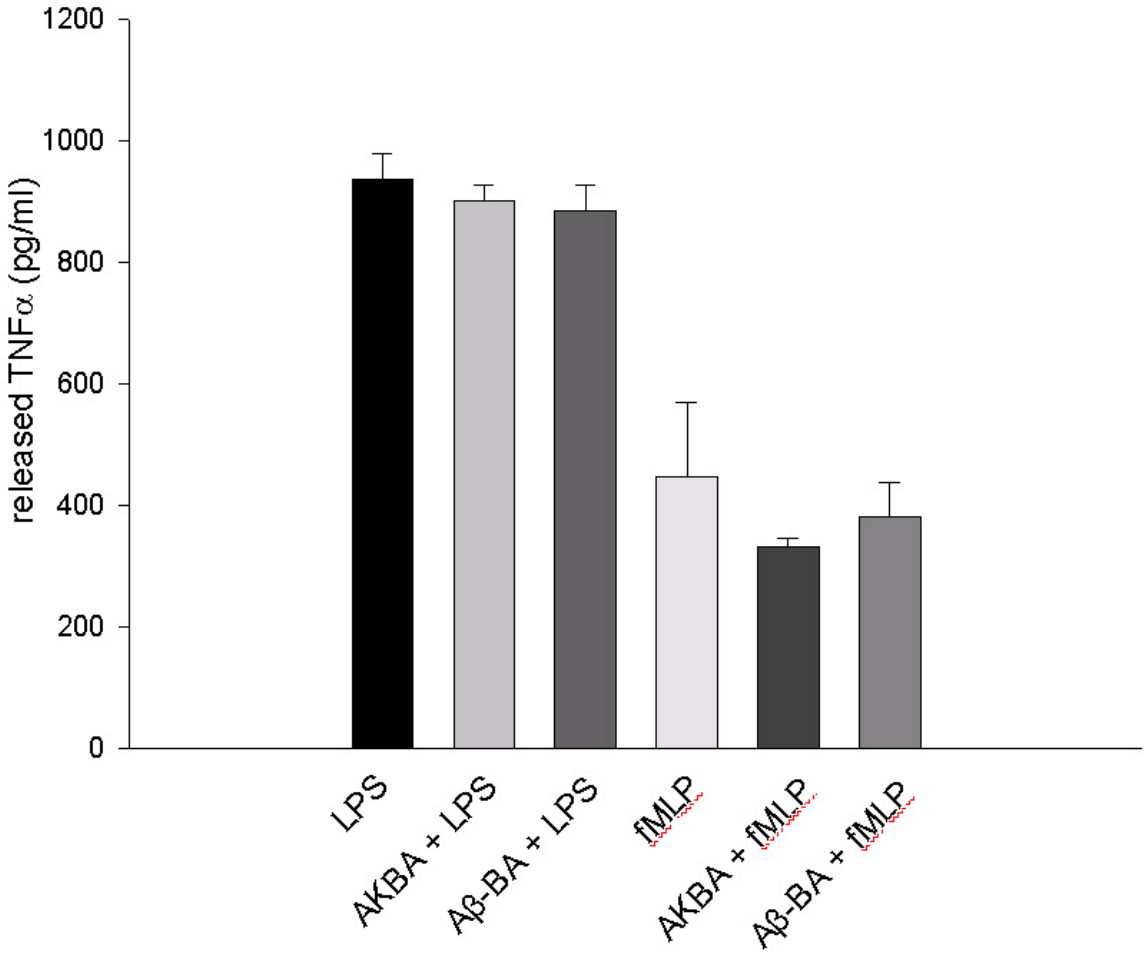

figure 4410: Effects of BAs on TNFα-release in MM6 cells. 3 x 10^6 MM6 cells were preincubated with AKBA or Aβ-BA (10 µM each) for 1 h and then stimulated with either LPS 50 ng/ml or fMLP 1 µM. Supernatants were tested by ELISA for TNFα as described in the methods section. Results are given as mean + s.e.m., n = 3.

4.4.8 Suppression of agonist-evoked Ca^{2+} mobilization in PMNL and HL-60 cells by boswellic acids

The influence of BAs on Ca^{2+}-influx in agonist stimulated PMNL and HL-60 was investigated. The following agents were used: PAF, LTB_4, 5-HETE and fMLP for PMNL (**fig. 4411A-D**) and PAF for the leukemic cell line HL-60 (**fig. 4411E**). Preincubation with AKBA results in a concentration-dependent inhibition of agonist-evoked Ca^{2+}-influx (**fig. 4411**), the IC_{50} values were determined at 5 to 15 µM. AKBA is the most potent boswellic acid, 11-methylene BAs are less effective and KBA is even inactive (not shown).

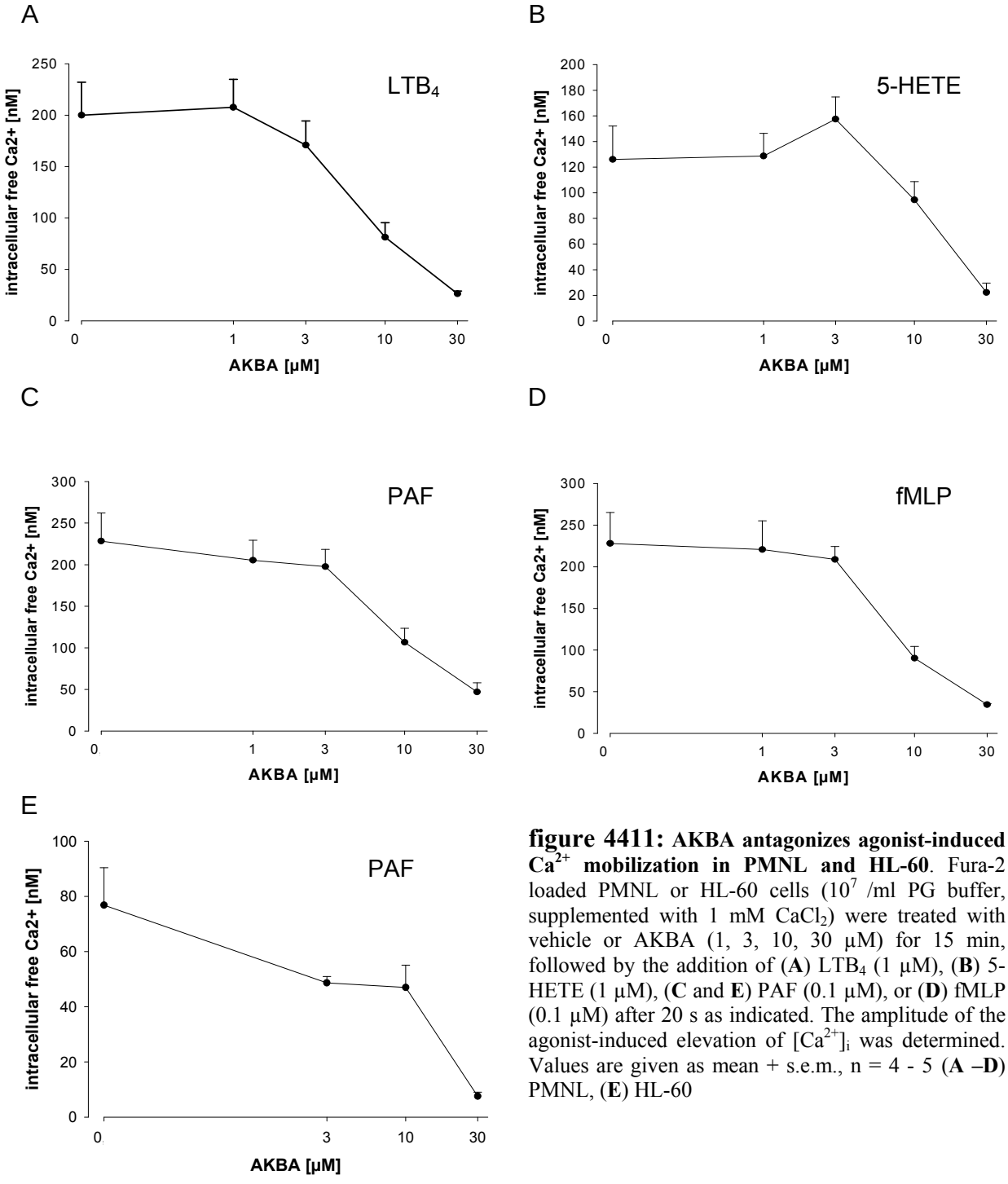

figure 4411: AKBA antagonizes agonist-induced Ca^{2+} mobilization in PMNL and HL-60. Fura-2 loaded PMNL or HL-60 cells (10^7 /ml PG buffer, supplemented with 1 mM $CaCl_2$) were treated with vehicle or AKBA (1, 3, 10, 30 µM) for 15 min, followed by the addition of (**A**) LTB_4 (1 µM), (**B**) 5-HETE (1 µM), (**C** and **E**) PAF (0.1 µM), or (**D**) fMLP (0.1 µM) after 20 s as indicated. The amplitude of the agonist-induced elevation of $[Ca^{2+}]_i$ was determined. Values are given as mean + s.e.m., n = 4 - 5 (**A –D**) PMNL, (**E**) HL-60

4.4.9 Suppression of agonist-evoked aggregation of washed human platelets by boswellic acids

Rapid and pronounced elevation of $[Ca^{2+}]_i$ in platelets is a determinant for platelet aggregation in response to various stimuli [69, 149]. Recently, β-BA (10 to 30 µM) strongly elevates $[Ca^{2+}]_i$ in platelets also causes platelet aggregation, although moderately and in a delayed manner, whereas in contrast AKBA was barely active even at high concentrations (30 µM). Since AKBA potently prevented the elevation of Ca^{2+} in platelets stimulated by collagen and U-46619 at rather low effective concentrations (≤ 3 µM), it seemed reasonable that keto-BAs could inhibit aggregation induced by these agonists in a similar manner. First, the capacity of selected agonists and BAs themselves were analyzed for their ability to induce aggregation of washed platelets. As shown in **fig. 4412A**, collagen, thrombin and U-46619 caused marked aggregation of platelets within seconds or a few minutes. Differential effects for the BAs were observed: Whereas both 11-methylene BAs at 30 µM efficiently induced platelet aggregation, the 11-keto-BAs AKBA as well as KBA (30 µM, each) failed in this respect (**fig. 4412B**).

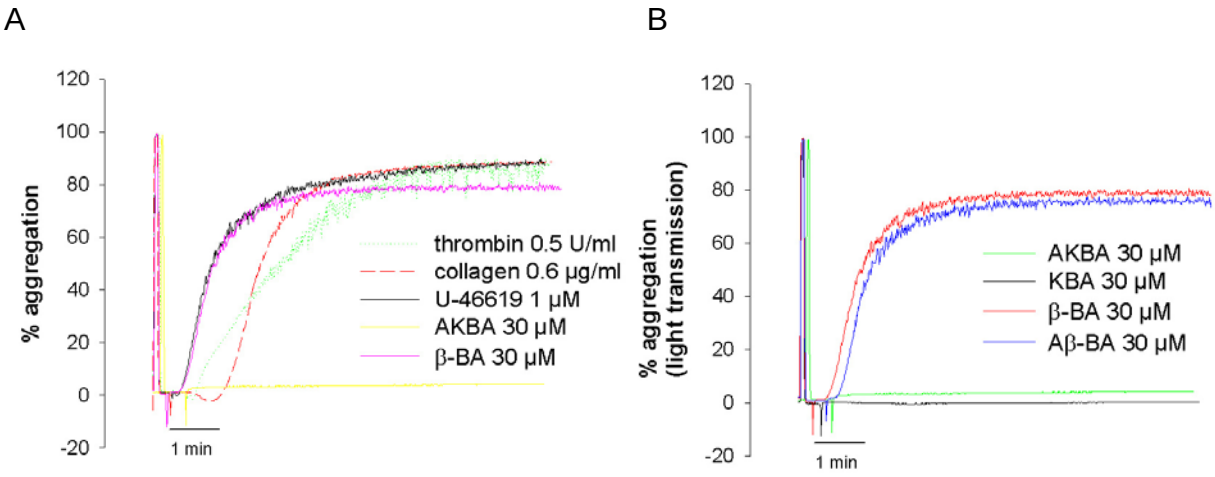

figure 4412: Aggregation of human platelets. To 500µl of prewarmed recalcified washed platelets (1mM $CaCl_2$) the indicated agents were added and aggregation was recorded for 7 min. (**A**) Aggregation induced by various stimuli; (**B**) BAs induced aggregation.

Next, washed platelets were preincubated with BAs (3 µM, each) for 15 min and subsequently stimulated with collagen, thrombin, and U-46619 and aggregation was analyzed. Among the four BAs, only AKBA potently suppressed collagen-induced aggregation (**fig. 4413B**). In contrast, thrombin-evoked aggregation was not prevented by AKBA (up to 30 µM) or any other BA (not shown). This is of interest since U-46619-induced aggregation AKBA was hardly efficient and KBA did not inhibit the effect of U-46619 (**fig. 4413A**). Detailed concentration-response studies showed that AKBA prevented platelet aggregation induced by collagen with an IC_{50} value of 1.1 µM, whereas for U-46619 the IC_{50} value was approximated at 25 µM (**fig. 4413C**). Despite the robust inhibition of collagen-induced aggregation by AKBA, only a moderate effect was measured with KBA (IC_{50} = 10 µM). Apparently, the 3-*O*-acetyl group and the 11-keto moiety present in AKBA render this β-configurated BA a potent inhibitor of collagen-evoked platelet aggregation, implying that defined structure-activity relationships exist excluding unspecific effects of AKBA.

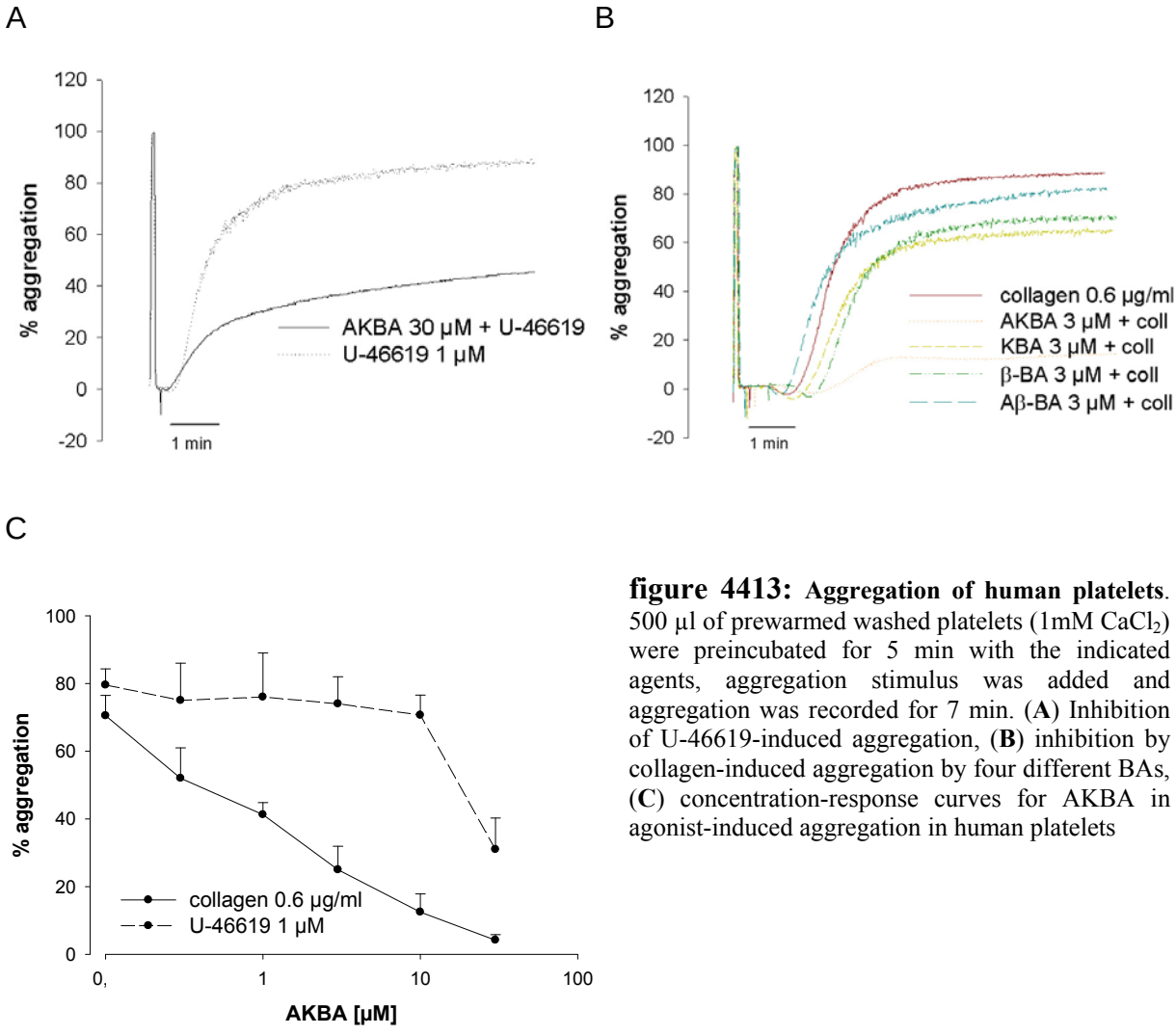

figure 4413: Aggregation of human platelets. 500 µl of prewarmed washed platelets (1mM $CaCl_2$) were preincubated for 5 min with the indicated agents, aggregation stimulus was added and aggregation was recorded for 7 min. (**A**) Inhibition of U-46619-induced aggregation, (**B**) inhibition by collagen-induced aggregation by four different BAs, (**C**) concentration-response curves for AKBA in agonist-induced aggregation in human platelets

4.5 Celecoxib

4.5.1 Suppression of 5-LO product formation in human whole blood

To investigate the effects of COX-2-selective inhibitors on eicosanoid formation, a human whole blood assay using Ca^{2+}-ionophore A23187 as stimulus was applied, equipped with a highly sensitive LC/MS-MS methodology capable of selectively detecting a broad number of eicosanoids [140]. Celecoxib but no other COX-2 inhibitor (up to 100 μM) concentration-dependently inhibited the formation of the 5-LO products LTB_4 and 5-HETE with IC_{50} values ≈ 30.9 and 42.3 μM, respectively **(fig. 451 A** and **B)**. Zileuton, a well-known iron-ligand inhibitor of 5-LO [150] used as positive control, caused significant reduction of LTB_4 and 5-HETE already at 1 μM. All COX inhibitors reduced PGE_2 formation with diclofenac and celecoxib showing the highest efficacy (**fig. 451 C**). Interestingly, celecoxib failed to significantly suppress the levels of 12(S)-HETE (**fig. 451D**), and the formation of 15(S)-HETE (**fig. 451E**) was only slightly decreased (IC_{50} > 100 μM). Therefore, besides inhibition of PGE_2 synthesis, celecoxib has the unique property among COX inhibitors tested to suppress the formation of 5-LO products[151]. This work was done in collaboration with Dr. T.J. Maier.

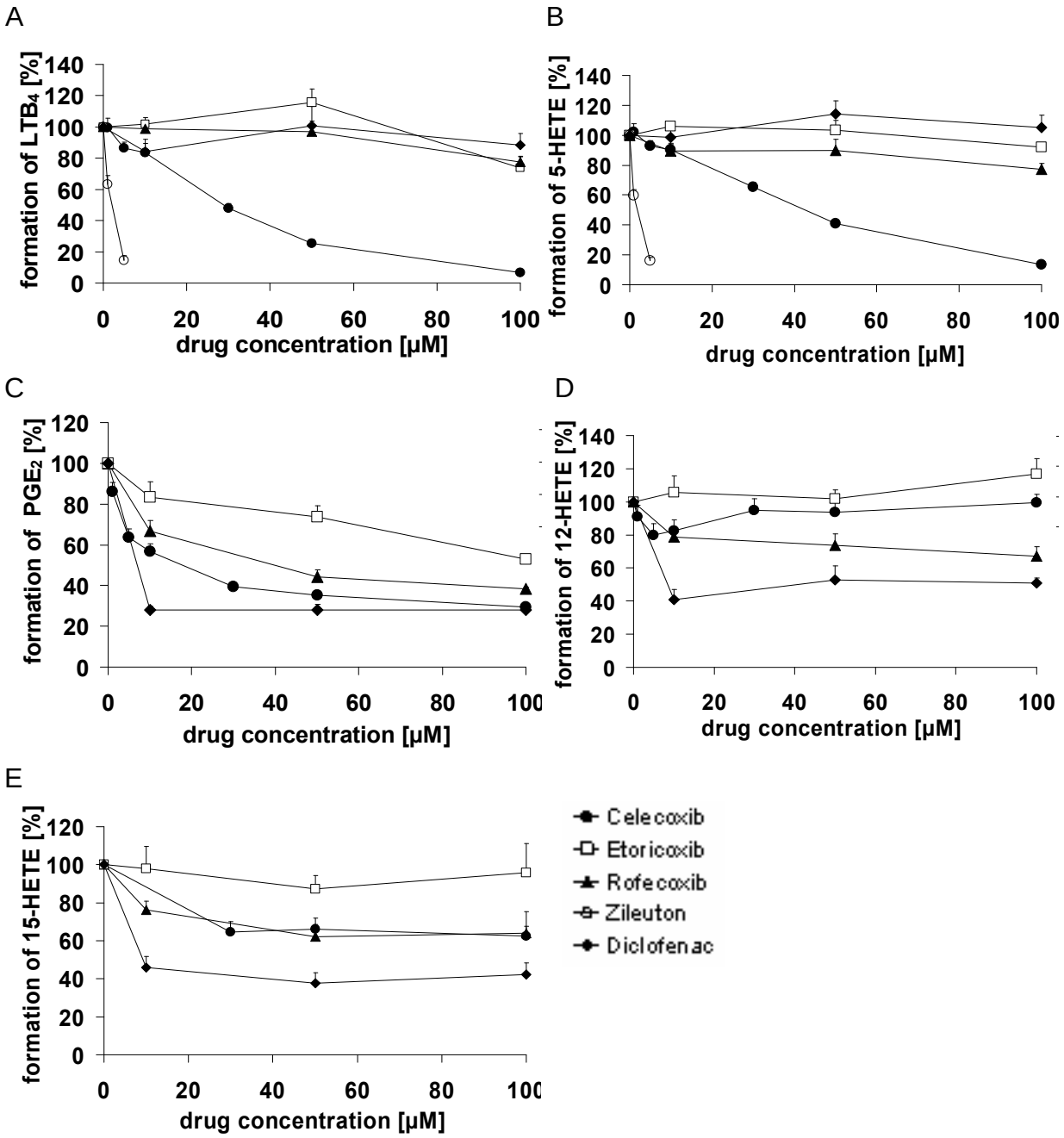

figure 451: Effects of COX inhibitors on eicosanoid formation in human whole blood. The experimental procedure is described in *Methods.* The eicosanoids in the plasma supernatant analyzed by LC/MS-MS were LTB_4 (**A**), 5-HETE (**B**), PGE_2 (**C**), 12(S)-HETE (**D**) and 15(S)-HETE (**E**). For LTB_4, 5-HETE and 12(S)-HETE data are given as mean + s.e.m. of 8 (celecoxib and zileuton; n = 14-26 values), 4 (etoricoxib, rofecoxib; n = 11-13 values) and 2 (diclofenac; n = 6 values) independent experiments. For PGE_2 and 15-HETE data are given as mean + s.e.m. of ≥ 4 (celecoxib, n = 12-15 values) or ≥ 2 (rofecoxib, etoricoxib, diclofenac, n = 5-6 values) independent experiments.

4.5.2 Inhibition of 5-LO product formation in activated human PMNL

The efficacy of celecoxib was assessed in A23187-stimulated human PMNL, a frequently used model for evaluation of 5-LO inhibitors [152]. Pretreatment (10 min) of PMNL with celecoxib caused a concentration-dependent inhibition of 5-LO product formation with an $IC_{50} \approx 8.4$ µM (**fig. 452A**). To exclude effects of celecoxib on the availability of endogenous AA as substrate and consequently circumvent $cPLA_2$ activity, exogenous AA (2, 10, or 20 µM) was provided. No alteration in the efficacy of celecoxib on 5-LO product formation was observed. Data are shown in **fig. 452A** for incubations with 20 µM AA ($IC_{50} \approx 7.0$ µM) and without AA. In agreement with the results obtained from whole blood assays, other coxibs (i.e. etoricoxib and rofecoxib) as well as the unselective COX-inhibitor diclofenac (up to 30 µM, each), showed no or only weak inhibition of 5-LO activity in A23187-activated PMNL, irrespective of the presence of exogenous AA (**fig. 452B**). BWA4C, a potent 5-LO inhibitor, structurally related to zileuton, was used as positive control. In summary, only celecoxib among various COX inhibitors suppresses 5-LO product synthesis in activated intact human PMNL.

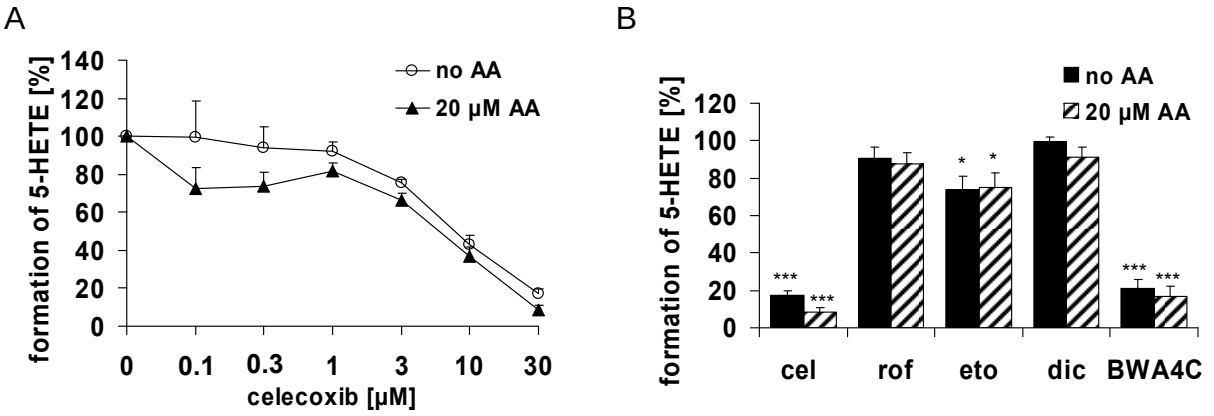

figure 452: (**A**) Inhibition of 5-LO product formation in intact PMNL by celecoxib. 5-LO activity in absence or presence of AA (20 µM) was assayed as described in *Methods* and expressed as percentage compared to vehicle control (100 %). Results are mean + s.e.m., n = 6. (**B**) 5-LO-inhibitory activity of celecoxib, rofecoxib, etoricoxib, diclofenac and BWA4C in intact PMNL in the absence (black bars) or presence (striped bars) of 20 µM AA as compared to vehicle control (100 %). For experimental procedures see *Methods.* Results are mean + s.e.m., n = 5. ***, $p \leq 0.001$; *, $p \leq 0.05$. cel, celecoxib; eto, etoricoxib; rof, rofecoxib; dic, diclofenac; AA, arachidonic acid

4.5.3 Inhibition of 5-LO activity of in cell-free assays

5-LO is a tightly regulated enzyme and suppression of cellular product formation by any compound does not unequivocally indicate a direct interference with 5-LO catalysis. Thus, cellular regulatory components or mechanisms such as FLAP, mitogen-activated protein kinases (MAPKs), Ca^{2+} mobilization, nuclear membrane association [79] and interaction with CLP [153] might theoretically be targeted by celecoxib. To demonstrate a direct action on 5-LO, the effects of celecoxib on 5-LO product synthesis were analyzed in cell free assays. Celecoxib concentration-dependently inhibited 5-LO product formation in homogenates supplemented with 20 μM AA, though less potent ($IC_{50} \approx 23.4$ μM, **fig. 453A**) as compared to intact cells ($IC_{50} \approx 8.4$ μM, **fig. 451A**). Such a loss of efficacy in cell-free assays was observed also for nonredox–type 5-LO inhibitors, [154] but addition of thiols (to reduce the lipid hydroperoxide levels via glutathione (GSH) peroxidases) restored potent inhibition. However, addition of GSH had no significant effect on the efficacy of celecoxib (**fig. 453A,** $IC_{50} \approx 20.5$ μM). In accordance with the results obtained from the whole blood assay, celecoxib (up to 30 μM) did not suppress the formation of 12(S)-HETE or 15(S)-HETE in homogenates of human platelets or eosinophils, respectively (**fig. 453B**). Finally, celecoxib concentration-dependently inhibited the activity of partially (ATP-affinity) purified human recombinant 5-LO with an $IC_{50} \approx 30.9$ μM (**fig. 453C**). Rofecoxib, etoricoxib and diclofenac (up to 100 μM) caused no or only modest inhibition of 5-LO activity in the cell free assays (**fig. 453D** and **E**). Taken together, celecoxib can thus be said to be a direct inhibitor of 5-LO.

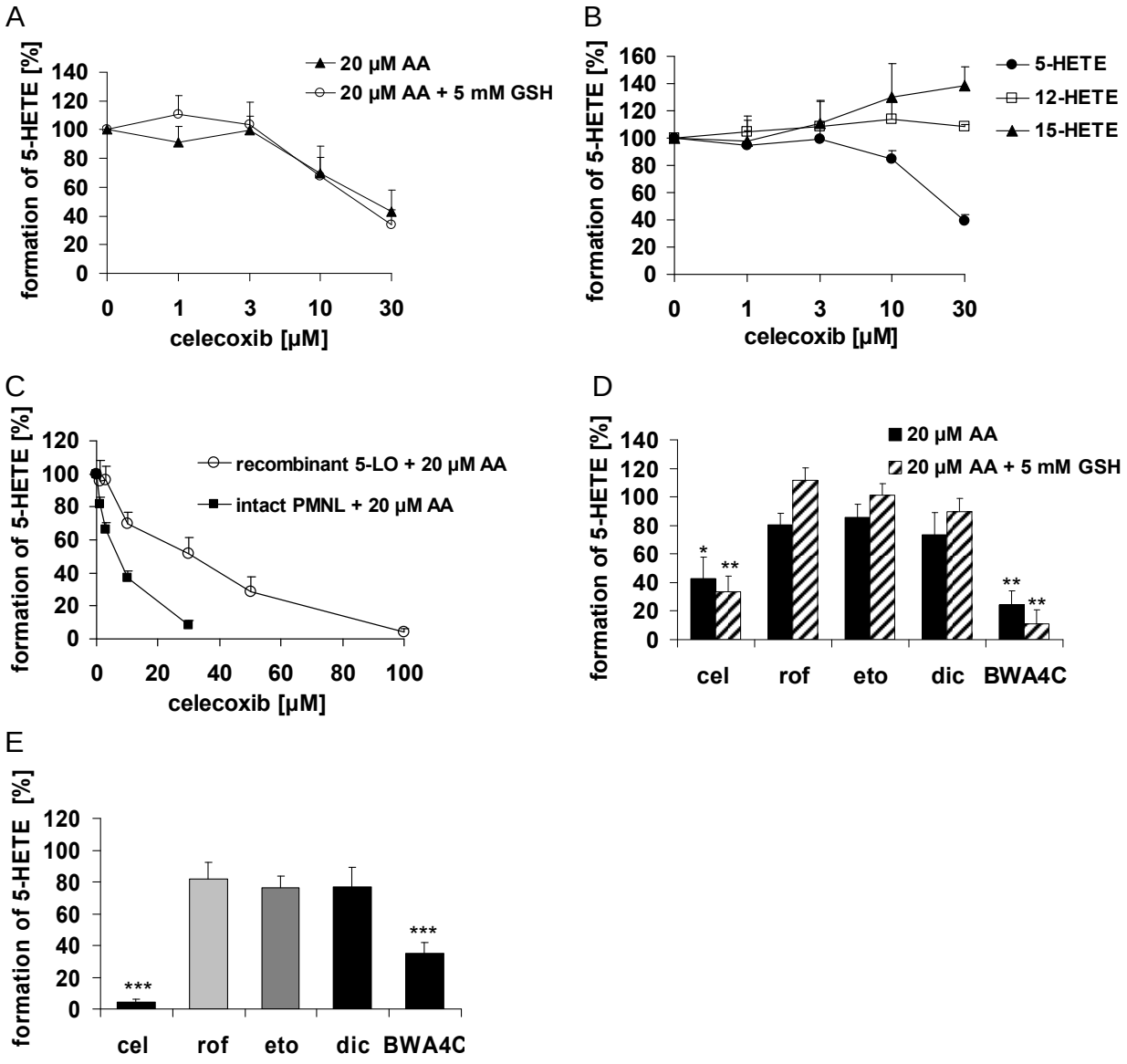

figure 453: Effect of celecoxib, etoricoxib, rofecoxib, diclofenac and BWA4C on 5-LO activity in cell-free assays. 5-LO activity is expressed as percentage compared to vehicle control (100 %). Respective 5-LO activities were determined as described in *Methods.* (**A**) Inhibition of 5-LO product formation in broken cell homogenates by celecoxib in presence or absence of 5 mM GSH. Results are given as mean + s.e.m., n = 4. (**B**) Determination of 5-, 12- and 15-LO product formation in broken cell homogenates in the presence of increasing concentrations of celecoxib, 20 µM AA and 25 mM GSH. Results are given as mean + s.e.m., n = 3. (**C**) Inhibition of partially purified human recombinant 5-LO by celecoxib as compared to intact PMNL. Results are given as mean + s.e.m., n ≥ 5. (**D**) Comparison of the 5-LO-inhibitory activity of celecoxib, rofecoxib, etoricoxib, diclofenac and BWA4C in PMNL homogenates in the absence (black bars) or presence (striped bars) of 5 mM GSH as compared to vehicle control (100 %). Results are given as mean + s.e.m., n = 4. (**E**) Effect of celecoxib, rofecoxib, etoricoxib, diclofenac and BWA4C on recombinant 5-LO activity as compared to vehicle control (100 %). Results are given as mean + s.e.m., n ≥ 3. ***, $p \leq 0.001$; **, $p \leq 0.01$; *, $p \leq 0.05$. cel, celecoxib; eto, etoricoxib; rof, rofecoxib; dic, diclofenac.

5 Discussion

5.1 Cathepsin G is a target of boswellic acids

Our findings provide strong evidence that human CatG is a high-affinity target of BAs. By means of a protein-fishing approach, besides several other proteins, a 25.8 kDa protein from lysates of human PMNL was found to selectively bind to an affinity matrix composed of KBA, linked covalently to insoluble EAH Sepharose 4B. MALDI-TOF-MS analysis combined with immunological detection revealed that this 25.8 kDa BA-binding protein is CatG. All four β-configurated BAs inhibited the activity of human CatG *in vitro*. With IC_{50} values of 0.6 and 0.7 μM, respectively, AKBA and β-BA were most potent. The proteolysis of related serine proteases was less efficiently inhibited, confirming the selectivity of BAs for CatG. Moreover, BAs potently inhibited CatG-mediated cellular responses such as chemoinvasion of PMNL, and Ca^{2+} mobilization in platelets evoked by fMLP-stimulated PMNL. Hence, BAs not only bind CatG but also functionally interact with this protease. Along these lines, AKBA with a high average docking score docked into the active site of CatG, where the proteolysis of the substrate takes place. Since CatG plays a role in inflammatory diseases such as asthma, psoriasis and rheumatoid arthritis [28, 155] for which *B. spec* extracts have proven to possess therapeutic benefit [5], the high-affinity BA-CatG interaction may provide a molecular basis for these beneficial effects and might be of pharmacological relevance.

BAs, in particular AKBA, have been proposed as the main active principles of *B. spec* preparations that are traditionally used to cure chronic inflammatory disorders [4, 5]. Initial attempts to elucidate the molecular mechanisms responsible for the pharmacological actions of *B. spec* extracts identified 5-LO as a reasonable target of AKBA. Thus, AKBA as well as *B. spec* extracts reduced the formation of LTs in activated leukocytes [8, 65, 156, 157] and AKBA inhibited 5-LO activity in cell-free assays [65, 101, 156] or isolated 5-LO enzyme [156]. Aside from AKBA, other BAs were either hardly active or not active at all [65]. Since LTs play pivotal roles in inflammatory reactions [79] and because *B. spec* extracts show clinical effects similar to typical 5-LO inhibitors, it appeared reasonable that intervention of BAs with 5-LO and thus with LT formation, is the molecular basis underlying the anti-inflammatory effectiveness of *B. spec* extracts observed *in vivo* [5].

Besides 5-LO, AKBA was shown to interfere with several other enzymes or signalling events that contribute to inflammation including HLE [10], p12-LO [9], the NFκB pathway [12],

intracellular Ca^{2+} levels and MAPKs activities [17]. However, the required concentrations in the respective experimental systems frequently appeared rather high (> 10 μM) [10, 18, 101, 157], whereas the plasma concentrations of AKBA obtained after oral application of standardised *B. spec* extracts are in the submicromolar range [26, 27]. The most affine AKBA target was proposed to be 5-LO, but strikingly different potencies (IC_{50} = 1.5 up to 50 μM) were reported [8, 65, 101, 104]. These discrepancies seemingly depend on the different experimental settings (intact cells or cell-free assays, different species and cell type, AA concentration etc.). Thus, AKBA was most efficient to inhibit 5-LO in Ca^{2+} ionophore-stimulated PMNL from rat (IC_{50} = 1.5) [8], whereas for direct interference with isolated human 5-LO, the IC_{50} was determined at 16 μM [156], a phenomenon that needs to be resolved. Taken together, the pharmacological relevance of most of the proposed target interactions and effects of AKBA observed *in vitro* and the pharmacological relevance *in vivo* are a matter of debate.

In fact, isolated CatG binds to KBA-Seph, but not to Seph without ligand, in the same manner as CatG in PMNL lysates. Most of the other identified proteins that selectively bind to KBA-Seph are directly or indirectly involved in inflammatory processes, immune responses or cancer formation [30, 53, 63, 134, 158].

The successful identification of CatG as target of BAs by means of the fishing approach using the affinity resin is the result of the combination of several fortunate circumstances. First, CatG is a rather abundant protein in PMNL. Second, the relatively high affinity of CatG to KBA-Seph enabled binding under the stringent conditions (1% Triton X-100) and the ability to endure the thorough and long-lasting washing (overnight) of the precipitates. Third, KBA is a highly rigid molecule with only few conformations favourable for binding to CatG. Finally, the C3-OH moiety used to link KBA to the resin via an ester bound is not detrimental for binding, in fact esterified BAs (i.e. AKBA or Aβ-BA) are virtually equipotent or even more potent than those with a free OH group (i.e. KBA and β-BA).

In collaboration with HLE, CatG is largely responsible for the destruction of bacteria by neutrophils [28]. Both proteases as well as proteinase-3 are not only involved in defence against bacterial infections, these enzymes are also important players in ulcerative colitis and rheumatoid arthritis [159-162] where BS extracts are beneficial [49, 163]. Moreover, this work demonstrates that CatG activity can be reduced by oral administration of BS extracts in healthy volunteers and patients with ulcerative colitis in remission (*ex vivo*). Our findings might prove useful for the development of new drugs for treatment of bowel diseases.

5.2 DNA-PK and Akt are targeted by BAs

The ability of apoptotic stimuli to induce cell death is counteracted by the activity of antiapoptotic proteins. The PI3K/Akt pathway downstream of RTKs plays an important role in cell survival. It was shown before that PKCξ acts as an antiapoptotic protein during TNFα-induced cell death [164] and that there is a cross-talk between PKCξ and Akt. PKCξ acts upstream of Akt/PKB to exert its antiapoptotic function [165]. Activation of Akt by PKCξ is mediated by DNA-PK, a member of the PIKK subfamily of protein kinases, and depletion of DNA-PK reversed the antiapoptotic function of PKCξ during TNFα-induced apoptosis [165]. The observation that inhibition of DNA-PK can reverse antiapoptotic signalling by Akt establishes a new role for DNA-PK in the extrinsic cell death pathway. Multiple signalling pathways that exist in certain cell types might regulate/influence the final outcome of cell death or survival. Cells that are resistant to TNFα contain constitutively active Akt [166]. Activation of Akt is an early event following binding of TNFα to its cell surface receptors. Complete activation of Akt requires phosphorylation at Thr308 and Ser473 by PDK1 and PDK2, respectively[167]. Since phosphorylation of Akt at Ser473 is mediated by PDK2 and since DNA-PK has been recently identified as PDK2 [55], the recruitment of DNA-PK during DNA damage-induced apoptosis is reasonable. In fact, DNA-PK is activated in response to DNA damage [168] and autophosphorylation of DNA-PK has been shown to inhibit DNA-PK activity [169]. These results suggest that DNA-PK may also play a critical role in receptor-initiated cell survival via activation of Akt/PKB. The mechanism of how DNA-PK localizes to the membrane is not clear, but DNA-PK has been reported to be associated with epidermal growth factor receptor [57].

It was shown, that activation of Akt via DNA-PK inhibits TNFα-induced apoptosis in breast cancer cells [165]. BAs inhibit LPS-mediated TNFα induction in monocytes [100]. The cross-talk between multiple signalling pathways is an important determinant of cell survival and cell death, but is currently not well understood. The involvement of DNA-PK during DNA damage induced apoptosis is well known and a new role for DNA-PK during receptor-initiated apoptosis was established [55]. DNA-PK is activated upon DNA damage by UV irradiation, as is Akt [58]. Induction of apoptosis by cisplatin was explained by a decrease in DNA-PK activity through proteolytic degradation of DNA-PK [60]. Interestingly, Akt activity and Ser473 phosphorylation are also inhibited by cisplatin treatment [61, 170]. Mouse and human cells deficient in DNA-PK are hypersensitive to ionizing radiation and to radiomimetic drugs [171-173]; a similar phenotype can be observed in Akt1/PKB knock-out mice [174] and with mouse

embryo fibroblasts derived from such mice [175]. It was often reported that BAs induce apoptosis in several cancer cell lines in vitro and reduce tumour growth in vivo [13, 14, 16, 18] Modulation of DNA-PK and inhibition of Akt by BAs may be responsible for induction of apoptosis in several tumour cell lines [13 14 16].

Akt is an upstream kinase of the IKK pathway which is indirectly inhibited by boswellic acids [12, 18]. Akt is bound selectively by immobilized KBA (KBA-Seph). Beneath NFκB pathway (IKK) and MAPK pathway, Akt influences several other pathways like cell growth, cell death, cardiovascular homoeostasis (eNOS), JNK and glycogen synthesis. Akt is inhibited potently (Aβ-BA IC_{50} = 300 nM) and directly in vitro but also in vivo by BAs. Phosphorylation of Akt on Ser473 was reduced by BAs and phosphorylation of the direct downstream-target Bad by Akt was inhibited (Bad phosphorylation in LNCaP). These results provide strong evidence that Akt is a high affinity target of BAs. The fact that also Akt phosphorylation by DNA-PK is inhibited *in vitro* and *in vivo* implies that BAs may inhibit the interaction of Akt and DNA-PK, which results in the inactivation of their activity.

The DNA-PK pathway plays a crucial role in controlling transcription, cell cycle progression, and apoptosis [171]. Similarly, Akt is also implicated in the regulation of many different cellular processes [53, 54]. It was shown that BAs induce apoptosis in cancer and cancer cell lines[13, 14, 18]. These anticarcinogenic effects may be influenced by inhibition of DNA-PK and Akt. Hyperproliferation and overactivation of RTKs in cancers lead to invasiveness and metastasis of tumours. BAs block the growth signal on an early stage of the pathway. Because Akt is potently inhibited by Aβ-BA (IC_{50} = 300 nM), *in vivo* relevance could be implicated; plasma levels up to 6.4 µM β-BA / 4.9 µM Aβ-BA have been achieved. In conclusion, the RTK/PI3K pathway is directly modulated by BAs, DNA-PK and Akt are the main targets.

Beneath Akt and DNA-PK, other BA-binding proteins are involved in cancer development and immune response [30, 53, 63, 134, 158]. Farnesyl pyrophosphate synthetase (FPPs) is the target of the bisphosphonates, which are effective in the treatment of osteoporosis. Though FPPs is not influenced by BAs *in vitro*, there could still be a certain relevance *in vivo* [176]. Proteinase-3 is a human protease involved in tissue degradation and penetration of macrophages. Proteinase-3 is very similar in sequence and structure to CatG and HLE, but inhibition by BAs is weak (IC_{50} ~ 30 µM). Moreover, other proteins found by pulldown experiments, e.g. cathelicidin antimicrobial peptide (hCAP18), UNC-112 and prohibitin are important key mediators in inflammation and the autocrine immune response, but the whole context still remains unclear [158].

5.3 Modulation of signal transduction and functionality of platelets and monocytes by boswellic acids

The current opinion regarding the molecular mechanisms underlying the anti-inflammatory properties of BS extracts or BAs, favours 5-LO as the most relevant target [5], but AKBA interferes with several other relevant enzymes or signalling events that contribute to inflammation as described above. In this work, additional anti-inflammatory implications of AKBA, that is, suppression of agonist-induced Ca^{2+} mobilization in platelets and platelet aggregation, are implicated. These inhibitory actions may contribute to the anti-inflammatory effectiveness of AKBA-containing extracts of B. *spec*. observed *in vivo* as well. Moreover, inhibition of platelet aggregation suggests novel beneficial properties of AKBA in cardiovascular diseases such as atherosclerosis, heart attack and stroke that are characterized by aggregating platelets and thrombotic states [177]. However, besides AKBA, BS extracts also contain 11-methylene-BAs that activate platelets and when BS extracts were analysed, the overall effects on platelets resembled those of 11-methylene-BAs.

As mentioned before, there is a discrepancy between plasma levels of BAs and the concentrations required for inhibition of proposed targets. Along these lines, it was previously shown that in platelets, AKBA at concentrations ≥ 30 μM caused moderate elevation of $[Ca^{2+}]_i$ and activation of MAPKs, accompanied by the release of AA [67]. Furthermore, our group showed before that relatively high concentrations of AKBA (10 up to 100 μM) stimulated the mobilization of Ca^{2+} and the activation of MAPK in PMNL [66], coupled to the formation of reactive oxygen species (ROS), the release of AA and its metabolism to leukotrienes, similarly as observed for the chemoattractants fMLP or PAF [104]. Such actions of AKBA suggest a pro-inflammatory rather than an anti-inflammatory potential. However, these events were evoked only at quite high concentrations of AKBA (≥ 10 μM) [17, 66, 67, 104] that we consider not pharmacologically relevant *in vivo*. Intriguingly, in the present study, effective concentrations of AKBA (≤ 3 μM) significantly antagonised Ca^{2+} mobilization evoked by the platelet agonist collagen and suppressed agonist-induced platelet aggregation. Note that AKBA itself is unable to activate platelets at such low concentrations [67]. AKBA was somewhat less efficient to suppress Ca^{2+} mobilization and platelet aggregation induced by U-46619, and when thrombin was used to evoke these responses, AKBA even failed. Presumably, AKBA targets a component pivotal in the signal transduction of collagen (and U-46619), which apparently is dispensable for thrombin-induced pathways leading to Ca^{2+} mobilization and platelet aggregation. It should be noted that the signal transduction pathways

of collagen and U-46619 or thrombin are quite distinct and, at least in part, utilize different types of signalling molecules. U-46619 and thrombin act on GPCRs and signals via $G_{i/q}$ proteins and PLC to rapidly release Ca^{2+} from IP_3-sensitive stores [178], whereas collagen binds integrin $\alpha_2\beta_1$ and glycoprotein VI and slowly allows Ca^{2+} entry via a Src family kinase/PLCγ-mediated pathway [179]. For β-BA, Src family kinases and the PLC/IP3 pathway seem to be involved in Ca^{2+} mobilization, and β-BA causes activation of ERK2 and the PI3K/Akt route. Moreover, β-BA induces the release of AA, a pronounced generation of thrombin, and Ca^{2+}-dependent platelet aggregation. In contrast, AKBA-induced Ca^{2+} mobilization is not connected to Src family kinases and PLC/IP3 signalling, and AKBA failed to induce phosphorylation of Akt and ERK2, as well as functional platelet responses. Detailed analysis of the interference of AKBA with these signalling pathways is needed to reveal the molecular modes of action.

Among the BAs tested for induction of Ca^{2+} mobilization, β-BA is the most potent analogue. At 10 μM, the effectiveness of β-BA exceeded that of PAF or collagen, and was comparable with that of the potent platelet agonist thrombin. Such β-BA concentrations are in the range of β-BA levels in human plasma (10.1 μM), determined after oral application of 4 x 786 mg BS extract/day within 10 days [27]. The 3-O-acetyl group slightly hampers (receptor-)activation and the 11-keto moiety significantly decreases the potency and also alters the signalling routes in platelets. In sharp contrast to platelets, only 11-keto BAs, but not 11-me-BAs, caused stimulation of PMNL [66, 104]. Possibly, PMNL and platelets selectively express closely related but not identical receptors specific for AKBA or 11-me-BAs, respectively. Important receptors for soluble agonists known to regulate $[Ca^{2+}]_i$ in platelets are the purinergic P_2X_1 and P_2Y_{12} receptors, the TXA_2 receptor, the PAF receptor, the $5\text{-}HT_{2A}$ receptor, and the PAR-1 and – 4 [180]. Whether β-BA acts at one (or more) of these receptors is unknown. However, antagonists of thrombin (argatroban), PAF (WEB 2086), and ADP (NF449 and MRS2179) did not affect β-BA-induced Ca^{2+} mobilization. Thrombin is the most potent platelet agonist acting via PAR-1 and -4 [181, 182] and the influence of 2-APB on cellular Ca^{2+} influx systems has been reported [183]. Interestingly, the proximal routes mediating PLC/IP3-dependent Ca^{2+} mobilization appear to be different for β-BA and thrombin (or PAF). Thus, Src family kinase inhibitors abolished the β-BA-induced response, but not the responses elicited by thrombin or PAF. PLCγ is the most abundant PLC isoform in platelets [184] and is an operative element in Ca^{2+} mobilization in response to activation by adhesion receptors [185]. Whereas, soluble ligands such as thrombin, ADP, PAF, or TXA_2 act via GPCRs to stimulate PLCβ isoenzymes,

the PLCγ isoforms are regulated through phosphorylation by Src family kinases [185]. In analogy to agonists that act via adhesion receptors but unlike thrombin, β-BA may utilise the Src family kinases/PLCγ pathway to induce Ca^{2+} mobilization. Another difference between β-BA- and thrombin-mediated Ca^{2+}-mobilization is the significant delay of the response to β-BA as compared to the rapid effect of thrombin. Aside from acting as a direct ligand at a certain (adhesion) receptor, β-BA may possibly first induce the generation of an endogenous agonist that in turn causes PLC-γ/IP3-coupled Ca^{2+} mobilization via (adhesion) receptors. Attempts to unravel a putative autocrine mode of action are in progress in our laboratory.

Typical platelet agonists such as thrombin, collagen, or TXA_2 activate PI3K and its downstream effector Akt, important mediators of agonist-induced platelet activation [186], as well as p38 MAPK and ERKs [71, 72, 187]. The MAPK are a point of convergence of complex signalling networks, regulating cell proliferation and differentiation [72]. In platelets, the functions of MAPK are mainly uncharacterised and the signal transduction steps are poorly understood. All BAs tested activated p38 MAPK with similar efficacy, but only β-BA (and Aβ-BA) rapidly and significantly activated ERK2. Also, β-BA, but not AKBA, evoked Akt phosphorylation, and in analogy to thrombin, the PI3K and/or the PLC/Ca^{2+} pathway are involved. Therefore, the receptor for BAs mediating p38 MAPK activation might differ from those transmitting signals to activate ERK2 and Akt. The latter (11-me-BA specific) receptor may also mediate increases in $[Ca^{2+}]_i$, generation of thrombin, release of AA and aggregation, since AKBA and KBA failed to elicit these events. Investigation of the platelet functions elicited by β-BA provided controversial results. As a rule, the distinct responses of activated platelets depend on the strength (potency) of the agonist, and these responses can be arranged in an activation sequence: (1) aggregation, (2) granule secretion, (3) AA liberation, and (4) acid hydrolase secretion [188]. The magnitude of Ca^{2+} mobilization is an important parameter for the induction of these responses. In fact, β-BA (10–30 μM) substantially elevated $[Ca^{2+}]_i$ and potently induced thrombin generation, being equipotent in this respect with collagen at 2 mg/ml in a model utilising native platelets. Also, β-BA potently evoked the liberation of free AA from washed platelets, although at concentrations slightly higher than those required for Ca^{2+} mobilization, probably due to the presence of fatty acid-free albumin that may bind BAs. In general, liberation of free AA is a response distal of aggregation and degranulation, and its induction normally requires potent agonist-activating platelets with high strength. Surprisingly, however, the efficacy of β-BA was greatly reduced by the induction of aggregation. In contrast to collagen, the response of β-BA was strictly dependent on the

presence of extracellular Ca^{2+}. Therefore, β-BA may facilitate aggregation by other factors rather than being a full agonist. Moreover, β-BA failed to induce degranulation and fibrinogen receptor activation (CD62, PAC-1 expression). Together, despite the pronounced elevation of $[Ca^{2+}]_i$, only select functional platelet responses were observed after stimulation with β-BA. Along these lines it was found that platelets in polycythaemia vera exhibit decreased aggregation after stimulation with PAF, although an equal increase in $[Ca^{2+}]_i$ was seen as compared to platelets from healthy donors [189]. Furthermore, a patient was described with defective platelet aggregation in response to Ca^{2+} ionophore A23187, despite normal increases in $[Ca^{2+}]_i$ [190]. Hence, elevation of $[Ca^{2+}]_i$ in platelets is one important signalling step for eliciting various platelet responses, but must not necessarily lead to the induction of all Ca^{2+}-dependent platelet functions. It is conceivable that β-BA on one hand is a platelet agonist that potently induces central signalling pathways (Ca^{2+} mobilization, MAPK/Akt phosphorylation) and select responses such as thrombin generation and AA release, but on the other hand lacks the stimulation of certain signalling components or executing molecules particularly important for a rapid aggregation, degranulation, and fibrinogen receptor activation. At the present time, the findings cannot be readily related to the antiinflammatory properties of BS extracts, observed in animal models or in studies with human subjects [6]. Nevertheless, due to its high effectiveness and the importance of the signalling molecules and the select platelet functions induced, the receptor(s) mediating the actions of β-BA in platelets warrant further elucidation. Effective concentrations of β-BA (10 μM) are in range of β-BA levels in human plasma (see above), but platelet agonism does not appear to be relevant *in vivo* (see above).

Besides the agonism of 11-me-BAs to Ca^{2+}-influx in human platelets, particularly the keto-BAs antagonize potently agonist-induced increases in $[Ca^{2+}]_i$ in monocytes, PMNL and HL-60-cells. These findings indicate that keto-BAs especially AKBA desensitize blood cells to endogenous inflammation-stimuli.

Based on present findings and previous studies, the 3-*O*-acetyl group and the 11-keto moiety strongly determine the pharmacodynamics in the particular assay system, and AKBA is frequently the most effective or the exclusive active analogue [9, 17, 65, 66]. In this work, AKBA suppressed Ca^{2+} mobilization induced by collagen or U-46619 with almost equal potencies (IC_{50} = 3 and 5 µM), implying the interference with a common type of target or pathway distal of Ca^{2+} release. Besides AKBA, also β-BA reduced U-46619- and collagen-induced Ca^{2+} mobilization, though less efficient (IC_{50} = 7 and 8 µM, respectively). Accordingly, one would expect that KBA, containing an 11-keto moiety or Aβ-BA, possessing a 3-*O*-acetyl-group should be more potent than β-BA. However, KBA caused no suppression at all but rather enhanced the signals induced by collagen, U-46619 and also by thrombin, and Aβ-BA was less effective than AKBA or β-BA. It is possible that AKBA and β-BA act at different targets both leading to suppression of Ca^{2+} mobilization.

The finding that β-BA (and Aβ-BA) suppressed agonist-induced Ca^{2+} mobilization was actually quite surprising, since these 11-methylene-BAs themselves cause a transient increase of $[Ca^{2+}]_i$ in platelets (this study and [67]). Such transient increase of $[Ca^{2+}]_i$ could desensitize platelets by unspecific actions (e.g. depletion of intracellular Ca^{2+} stores) and thus be the reason for the subsequent failure of Ca^{2+} release evoked by a second agonist. However, elicitation of Ca^{2+} mobilization by U-46619 and subsequent stimulation of platelets with collagen or thrombin did not substantially prevent the effects of the agonists as in the case of BAs.

At the moment it is not possible to provide a molecular basis explaining the puzzling effects of the various BAs on the Ca^{2+} homeostasis in platelets. Nonetheless, since elevation of $[Ca^{2+}]_i$ is a determinant for aggregation of washed platelets [69, 149], it is reasonable to speculate that inhibition of collagen-induced aggregation by AKBA could be the result of suppressed Ca^{2+} mobilization. On the other hand, lower concentrations of AKBA were sufficient to suppress collagen-evoked aggregation (IC_{50} = 1.1 µM) as compared to those required to inhibit Ca^{2+} mobilization (IC_{50} = 3 µM). Moreover, AKBA was about equipotent for suppression of Ca^{2+} mobilization in response to U-46619 as compared to collagen, but U-46619-evoked aggregation was hardly affected by AKBA (IC_{50} = 25 µM) . Therefore, the inhibitory effects of ABKA on agonist-induced Ca^{2+} mobilization and on aggregation also might be separated. However, it is possible that already a minimal impairment of $[Ca^{2+}]_i$ as in the case of collagen is sufficient to substantially affect aggregation. In contrast to AKBA, β-BA at higher concentrations caused aggregation itself [67]. Once again, this indicates that

AKBA interacts with other molecules required for aggregation, and thus concrete structure-activity relationships may exist in this respect.

In summary, AKBA (and to a minor extent also β-BA) acts as an efficient blocker of select agonist-induced Ca^{2+} mobilization, and AKBA but no other BA, potently inhibits collagen-evoked aggregation of platelets. Importantly, the concentrations of AKBA needed to block aggregation are in the range of plasma levels of AKBA detected *in vivo* after oral administration of standardized doses of B. *spec* extracts. For patients taking such BS preparations, the amounts of AKBA reached in the blood may be sufficient to antagonise collagen-mediated pathophysiological events, particularly platelet aggregation.

5.4 Celecoxib is an inhibitor of 5-LO

Celecoxib, a well-tolerated antirheumatic drug, reduces familial adenomatous polyp formation[92]. This effect could not merely be explained by COX-2 inhibition. The COX-2-selective drug is, as shown here, also an inhibitor of 5-LO both *in vitro* and *in vivo*. Celecoxib inhibited 5-LO product synthesis in different cellular models using A23187 as agonist, that is, in human whole blood and human isolated PMNL. A direct interaction between 5-LO and celecoxib is visualized in cell-free assays, where celecoxib blocked the activity of isolated human recombinant 5-LO or 5-LO in homogenates from human PMNL. Together, the data strongly suggest that pharmacologically relevant doses of celecoxib affect 5-LO activity in leukocytes and may thus contribute to the unique pharmacology of this drug.

5-LO contains a non-heme iron in the active site coordinated by three His and a C-terminal Ile residue that cycles between the ferrous and the ferric state, being essential for catalysis [191]. Most pharmacological 5-LO inhibitors target this iron by retaining the ferrous state and/or by chelation, whereas nonredox-type inhibitors interfere with fatty acid binding cleft(s) [191]. Based on the structure of celecoxib, an iron-chelating- or a redox-related mechanism for inhibition can be excluded and a typical pattern of a nonredox-type 5-LO inhibitor is not evident. Besides direct inhibition of 5-LO, interference with FLAP (by e.g. MK-886) blocks cellular 5-LO product formation [192]. Although the cellular environment influences inhibition of 5-LO product synthesis by celecoxib, FLAP is apparently not involved in 5-LO inhibition in intact cells.

A number of studies were conducted to identify non-COX-2 targets of celecoxib responsible for its pharmacological profile. The pharmacological effects include a distinctive chemo-preventive and tumour-regressive efficacy at higher celecoxib doses as well as a favourable gastrointestinal tolerability as compared to classical NSAIDs. Various COX-independent mechanisms predominantly in the higher μM range were considered to explain the unique pharmacology of celecoxib such as inhibition of 3-phosphoinositide-dependent kinase-1 (PDK-1, IC_{50} = 48 μM) [97] or endoplasmatic reticulum Ca^{2+}-ATPase ($IC_{50} \approx$ 35 μM) [95] in human prostate cancer cells, degradation of the oncogenic survival factor beta-catenin in human colon carcinoma cells at 60-100 μM [98] or inhibition of adenylyl-cyclases (IC_{50} = 375 μM) [96]. However, due to the strong discrepancy between the plasma concentrations of celecoxib after a single intake of 800 mg ($c_{max} \approx$ 8 μM) [99] and those concentrations required to affect non-COX-2 targets (≥ 30 μM, *in vitro* assays) the relevance of these findings is discussed controversially.

Inhibition of 5-LO product synthesis occurs at comparably low celecoxib concentrations (IC_{50} ≈ 8 μM, cellular assay) similar to the plasma levels in humans after intake of high celecoxib doses [99]. The findings are supported by a study of Chen et al. demonstrating that high doses of celecoxib in chow (1000 ppm) reduced the content of LTB_4 by approx. 50 % in oesophageal adenocarcinoma xenografts of rats, whereas lower doses were almost ineffective [193]. Also, a 50% reduction of LTB_4 and 5-HETE formation in A23187-stimulated human whole blood by 100 μM celecoxib was described using different experimental conditions as compared to the present study [194]. In contrast, Mao et al. showed that administration of celecoxib 400 mg twice daily to active smokers increased the production of LTB_4 in broncho alveolar lavage fluids (BAL) by around 36 % [195] , indicating that modulation of 5-LO product synthesis by celecoxib may depend on the tissue type and its state of health.

Distinctive inhibition of tumour growth as a pharmacological effect arising from 5-LO inhibition was reported for human prostate, oesophageal, pancreatic, lung and colorectal cancer [196]. Interestingly, all these tumour types were susceptible to celecoxib treatment [197] providing a possible link between the antiproliferative potency of celecoxib and inhibition of 5-LO. Indeed, the celecoxib-mediated antiproliferative effects are mechanistically similar to those observed during 5-LO inhibitor-triggered cell death. For instance, both 5-LO inhibitors and celecoxib attenuated the growth of human carcinoma cells by releasing cytochrome c from mitochondria, by activating caspase-3 and -9 followed by cleavage of poly(ADP-ribose)polymerase (PARP), and by inducing the cell cycle inhibitor $p21^{kip1}$ [94, 198, 199]. Moreover, inhibition of 5-LO was described to implicate downregulation of LTD_4-mediated beta-catenin-signalling [200] , and this pathway is suppressed also by celecoxib [98]. Finally, LTB_4 was reported to activate Akt by PI3-kinase/PDK-1-mediated phosphorylation [201] , suggesting that inhibition of LTB_4 formation by celecoxib may contribute to the downregulation of cellular Akt activity as described for this drug few years ago [97]. Taken together, celecoxib may exert its antiproliferative effects via inhibition of 5-LO product synthesis.

Dual inhibitors of COXs and the 5-LO pathway, such as licofelone, constitute a valuable alternative to classical NSAIDs since they cause less severe gastrointestinal (GI) side effects than non selective COX-inhibitors alone [202]. Recent studies showed that the gastroprotective effects of licofelone can substantially be attributed to an inhibition of LT-mediated leukocyte adhesion to intestinal blood vessels and subsequent mucosal inflammation [203]. Together, since celecoxib combines COX-2 selectivity with 5-LO-inhibitory activity, it may counteract such ulcerogenic effects by reducing LTB_4 levels which is highly chemotactic for leukocytes and plays an important role in the development of NSAID-induced gastrointestinal lesions [204].

Interestingly, it has been shown that celecoxib has a favourable gastrointestinal tolerability profile superior to that of unselective NSAIDs [205-207], perhaps partly due to its 5-LO-inhibitory activity.

In conclusion, this work shows that celecoxib inhibits human 5-LO in cell-free assays, in cellular systems and in human whole blood. These findings may contribute to a better understanding of the unique pharmacological profile of celecoxib among coxibes, characterized by a distinctive antiproliferative efficacy and a favourable gastrointestinal tolerability.

6 Summary

Extracts of Boswellia serrata, also known as Indian frankincense, have been used to treat inflammatory diseases in the Indian ayurvedic medicine or Chinese traditional medicine (TCM) for over 3000 years, but the molecular mechanisms of the anti-inflammatory effects are still not well understood. It is obvious that the boswellic acids, the major compounds in the extracts, are responsible for the efficacy. This work employed a protein fishing technique to identify putative targets of boswellic acids at different stages within the inflammatory cascade. For fishing experiments, boswellic acids were immobilized to sepharose and incubated with cell lysates. After washing and boiling, fished proteins were separated by SDS-PAGE and analysed by MALDI-TOF-MS. CatG, DNA-PK and the protein kinase Akt were identified by protein pulldowns with immobilised BAs and characterised as selective and important targets for BAs with an IC_{50} in the range of physiologically achievable plasma levels up to 5 μM. In addition, the influence on several signal transductions by BAs was tested. Calcium influx, arachidonic acid release, platelet aggregation and TNFα-release were assayed to reveal further pharmacological effects of BAs.

Celecoxib is a well-known selective COX-2 inhibitor that is in clinical use. In this work, it is demonstrated that celecoxib is also a highly potent direct 5-LO inhibitor. Celecoxib is used in arthritis and its gastro-intestinal side effects are reduced compared to non-selective NSAIDs. In patients with a familiar disposition to polyp forming, celecoxib reduced polyps and the incidence of colon cancer. Because of lowered leukotriene levels in patients under celecoxib therapy it was plausible to test whether celecoxib interferes with 5-LO. Here it is shown that the activity of 5-LO is inhibited in PMNL and cell-free assays with IC_{50} of 8 μM in intact cells, 20 μM with supplemented arachidonic acid and 30 μM in cell-free systems. Thus, celecoxib is a dual inhibitor of COX-2 and 5-LO. Since 2006, celecoxib has been approved as an orphan drug for the treatment of familial adenomatous polyposis. Aside from this indication, it could be useful for treatment of asthma and other diseases where 5-LO is implicated.

7 Zusammenfassung

Extrakte des indischen Weihrauchs werden seit mehr als 3000 Jahren in der Volksmedizin zur Behandlung chronisch entzündlicher Erkrankungen sowie in der ayurvedischen Medizin in Indien und in der Traditionellen Chinesischen Medizin (TCM) verwendet. Pharmakologisch wirksame Inhaltsstoffe sind vor allem Boswelliasäuren, die den Hauptbestandteil der Säurefraktion des Harzes ausmachen. Bislang sind die molekularen Mechanismen nur unvollständig aufgeklärt. Diese Arbeit befasst sich mit der Auffindung und Charakterisierung von Zielstrukturen, die innerhalb der Entzündungskaskade von Boswelliasäuren moduliert werden. Zur Identifizierung wurden 11-Keto-Boswelliasäure sowie β-Boswelliasäure an Sepharose-Beads gebunden und damit immobilisiert. Die immobilisierten Boswelliasäuren wurden zusammen mit Zelllysaten aus verschiedenen Zelltypen (PMNL, Thrombozyten, MM6, LNCaP, MCF-7, HL-60 und RBL-1) inkubiert. Die Beads wurden von dem Überstand getrennt, gewaschen und mittels SDS-PAGE aufgetrennt. Als Vergleichsprobe diente ungebundene Sepharose, die unter gleichen Bedingungen behandelt wurde. Banden, die nur in den Präzipitaten der BA-Sepharosen auftraten, wurden mittels MALDI-TOF-MS analysiert. Bei diesem als „Fischen“ bezeichneten Verfahren wurden selektiv folgende Proteine als mögliche Interaktionspartner von BAs gefunden: CatG, Rap1b, DNA-PK, Akt, Proteinase-3, Prohibitin, UNC-112, cathelicidin antimicrobial peptide (hCAP18), farnesylpyrophosphate synthase (FPPs), VAT-1 und ATP-synthase.

Die meisten dieser Proteine sind wichtige Mediatoren in der Zelltransduktion, im Immunsystem oder spielen eine Rolle im Entzündungsgeschehen sowie bei der Apoptose. Der Einfluss der BAs auf PKC und FPPs ist noch unklar, da *ex vivo* und *in vitro* Experimente zwar negativ ausfielen, Untersuchungen in klinischen Studien aber auf eine Beeinflussung schließen lassen[176]. Rap1b wird durch BAs in seiner Aktivität gehemmt, hier sind noch weitere Studien zur genaueren Charakterisierung nötig. CatG, DNA-PK und die Proteinkinase Akt konnten als Zielstrukturen von BAs mit hoher Affinität (IC_{50}-Werte < 5 µM) identifiziert werden, wobei die erreichbaren Plasmakonzentrationen mancher BAs pharmakologische Relevanz implizieren. Andere in der Literatur beschriebene Interaktionspartner benötigen für eine Hemmung sehr hohe Konzentrationen an BAs (z.B. 5-LO: 15-30 µM), so dass eine pharmakologische Relevanz *in vivo* bei der 5-LO und der HLE fraglich erscheint. Die proteolytische Aktivität von CatG wird konzentrationsabhängig, kompetitiv und reversibel mit IC_{50}-Werten von 0,6 µM (AKBA), 0,8 µM (β-BA), 1,1µM (Aβ-BA) und 3,7 µM (KBA)

gehemmt. Den BAs ähnliche Triterpene wie Amyrin oder Ursolsäure konnten die Aktivität von CatG bis zu einer Konzentration von 30 µM nicht signifikant supprimmieren. Auch die Aktivität anderer Serinproteasen wurde zum Teil sehr potent inhibiert, so konnte für Chymotrypsin ein IC_{50}-Wert von 4,8 µM (Aβ-BA) ermittelt werden, die anderen BAs waren weniger stark wirksam. Insgesamt ist die Effektivität bei CatG aber am höchsten. Nicht nur die proteolytische Aktivität von CatG wird in vitro inhibiert, auch die CatG-induzierte Migration von PMNL durch Matrigel wird mit einem IC_{50} von 2,9 µM (Aβ-BA) gehemmt. In unserem kleinen pharmakokinetischen Test (Phase I) konnte gezeigt werden, dass bei einem Plasmaspiegel von 6 µg/ml Aβ-BA die proteolytische Aktivität von CatG nur noch ca. 75% des Ausgangswertes beträgt.

DNA-PK und Akt sind Kinasen in der Signaltransduktion von Rezeptor-Tyrosinkinasen, deren Liganden Wachstumsfaktoren sind. Durch zellbasierte und zellfreie Experimente wurde gezeigt, dass BAs die Aktivität von DNA-PK und Akt hemmen und somit Wachstumssignale inhibieren. Die Phosphorylierung von Akt wird intrazellulär und im zellfreien System durch BAs stark reduziert, und die Aktivität von Akt wird extrazellulär durch BAs konzentrationsabhängig im nanomolaren Bereich inhibiert.

Weiterhin wurde der Einfluss von BAs auf verschiedene Elemente der Signaltransduktionskette untersucht. Hierbei stellen vor allem Ca^{2+}-Einstrom, Beeinflussung des MAP-Kinaseweges, Arachidonsäurefreisetzung, Thrombozytenaggregation und TNFα-Freisetzung interessante Ansatzpunkte dar. Die gefundenen Ergebnisse beleuchten die pharmakologischen Wirkungen der Weihrauchextrakte ein wenig besser, vor allem die sehr guten Ergebnisse bei chronisch entzündlichen Darmerkrankungen könnten nun aufgrund der sehr potenten Hemmung von Cathepsin G erklärbar sein.
Mittels sepharose-gebundener Boswelliasäuren konnten Zielstrukturen entdeckt werden, die selektiv und hochaffin an die BA-Sepharosen binden. Diese Strukturen sind größtenteils in wichtige Prozesse der zellulären Signalkaskade involviert. Durch die Identifizierung dieser hochaffinen Targets ist es möglich, die zelluläre Wirkung der BAs genauer aufzuklären und die BA-Grundstruktur zur Entwicklung neuer selektiver Arzneistoffe gegen chronisch entzündliche Erkrankungen und Krebs zu nutzen.

Des Weiteren wurde gezeigt, daß Celecoxib, ein gut charakterisierter, selektiver COX-2-Inhibitor, als hoch potenter 5-LO Inhibitor fungiert. Der Wirkstoff wird zur Therapie von Arthrosen und Rheumatoider Arthritis angewendet und kam als erster selektiver COX-2-Hemmer auf dem Markt. Die gastrointestinalen Nebenwirkungen sind gegenüber den unselektiven NSAR deutlich reduziert, zusätzlich konnte durch klinische Studien gezeigt werden, dass die Gefahr für kardiovaskuläre Ereignisse im Vergleich zu den anderen Coxiben – Rofecoxib (Vioxx®) wurde deshalb vom Markt genommen – stark erniedrigt ist und auf dem Niveau der klassischen Antirheumatika wie Ibuprofen oder Diclofenac liegt.
Durch Zufall wurde entdeckt, dass neben der bisher bekannten Wirkung Celecoxib bei Patienten mit familiärer Prädisposition die Polypentstehung im Darm stoppen kann. Diese Darmpolypen sind eine Vorstufe von Darmkrebs. Dieser Effekt konnte weder mit klassischen NSAR noch mit den anderen Coxiben erzielt werden, weshalb neben der COX-2 noch weitere Zielstrukturen beeinflusst werden mussten. Bei weiteren Studien konnte mit 800 mg/d Celecoxib bei einigen Patienten eine Remission von Darmtumorvorstufen erreicht werden, unzureichend mit einer COX-Hemmung erklärbar ist. Durch Untersuchungen an Patientenvollblut konnten verminderte Level an Leukotrienen unter Therapie gezeigt werden, die auf eine Beeinflussung des Leukotrienstoffwechsels hindeuten. Als interessante Zielstrukturen wurden FLAP und die 5-LO ausgewählt und bearbeitet. Schon schnell stellte sich heraus, dass FLAP nicht gehemmt wird (Untersuchungen von Dr. Maier und M. Hörnig). Die Aktivität der 5-LO wird sowohl in PMNL als auch in zellfreien Systemen inhibiert und zwar mit folgenden IC_{50}-Werten: 8 µM in intakten PMNL, 20 µM nach Zugabe von 20 µM Arachidonsäure und 30 µM im zellfreien System.
Seit 2006 ist Celecoxib in Europa als Orphan Drug zur Therapie der adenomatösen familiären Polyposis zugelassen. Weitere Anwendungen bei Erkrankungen mit hoher Beteiligung der 5-LO wie zum Beispiel Asthma bronchiale, entzündliche Erkrankungen oder bestimmte Krebsarten sind sinnvoll. Die duale Hemmung von 5-LO und COX eröffnet neue Behandlungsmöglichkeiten, so dass neben verstärkter antientzündlicher Wirkung die Nebenwirkungsrate gesenkt werden kann. Celecoxib ist zur Zeit der einzige zugelassene Arzneistoff, der über diesen dualen Wirkmechanismus verfügt.

8 References

1. Jauch, J., and J. Bergmann. 2003. An Efficient Method for the Large-Scale Preparation of 3-O-Acetyl-11-oxo-b-boswellic acid and Other Boswellic acids.
2. Werz, O., M. Brungs, and D. Steinhilber. 1996. Purification of transforming growth factor beta 1 from human platelets. *Pharmazie 51:893*.
3. Martinez, D., K. Lohs, and J. Janzen. 1988. *Weihrauch und Myrrhe. Kulturgeschichte und wirtschaftliche Bedeutung. Botanik*. Wissenschaftliche Verlagsgesellschaft, Stuttgart.
4. Poeckel, D., and O. Werz. 2006. Boswellic acids: biological actions and molecular targets. *Curr Med Chem 13:3359*.
5. Ammon, H. P. 2006. Boswellic acids in chronic inflammatory diseases. *Planta Med 72:1100*.
6. Safayhi, H., and E. R. Sailer. 1997. Anti-inflammatory actions of pentacyclic triterpenes. *Planta Med 63:487*.
7. Ammon, H. P. 2002. [Boswellic acids (components of frankincense) as the active principle in treatment of chronic inflammatory diseases]. *Wien Med Wochenschr 152:373*.
8. Safayhi, H., T. Mack, J. Sabieraj, M. I. Anazodo, L. R. Subramanian, and H. P. Ammon. 1992. Boswellic acids: novel, specific, nonredox inhibitors of 5-lipoxygenase. *J Pharmacol Exp Ther 261:1143*.
9. Poeckel, D., L. Tausch, N. Kather, J. Jauch, and O. Werz. 2006. Boswellic acids stimulate arachidonic acid release and 12-lipoxygenase activity in human platelets independent of Ca2+ and differentially interact with platelet-type 12-lipoxygenase. *Mol Pharmacol 70:1071*.
10. Safayhi, H., B. Rall, E. R. Sailer, and H. P. Ammon. 1997. Inhibition by boswellic acids of human leukocyte elastase. *J Pharmacol Exp Ther 281:460*.
11. Syrovets, T., B. Buchele, E. Gedig, J. R. Slupsky, and T. Simmet. 2000. Acetyl-boswellic acids are novel catalytic inhibitors of human topoisomerases I and IIalpha. *Mol Pharmacol 58:71*.
12. Syrovets, T., J. E. Gschwend, B. Buchele, Y. Laumonnier, W. Zugmaier, F. Genze, and T. Simmet. 2005. Inhibition of IkappaB kinase activity by acetyl-boswellic acids promotes apoptosis in androgen-independent PC-3 prostate cancer cells in vitro and in vivo. *J Biol Chem 280:6170*.
13. Glaser, T., S. Winter, P. Groscurth, H. Safayhi, E. R. Sailer, H. P. Ammon, M. Schabet, and M. Weller. 1999. Boswellic acids and malignant glioma: induction of apoptosis but no modulation of drug sensitivity. *Br J Cancer 80:756*.
14. Liu, J. J., A. Nilsson, S. Oredsson, V. Badmaev, W. Z. Zhao, and R. D. Duan. 2002. Boswellic acids trigger apoptosis via a pathway dependent on caspase-8 activation but independent on Fas/Fas ligand interaction in colon cancer HT-29 cells. *Carcinogenesis 23:2087*.
15. Koehler. 1887. *Koehler´s medical plants*.
16. Park, Y. S., J. H. Lee, J. A. Harwalkar, J. Bondar, H. Safayhi, and M. Golubic. 2002. Acetyl-11-keto-beta-boswellic acid (AKBA) is cytotoxic for meningioma cells and inhibits phosphorylation of the extracellular-signal regulated kinase 1 and 2. *Adv Exp Med Biol 507:387*.
17. Poeckel, D., L. Tausch, S. George, J. Jauch, and O. Werz. 2006. 3-O-Acetyl-11-keto-boswellic Acid Decreases Basal Intracellular Ca2+ Levels and Inhibits Agonist-Induced Ca2+ Mobilization and Mitogen-Activated Protein Kinase Activation in Human Monocytic Cells. *J Pharmacol Exp Ther 316:224*.

18. Takada, Y., H. Ichikawa, V. Badmaev, and B. B. Aggarwal. 2006. Acetyl-11-Keto-beta-Boswellic Acid Potentiates Apoptosis, Inhibits Invasion, and Abolishes Osteoclastogenesis by Suppressing NF-{kappa}B and NF-{kappa}B-Regulated Gene Expression. *J Immunol 176:3127*.
19. Liu, J. J., B. Huang, and S. C. Hooi. 2006. Acetyl-keto-beta-boswellic acid inhibits cellular proliferation through a p21-dependent pathway in colon cancer cells. *Br J Pharmacol 148:1099*.
20. Singh, G. B., and C. K. Atal. 1986. Pharmacology of an extract of salai guggal ex-Boswellia serrata, a new non-steroidal anti-inflammatory agent. *Agents Actions 18:407*.
21. Kimmatkar, N., V. Thawani, L. Hingorani, and R. Khiyani. 2003. Efficacy and tolerability of Boswellia serrata extract in treatment of osteoarthritis of knee--a randomized double blind placebo controlled trial. *Phytomedicine 10:3*.
22. Gupta, I., A. Parihar, P. Malhotra, G. B. Singh, R. Ludtke, H. Safayhi, and H. P. Ammon. 1997. Effects of Boswellia serrata gum resin in patients with ulcerative colitis. *Eur J Med Res 2:37*.
23. Gerhardt, H., F. Seifert, P. Buvari, H. Vogelsang, and R. Repges. 2001. [Therapy of active Crohn disease with Boswellia serrata extract H 15]. *Z Gastroenterol 39:11*.
24. Gupta, I., A. Parihar, P. Malhotra, S. Gupta, R. Ludtke, H. Safayhi, and H. P. Ammon. 2001. Effects of gum resin of Boswellia serrata in patients with chronic colitis. *Planta Med 67:391*.
25. Streffer, J. R., M. Bitzer, M. Schabet, J. Dichgans, and M. Weller. 2001. Response of radiochemotherapy-associated cerebral edema to a phytotherapeutic agent, H15. *Neurology 56:1219*.
26. Sterk, V., B. Buchele, and T. Simmet. 2004. Effect of food intake on the bioavailability of boswellic acids from a herbal preparation in healthy volunteers. *Planta Med 70:1155*.
27. Buchele, B., and T. Simmet. 2003. Analysis of 12 different pentacyclic triterpenic acids from frankincense in human plasma by high-performance liquid chromatography and photodiode array detection. *J Chromatogr B Analyt Technol Biomed Life Sci 795:355*.
28. Pham, C. T. 2006. Neutrophil serine proteases: specific regulators of inflammation. *Nat Rev Immunol 6:541*.
29. Campbell, E. J. 1982. Human leukocyte elastase, cathepsin G, and lactoferrin: family of neutrophil granule glycoproteins that bind to an alveolar macrophage receptor. *Proc Natl Acad Sci U S A 79:6941*.
30. Wiedow, O., and U. Meyer-Hoffert. 2005. Neutrophil serine proteases: potential key regulators of cell signalling during inflammation. *J Intern Med 257:319*.
31. Shafer, W. M., S. Katzif, S. Bowers, M. Fallon, M. Hubalek, M. S. Reed, P. Veprek, and J. Pohl. 2002. Tailoring an antibacterial peptide of human lysosomal cathepsin G to enhance its broad-spectrum action against antibiotic-resistant bacterial pathogens. *Curr Pharm Des 8:695*.
32. Reeves, E. P., H. Lu, H. L. Jacobs, C. G. Messina, S. Bolsover, G. Gabella, E. O. Potma, A. Warley, J. Roes, and A. W. Segal. 2002. Killing activity of neutrophils is mediated through activation of proteases by K+ flux. *Nature 416:291*.
33. Tkalcevic, J., M. Novelli, M. Phylactides, J. P. Iredale, A. W. Segal, and J. Roes. 2000. Impaired immunity and enhanced resistance to endotoxin in the absence of neutrophil elastase and cathepsin G. *Immunity 12:201*.
34. Salaun, C., D. J. James, J. Greaves, and L. H. Chamberlain. 2004. Plasma membrane targeting of exocytic SNARE proteins. *Biochim Biophys Acta 1693:81*.

35. Rest, R. F. 1988. Human neutrophil and mast cell proteases implicated in inflammation. *Methods Enzymol 163:309*.
36. Capodici, C., and R. A. Berg. 1989. Cathepsin G degrades denatured collagen. *Inflammation 13:137*.
37. Williams, S. E., T. I. Brown, A. Roghanian, and J. M. Sallenave. 2006. SLPI and elafin: one glove, many fingers. *Clin Sci (Lond) 110:21*.
38. Liu, Z., X. Zhou, S. D. Shapiro, J. M. Shipley, S. S. Twining, L. A. Diaz, R. M. Senior, and Z. Werb. 2000. The serpin alpha1-proteinase inhibitor is a critical substrate for gelatinase B/MMP-9 in vivo. *Cell 102:647*.
39. Churg, A., J. Dai, K. Zay, A. Karsan, R. Hendricks, C. Yee, R. Martin, R. MacKenzie, C. Xie, L. Zhang, S. Shapiro, and J. L. Wright. 2001. Alpha-1-antitrypsin and a broad spectrum metalloprotease inhibitor, RS113456, have similar acute anti-inflammatory effects. *Lab Invest 81:1119*.
40. Carden, D. L., and R. J. Korthuis. 1996. Protease inhibition attenuates microvascular dysfunction in postischemic skeletal muscle. *Am J Physiol 271:H1947*.
41. Kawabata, K., T. Hagio, S. Matsumoto, S. Nakao, S. Orita, Y. Aze, and H. Ohno. 2000. Delayed neutrophil elastase inhibition prevents subsequent progression of acute lung injury induced by endotoxin inhalation in hamsters. *Am J Respir Crit Care Med 161:2013*.
42. Kakimoto, K., A. Matsukawa, M. Yoshinaga, and H. Nakamura. 1995. Suppressive effect of a neutrophil elastase inhibitor on the development of collagen-induced arthritis. *Cell Immunol 165:26*.
43. Adkison, A. M., S. Z. Raptis, D. G. Kelley, and C. T. Pham. 2002. Dipeptidyl peptidase I activates neutrophil-derived serine proteases and regulates the development of acute experimental arthritis. *J Clin Invest 109:363*.
44. Hu, Y., and C. T. Pham. 2005. Dipeptidyl peptidase I regulates the development of collagen-induced arthritis. *Arthritis Rheum 52:2553*.
45. Sambrano, G. R., W. Huang, T. Faruqi, S. Mahrus, C. Craik, and S. R. Coughlin. 2000. Cathepsin G activates protease-activated receptor-4 in human platelets. *J Biol Chem 275:6819*.
46. Berahovich, R. D., Z. Miao, Y. Wang, B. Premack, M. C. Howard, and T. J. Schall. 2005. Proteolytic activation of alternative CCR1 ligands in inflammation. *J Immunol 174:7341*.
47. Sun, R., P. Iribarren, N. Zhang, Y. Zhou, W. Gong, E. H. Cho, S. Lockett, O. Chertov, F. Bednar, T. J. Rogers, J. J. Oppenheim, and J. M. Wang. 2004. Identification of neutrophil granule protein cathepsin G as a novel chemotactic agonist for the G protein-coupled formyl peptide receptor. *J Immunol 173:428*.
48. Chertov, O., H. Ueda, L. L. Xu, K. Tani, W. J. Murphy, J. M. Wang, O. M. Howard, T. J. Sayers, and J. J. Oppenheim. 1997. Identification of human neutrophil-derived cathepsin G and azurocidin/CAP37 as chemoattractants for mononuclear cells and neutrophils. *J Exp Med 186:739*.
49. Joos, S., T. Rosemann, J. Szecsenyi, E. G. Hahn, S. N. Willich, and B. Brinkhaus. 2006. Use of complementary and alternative medicine in Germany - a survey of patients with inflammatory bowel disease. *BMC Complement Altern Med 6:19*.
50. Lees-Miller, S. P., K. Sakaguchi, S. J. Ullrich, E. Appella, and C. W. Anderson. 1992. Human DNA-activated protein kinase phosphorylates serines 15 and 37 in the amino-terminal transactivation domain of human p53. *Mol Cell Biol 12:5041*.
51. Dragoi, A. M., X. Fu, S. Ivanov, P. Zhang, L. Sheng, D. Wu, G. C. Li, and W. M. Chu. 2005. DNA-PKcs, but not TLR9, is required for activation of Akt by CpG-DNA. *EMBO J 24:779*.

52. Sester, D. P., K. Brion, A. Trieu, H. S. Goodridge, T. L. Roberts, J. Dunn, D. A. Hume, K. J. Stacey, and M. J. Sweet. 2006. CpG DNA activates survival in murine macrophages through TLR9 and the phosphatidylinositol 3-kinase-Akt pathway. *J Immunol 177:4473*.
53. Datta, S. R., A. Brunet, and M. E. Greenberg. 1999. Cellular survival: a play in three Akts. *Genes Dev 13:2905*.
54. Brazil, D. P., and B. A. Hemmings. 2001. Ten years of protein kinase B signalling: a hard Akt to follow. *Trends Biochem Sci 26:657*.
55. Feng, J., J. Park, P. Cron, D. Hess, and B. A. Hemmings. 2004. Identification of a PKB/Akt hydrophobic motif Ser-473 kinase as DNA-dependent protein kinase. *J Biol Chem 279:41189*.
56. Mendelsohn, J., and Z. Fan. 1997. Epidermal growth factor receptor family and chemosensitization. *J Natl Cancer Inst 89:341*.
57. Bandyopadhyay, D., M. Mandal, L. Adam, J. Mendelsohn, and R. Kumar. 1998. Physical interaction between epidermal growth factor receptor and DNA-dependent protein kinase in mammalian cells. *J Biol Chem 273:1568*.
58. Huang, C., J. Li, M. Ding, S. S. Leonard, L. Wang, V. Castranova, V. Vallyathan, and X. Shi. 2001. UV Induces phosphorylation of protein kinase B (Akt) at Ser-473 and Thr-308 in mouse epidermal Cl 41 cells through hydrogen peroxide. *J Biol Chem 276:40234*.
59. Friedberg, J. W., H. Kim, M. McCauley, E. M. Hessel, P. Sims, D. C. Fisher, L. M. Nadler, R. L. Coffman, and A. S. Freedman. 2005. Combination immunotherapy with a CpG oligonucleotide (1018 ISS) and rituximab in patients with non-Hodgkin lymphoma: increased interferon-alpha/beta-inducible gene expression, without significant toxicity. *Blood 105:489*.
60. Henkels, K. M., and J. J. Turchi. 1997. Induction of apoptosis in cisplatin-sensitive and -resistant human ovarian cancer cell lines. *Cancer Res 57:4488*.
61. Piccolo, E., S. Vignati, T. Maffucci, P. F. Innominato, A. M. Riley, B. V. Potter, P. P. Pandolfi, M. Broggini, S. Iacobelli, P. Innocenti, and M. Falasca. 2004. Inositol pentakisphosphate promotes apoptosis through the PI 3-K/Akt pathway. *Oncogene 23:1754*.
62. Skorski, T., A. Bellacosa, M. Nieborowska-Skorska, M. Majewski, R. Martinez, J. K. Choi, R. Trotta, P. Wlodarski, D. Perrotti, T. O. Chan, M. A. Wasik, P. N. Tsichlis, and B. Calabretta. 1997. Transformation of hematopoietic cells by BCR/ABL requires activation of a PI-3k/Akt-dependent pathway. *Embo J 16:6151*.
63. Chu, W., X. Gong, Z. Li, K. Takabayashi, H. Ouyang, Y. Chen, A. Lois, D. J. Chen, G. C. Li, M. Karin, and E. Raz. 2000. DNA-PKcs is required for activation of innate immunity by immunostimulatory DNA. *Cell 103:909*.
64. Kostyuk, P., and A. Verkhratsky. 1994. Calcium stores in neurons and glia. *Neuroscience 63:381*.
65. Sailer, E. R., L. R. Subramanian, B. Rall, R. F. Hoernlein, H. P. Ammon, and H. Safayhi. 1996. Acetyl-11-keto-beta-boswellic acid (AKBA): structure requirements for binding and 5-lipoxygenase inhibitory activity. *Br J Pharmacol 117:615*.
66. Altmann, A., L. Fischer, M. Schubert-Zsilavecz, D. Steinhilber, and O. Werz. 2002. Boswellic acids activate p42(MAPK) and p38 MAPK and stimulate Ca(2+) mobilization. *Biochem Biophys Res Commun 290:185*.
67. Poeckel, D., L. Tausch, A. Altmann, C. Feisst, U. Klinkhardt, J. Graff, S. Harder, and O. Werz. 2005. Induction of central signalling pathways and select functional effects in human platelets by beta-boswellic acid. *Br J Pharmacol 146:514*.
68. Ruggeri, Z. M. 2002. Platelets in atherothrombosis. *Nat Med 8:1227*.

69. Holmsen, H. 1994. Significance of testing platelet functions in vitro. *Eur J Clin Invest 24 Suppl 1:3*.
70. Holmsen, H. 1991. Signal transducing mechanisms in platelets. *Proc Natl Sci Counc Repub China B 15:147*.
71. Kramer, R. M., E. F. Roberts, B. A. Strifler, and E. M. Johnstone. 1995. Thrombin induces activation of p38 MAP kinase in human platelets. *J Biol Chem 270:27395*.
72. Papkoff, J., R. H. Chen, J. Blenis, and J. Forsman. 1994. p42 mitogen-activated protein kinase and p90 ribosomal S6 kinase are selectively phosphorylated and activated during thrombin-induced platelet activation and aggregation. *Mol Cell Biol 14:463*.
73. Roberts, P. J., and C. J. Der. 2007. Targeting the Raf-MEK-ERK mitogen-activated protein kinase cascade for the treatment of cancer. *Oncogene 26:3291*.
74. McKay, M. M., and D. K. Morrison. 2007. Integrating signals from RTKs to ERK/MAPK. *Oncogene 26:3113*.
75. Ward, P. A., and M. S. Mulligan. 1994. Blocking of adhesion molecules in vivo as anti-inflammatory therapy. *Ther Immunol 1:165*.
76. Celotti, F., and S. Laufer. 2001. Anti-inflammatory drugs: new multitarget compounds to face an old problem. The dual inhibition concept. *Pharmacol Res 43:429*.
77. Vane, J. R., and R. M. Botting. 1996. Mechanism of action of anti-inflammatory drugs. *Scand J Rheumatol Suppl 102:9*.
78. Furst, D. E. 1999. Pharmacology and efficacy of cyclooxygenase (COX) inhibitors. *Am J Med 107:18S*.
79. Werz, O., and D. Steinhilber. 2006. Therapeutic options for 5-lipoxygenase inhibitors. *Pharmacol Ther 112:701*.
80. Gupta, S., M. Srivastava, N. Ahmad, K. Sakamoto, D. G. Bostwick, and H. Mukhtar. 2001. Lipoxygenase-5 is overexpressed in prostate adenocarcinoma. *Cancer 91:737*.
81. Werz, O. 2002. 5-lipoxygenase: cellular biology and molecular pharmacology. *Curr Drug Targets Inflamm Allergy 1:23*.
82. Peters-Golden, M., and T. G. Brock. 2003. 5-lipoxygenase and FLAP. *Prostaglandins Leukot Essent Fatty Acids 69:99*.
83. Luo, M., S. M. Jones, S. M. Phare, M. J. Coffey, M. Peters-Golden, and T. G. Brock. 2004. Protein kinase A inhibits leukotriene synthesis by phosphorylation of 5-lipoxygenase on serine 523. *J Biol Chem 279:41512*.
84. Werz, O., J. Klemm, O. Radmark, and B. Samuelsson. 2001. p38 MAP kinase mediates stress-induced leukotriene synthesis in a human B-lymphocyte cell line. *J Leukoc Biol 70:830*.
85. Werz, O., E. Burkert, B. Samuelsson, O. Radmark, and D. Steinhilber. 2002. Activation of 5-lipoxygenase by cell stress is calcium independent in human polymorphonuclear leukocytes. *Blood 99:1044*.
86. Borgeat, P., and B. Samuelsson. 1979. Arachidonic acid metabolism in polymorphonuclear leukocytes: effects of ionophore A23187. *Proc Natl Acad Sci U S A 76:2148*.
87. Fischer, L., D. Poeckel, E. Buerkert, D. Steinhilber, and O. Werz. 2005. Inhibitors of actin polymerisation stimulate arachidonic acid release and 5-lipoxygenase activation by upregulation of Ca2+ mobilisation in polymorphonuclear leukocytes involving Src family kinases. *Biochim Biophys Acta 1736:109*.
88. Rådmark, O., and B. Samuelsson. 2005. Regulation of 5-lipoxygenase enzyme activity. *Biochem Biophys Res Commun 338:102*.
89. Perkins, D. J., and D. A. Kniss. 1997. Rapid and transient induction of cyclo-oxygenase 2 by epidermal growth factor in human amnion-derived WISH cells. *Biochem J 321:677*.

90. Diaz, A., K. P. Chepenik, J. H. Korn, A. M. Reginato, and S. A. Jimenez. 1998. Differential regulation of cyclooxygenases 1 and 2 by interleukin-1 beta, tumor necrosis factor-alpha, and transforming growth factor-beta 1 in human lung fibroblasts. *Exp Cell Res 241:222*.
91. Silverstein, F. E., G. Faich, J. L. Goldstein, L. S. Simon, T. Pincus, A. Whelton, R. Makuch, G. Eisen, N. M. Agrawal, W. F. Stenson, A. M. Burr, W. W. Zhao, J. D. Kent, J. B. Lefkowith, K. M. Verburg, and G. S. Geis. 2000. Gastrointestinal toxicity with celecoxib vs nonsteroidal anti-inflammatory drugs for osteoarthritis and rheumatoid arthritis: the CLASS study: A randomized controlled trial. Celecoxib Long-term Arthritis Safety Study. *JAMA 284:1247*.
92. Steinbach, G., P. M. Lynch, R. K. Phillips, M. H. Wallace, E. Hawk, G. B. Gordon, N. Wakabayashi, B. Saunders, Y. Shen, T. Fujimura, L. K. Su, and B. Levin. 2000. The effect of celecoxib, a cyclooxygenase-2 inhibitor, in familial adenomatous polyposis. *N Engl J Med 342:1946*.
93. Grosch, S., I. Tegeder, E. Niederberger, L. Brautigam, and G. Geisslinger. 2001. COX-2 independent induction of cell cycle arrest and apoptosis in colon cancer cells by the selective COX-2 inhibitor celecoxib. *FASEB J 15:2742*.
94. Maier, T. J., K. Schilling, R. Schmidt, G. Geisslinger, and S. Grosch. 2004. Cyclooxygenase-2 (COX-2)-dependent and -independent anticarcinogenic effects of celecoxib in human colon carcinoma cells. *Biochem Pharmacol 67:1469*.
95. Johnson, A. J., A. L. Hsu, H. P. Lin, X. Song, and C. S. Chen. 2002. The cyclo-oxygenase-2 inhibitor celecoxib perturbs intracellular calcium by inhibiting endoplasmic reticulum Ca2+-ATPases: a plausible link with its anti-tumour effect and cardiovascular risks. *Biochem J 366:831*.
96. Saini, S. S., D. L. Gessell-Lee, and J. W. Peterson. 2003. The cox-2-specific inhibitor celecoxib inhibits adenylyl cyclase. *Inflammation 27:79*.
97. Kulp, S. K., Y. T. Yang, C. C. Hung, K. F. Chen, J. P. Lai, P. H. Tseng, J. W. Fowble, P. J. Ward, and C. S. Chen. 2004. 3-phosphoinositide-dependent protein kinase-1/Akt signaling represents a major cyclooxygenase-2-independent target for celecoxib in prostate cancer cells. *Cancer Res 64:1444*.
98. Maier, T. J., A. Janssen, R. Schmidt, G. Geisslinger, and S. Grosch. 2005. Targeting the beta-catenin/APC pathway: a novel mechanism to explain the cyclooxygenase-2-independent anticarcinogenic effects of celecoxib in human colon carcinoma cells. *FASEB J 19:1353*.
99. McAdam, B. F., F. Catella-Lawson, I. A. Mardini, S. Kapoor, J. A. Lawson, and G. A. FitzGerald. 1999. Systemic biosynthesis of prostacyclin by cyclooxygenase (COX)-2: the human pharmacology of a selective inhibitor of COX-2. *Proc Natl Acad Sci U S A 96:272*.
100. Syrovets, T., B. Buchele, C. Krauss, Y. Laumonnier, and T. Simmet. 2005. Acetyl-boswellic acids inhibit lipopolysaccharide-mediated TNF-alpha induction in monocytes by direct interaction with IkappaB kinases. *J Immunol 174:498*.
101. Werz, O., D. Szellas, M. Henseler, and D. Steinhilber. 1998. Nonredox 5-lipoxygenase inhibitors require glutathione peroxidase for efficient inhibition of 5-lipoxygenase activity. *Mol Pharmacol 54:445*.
102. Altmann, A. Boswelliasäuren : Modulation zellulärer Signaltransduktionsmechanismen in Leukozyten und Thrombozyten und Korrelation zu funktionellen Eigenschaften. In *Institut für Pharmazeutische Chemie*, (2003); Vol. Johann Wolfgang Goethe-Universität, Frankfurt.
103. Poeckel, D. Pharmacological actions and targets of boswellic acids in human leukocytes and platelets. In *Institut für Pharmazeutische Chemie*, (2006); Vol. Johann Wolfgang Goethe-Universität, Frankfurt, p. 152.

104. Altmann, A., D. Poeckel, L. Fischer, M. Schubert-Zsilavecz, D. Steinhilber, and O. Werz. 2004. Coupling of boswellic acid-induced Ca2+ mobilisation and MAPK activation to lipid metabolism and peroxide formation in human leucocytes. *British Journal of Pharmacology 141:223*.
105. Brungs, M., O. Radmark, B. Samuelsson, and D. Steinhilber. 1995. Sequential induction of 5-lipoxygenase gene expression and activity in Mono Mac 6 cells by transforming growth factor beta and 1,25-dihydroxyvitamin D3. *Proc Natl Acad Sci U S A 92:107*.
106. Boyum, A. 1968. Isolation of leucocytes from human blood. A two-phase system for removal of red cells with methylcellulose as erythrocyte-aggregating agent. *Scand J Clin Lab Invest Suppl 97:9*.
107. Albert, D., I. Zundorf, T. Dingermann, W. E. Muller, D. Steinhilber, and O. Werz. 2002. Hyperforin is a dual inhibitor of cyclooxygenase-1 and 5-lipoxygenase. *Biochem Pharmacol 64:1767*.
108. Fischer, L., D. Szellas, O. Rådmark, D. Steinhilber, and O. Werz. 2003. Phosphorylation- and stimulus-dependent inhibition of cellular 5-lipoxygenase activity by nonredox-type inhibitors. *FASEB J 17:949*.
109. Werz, O., and D. Steinhilber. 1996. Selenium-dependent peroxidases suppress 5-lipoxygenase activity in B-lymphocytes and immature myeloid cells. The presence of peroxidase-insensitive 5-lipoxygenase activity in differentiated myeloid cells. *Eur J Biochem 242:90*.
110. Maurer-Spurej, E., G. Pfeiler, N. Maurer, H. Lindner, O. Glatter, and D. V. Devine. 2001. Room temperature activates human blood platelets. *Lab Invest 81:581*.
111. Neuhoff, V., R. Stamm, I. Pardowitz, N. Arold, W. Ehrhardt, and D. Taube. 1990. Essential problems in quantification of proteins following colloidal staining with coomassie brilliant blue dyes in polyacrylamide gels, and their solution. *Electrophoresis 11:101*.
112. Shevchenko, A., M. Wilm, O. Vorm, and M. Mann. 1996. Mass spectrometric sequencing of proteins silver-stained polyacrylamide gels. *Anal Chem 68:850*.
113. Rosenfeld, J., J. Capdevielle, J. C. Guillemot, and P. Ferrara. 1992. In-gel digestion of proteins for internal sequence analysis after one- or two-dimensional gel electrophoresis. *Anal Biochem 203:173*.
114. Corvey, C., P. Koetter, T. Beckhaus, J. Hack, S. Hofmann, M. Hampel, T. Stein, M. Karas, and K. D. Entian. 2005. Carbon Source-dependent assembly of the Snf1p kinase complex in Candida albicans. *J Biol Chem 280:25323*.
115. Chen, H., J. Kovar, S. Sissons, K. Cox, W. Matter, F. Chadwell, P. Luan, C. J. Vlahos, A. Schutz-Geschwender, and D. M. Olive. 2005. A cell-based immunocytochemical assay for monitoring kinase signaling pathways and drug efficacy. *Anal Biochem 338:136*.
116. Johansson, A., R. Claesson, G. Belibasakis, E. Makoveichuk, L. Hanstrom, G. Olivecrona, G. Sandstrom, and S. Kalfas. 2001. Protease inhibitors, the responsible components for the serum-dependent enhancement of Actinobacillus actinomycetemcomitans leukotoxicity. *Eur J Oral Sci 109:335*.
117. Attucci, S., B. Korkmaz, L. Juliano, E. Hazouard, C. Girardin, M. Brillard-Bourdet, S. Rehault, P. Anthonioz, and F. Gauthier. 2002. Measurement of free and membrane-bound cathepsin G in human neutrophils using new sensitive fluorogenic substrates. *Biochem J 366:965*.
118. Jones, G., P. Willett, and R. C. Glen. 1995. A genetic algorithm for flexible molecular overlay and pharmacophore elucidation. *J Comput Aided Mol Des 9:532*.
119. Ponder, J. W., and D. A. Case. 2003. Force fields for protein simulations. *Adv Protein Chem 66:27*.

120. Halgren, T. A. 1995. Potential energy functions. *Curr Opin Struct Biol 5:205*.
121. DeLano, W. L. 2002. Unraveling hot spots in binding interfaces: progress and challenges. *Curr Opin Struct Biol 12:14*.
122. Hemker, H. C., P. L. Giesen, M. Ramjee, R. Wagenvoord, and S. Beguin. 2000. The thrombogram: monitoring thrombin generation in platelet-rich plasma. *Thromb Haemost 83:589*.
123. Grynkiewicz, G., M. Poenie, and R. Y. Tsien. 1985. A new generation of Ca2+ indicators with greatly improved fluorescence properties. *J Biol Chem 260:3440*.
124. Cavarra, E., A. Santucci, and G. Lungarella. 1995. Purification and N-terminal amino-acid sequence analysis of rabbit neutrophil cathepsin G. *Biol Chem Hoppe Seyler 376:371*.
125. Lowry, O. H., N. J. Rosebrough, A. L. Farr, and R. J. Randall. 1951. Protein measurement with the Folin phenol reagent. *J Biol Chem 193:265*.
126. Legler, G., C. M. Muller-Platz, M. Mentges-Hettkamp, G. Pflieger, and E. Julich. 1985. On the chemical basis of the Lowry protein determination. *Anal Biochem 150:278*.
127. Bradford, M. M. 1976. A rapid and sensitive method for the quantitation of microgram quantities of protein utilizing the principle of protein-dye binding. *Anal Biochem 72:248*.
128. Read, S. M., and D. H. Northcote. 1981. Minimization of variation in the response to different proteins of the Coomassie blue G dye-binding assay for protein. *Anal Biochem 116:53*.
129. de Garavilla, L., M. N. Greco, N. Sukumar, Z. W. Chen, A. O. Pineda, F. S. Mathews, E. Di Cera, E. C. Giardino, G. I. Wells, B. J. Haertlein, J. A. Kauffman, T. W. Corcoran, C. K. Derian, A. J. Eckardt, B. P. Damiano, P. Andrade-Gordon, and B. E. Maryanoff. 2005. A novel, potent dual inhibitor of the leukocyte proteases cathepsin G and chymase: molecular mechanisms and anti-inflammatory activity in vivo. *J Biol Chem 280:18001*.
130. Rashid, U. J., D. Paterok, A. Koglin, H. Gohlke, J. Piehler, and J. C. Chen. 2007. Structure of Aquifex aeolicus argonaute highlights conformational flexibility of the PAZ domain as a potential regulator of RISC function. *J Biol Chem 282:13824*.
131. Burdine, L., and T. Kodadek. 2004. Target identification in chemical genetics: the (often) missing link. *Chem Biol 11:593*.
132. Taunton, J., C. A. Hassig, and S. L. Schreiber. 1996. A mammalian histone deacetylase related to the yeast transcriptional regulator Rpd3p. *Science 272:408*.
133. Harding, M. W., A. Galat, D. E. Uehling, and S. L. Schreiber. 1989. A receptor for the immunosuppressant FK506 is a cis-trans peptidyl-prolyl isomerase. *Nature 341:758*.
134. Fischer, T. H., M. N. Gatling, F. McCormick, C. M. Duffy, and G. C. White, 2nd. 1994. Incorporation of Rap 1b into the platelet cytoskeleton is dependent on thrombin activation and extracellular calcium. *J Biol Chem 269:17257*.
135. de Bruyn, K. M., F. J. Zwartkruis, J. de Rooij, J. W. Akkerman, and J. L. Bos. 2003. The small GTPase Rap1 is activated by turbulence and is involved in integrin [alpha]IIb[beta]3-mediated cell adhesion in human megakaryocytes. *J Biol Chem 278:22412*.
136. Franke, B., J. W. Akkerman, and J. L. Bos. 1997. Rapid Ca2+-mediated activation of Rap1 in human platelets. *Embo J 16:252*.
137. Lova, P., S. Paganini, F. Sinigaglia, C. Balduini, and M. Torti. 2002. A Gi-dependent pathway is required for activation of the small GTPase Rap1B in human platelets. *J Biol Chem 277:12009*.
138. Woulfe, D., H. Jiang, R. Mortensen, J. Yang, and L. F. Brass. 2002. Activation of Rap1B by G(i) family members in platelets. *J Biol Chem 277:23382*.

139. Danielewski, O., J. Schultess, and A. Smolenski. 2005. The NO/cGMP pathway inhibits Rap 1 activation in human platelets via cGMP-dependent protein kinase I. *Thromb Haemost 93:319*.
140. Skarke, C., M. Reus, R. Schmidt, I. Grundei, P. Schuss, G. Geisslinger, and J. Lotsch. 2006. The cyclooxygenase 2 genetic variant -765G>C does not modulate the effects of celecoxib on prostaglandin E2 production. *Clin Pharmacol Ther 80:621*.
141. Hof, P., I. Mayr, R. Huber, E. Korzus, J. Potempa, J. Travis, J. C. Powers, and W. Bode. 1996. The 1.8 A crystal structure of human cathepsin G in complex with Suc-Val-Pro-PheP-(OPh)2: a Janus-faced proteinase with two opposite specificities. *EMBO J 15:5481*.
142. Hanke, J. H., J. P. Gardner, R. L. Dow, P. S. Changelian, W. H. Brissette, E. J. Weringer, B. A. Pollok, and P. A. Connelly. 1996. Discovery of a novel, potent, and Src family-selective tyrosine kinase inhibitor. Study of Lck- and FynT-dependent T cell activation. *J Biol Chem 271:695*.
143. Blake, R. A., M. A. Broome, X. Liu, J. Wu, M. Gishizky, L. Sun, and S. A. Courtneidge. 2000. SU6656, a selective src family kinase inhibitor, used to probe growth factor signaling. *Mol Cell Biol 20:9018*.
144. Gijon, M. A., and C. C. Leslie. 1999. Regulation of arachidonic acid release and cytosolic phospholipase A2 activation. *J Leukoc Biol 65:330*.
145. Bae, Y. S., T. G. Lee, J. C. Park, J. H. Hur, Y. Kim, K. Heo, J. Y. Kwak, P. G. Suh, and S. H. Ryu. 2003. Identification of a compound that directly stimulates phospholipase C activity. *Mol Pharmacol 63:1043*.
146. Vassalli, P. 1992. The pathophysiology of tumor necrosis factors. *Annu Rev Immunol 10:411*.
147. Greaves, D. R., and K. M. Channon. 2002. Inflammation and immune responses in atherosclerosis. *Trends Immunol 23:535*.
148. Watanabe, N., K. Nakada, and Y. Kobayashi. 1998. Processing and release of tumor necrosis factor alpha. *Eur J Biochem 253:576*.
149. Heemskerk, J. W., E. M. Bevers, and T. Lindhout. 2002. Platelet activation and blood coagulation. *Thromb Haemost 88:186*.
150. Carter, G. W., P. R. Young, D. H. Albert, J. Bouska, R. Dyer, R. L. Bell, J. B. Summers, and D. W. Brooks. 1991. 5-lipoxygenase inhibitory activity of zileuton. *J Pharmacol Exp Ther 256:929*.
151. Brautigam, L., G. Vetter, I. Tegeder, G. Heinkele, and G. Geisslinger. 2001. Determination of celecoxib in human plasma and rat microdialysis samples by liquid chromatography tandem mass spectrometry. *J Chromatogr B Biomed Sci Appl 761:203*.
152. Werz, O., D. Szellas, D. Steinhilber, and O. Radmark. 2002. Arachidonic acid promotes phosphorylation of 5-lipoxygenase at Ser-271 by MAPK-activated protein kinase 2 (MK2). *J Biol Chem 277:14793*.
153. Rakonjac, M., L. Fischer, P. Provost, O. Werz, D. Steinhilber, B. Samuelsson, and O. Radmark. 2006. Coactosin-like protein supports 5-lipoxygenase enzyme activity and up-regulates leukotriene A4 production. *Proc Natl Acad Sci U S A 103:13150*.
154. Fischer, L., D. Steinhilber, and O. Werz. 2004. Molecular pharmacological profile of the nonredox-type 5-lipoxygenase inhibitor CJ-13,610. *Br J Pharmacol 142:861*.
155. Maryanoff, B. E. 2004. Inhibitors of serine proteases as potential therapeutic agents: the road from thrombin to tryptase to cathepsin G. *J Med Chem 47:769*.
156. Safayhi, H., E. R. Sailer, and H. P. Ammon. 1995. Mechanism of 5-lipoxygenase inhibition by acetyl-11-keto-beta-boswellic acid. *Mol Pharmacol 47:1212*.
157. Werz, O., N. Schneider, M. Brungs, E. R. Sailer, H. Safayhi, H. P. Ammon, and D. Steinhilber. 1997. A test system for leukotriene synthesis inhibitors based on the in-

vitro differentiation of the human leukemic cell lines HL-60 and Mono Mac 6. *Naunyn Schmiedebergs Arch Pharmacol 356:441*.

158. Elsbach, P. 2003. What is the real role of antimicrobial polypeptides that can mediate several other inflammatory responses? *J Clin Invest 111:1643*.
159. Sobajima, J., S. Ozaki, T. Okazaki, F. Osakada, S. Sumita, K. Mori, and K. Nakao. 1996. Anti-neutrophil cytoplasmic antibodies (ANCA) in ulcerative colitis: anti-cathepsin G and a novel antibody correlate with a refractory type. *Clin Exp Immunol 105:120*.
160. Kossa, K., A. Coulthart, C. T. Ives, C. D. Pusey, and H. J. Hodgson. 1995. Antigen specificity of circulating anti-neutrophil cytoplasmic antibodies in inflammatory bowel disease. *Eur J Gastroenterol Hepatol 7:783*.
161. Kuwana, T., Y. Sato, M. Saka, Y. Kondo, M. Miyata, K. Obara, T. Nishimaki, and R. Kasukawa. 2000. Anti-cathepsin G antibodies in the sera of patients with ulcerative colitis. *J Gastroenterol 35:682*.
162. Locht, H., T. Skogh, and A. Wiik. 2000. Characterisation of autoantibodies to neutrophil granule constituents among patients with reactive arthritis, rheumatoid arthritis, and ulcerative colitis. *Ann Rheum Dis 59:898*.
163. Anthoni, C., M. G. Laukoetter, E. Rijcken, T. Vowinkel, R. Mennigen, S. Muller, N. Senninger, J. Russell, J. Jauch, J. Bergmann, D. N. Granger, and C. F. Krieglstein. Mechanisms underlying the anti-inflammatory actions of boswellic acid derivatives in experimental colitis.
164. Basu, A., D. Lu, B. Sun, A. N. Moor, G. R. Akkaraju, and J. Huang. 2002. Proteolytic activation of protein kinase C-epsilon by caspase-mediated processing and transduction of antiapoptotic signals. *J Biol Chem 277:41850*.
165. Lu, D., J. Huang, and A. Basu. 2006. Protein kinase Cepsilon activates protein kinase B/Akt via DNA-PK to protect against tumor necrosis factor-alpha-induced cell death. *J Biol Chem 281:22799*.
166. Lu, D., J. Huang, and A. Basu. 2004. Deregulation of PKB influences antiapoptotic signaling by PKC in breast cancer cells. *Int J Oncol 25:671*.
167. O'Toole, A., S. K. Moule, P. J. Lockyer, and A. P. Halestrap. 2001. Tumour necrosis factor-alpha activation of protein kinase B in WEHI-164 cells is accompanied by increased phosphorylation of Ser473, but not Thr308. *Biochem J 359:119*.
168. Gottlieb, T. M., and S. P. Jackson. 1993. The DNA-dependent protein kinase: requirement for DNA ends and association with Ku antigen. *Cell 72:131*.
169. Chan, D. W., and S. P. Lees-Miller. 1996. The DNA-dependent protein kinase is inactivated by autophosphorylation of the catalytic subunit. *J Biol Chem 271:8936*.
170. Damia, G., L. Filiberti, F. Vikhanskaya, L. Carrassa, Y. Taya, M. D'Incalci, and M. Broggini. 2001. Cisplatinum and taxol induce different patterns of p53 phosphorylation. *Neoplasia 3:10*.
171. Smith, G. C., and S. P. Jackson. 1999. The DNA-dependent protein kinase. *Genes Dev 13:916*.
172. Taccioli, G. E., A. G. Amatucci, H. J. Beamish, D. Gell, X. H. Xiang, M. I. Torres Arzayus, A. Priestley, S. P. Jackson, A. Marshak Rothstein, P. A. Jeggo, and V. L. Herrera. 1998. Targeted disruption of the catalytic subunit of the DNA-PK gene in mice confers severe combined immunodeficiency and radiosensitivity. *Immunity 9:355*.
173. Gao, Y., J. Chaudhuri, C. Zhu, L. Davidson, D. T. Weaver, and F. W. Alt. 1998. A targeted DNA-PKcs-null mutation reveals DNA-PK-independent functions for KU in V(D)J recombination. *Immunity 9:367*.
174. Chen, W. S., P. Z. Xu, K. Gottlob, M. L. Chen, K. Sokol, T. Shiyanova, I. Roninson, W. Weng, R. Suzuki, K. Tobe, T. Kadowaki, and N. Hay. 2001. Growth retardation

and increased apoptosis in mice with homozygous disruption of the Akt1 gene. *Genes Dev 15:2203*.

175. Feng, J., R. Tamaskovic, Z. Yang, D. P. Brazil, A. Merlo, D. Hess, and B. A. Hemmings. 2004. Stabilization of Mdm2 via decreased ubiquitination is mediated by protein kinase B/Akt-dependent phosphorylation. *J Biol Chem 279:35510*.
176. Bouhmidi-Boumariz, Z. 2004. Veränderung der Kochendichte bei der Therapie mit dem Boswellia serrata Extrakt H15 bei chronisch entzündlichen Darmerkrankungen. *Dissertationen der Ruprecht-Karls-Universität Heidelberg*.
177. Wootton, D. M., and D. N. Ku. 1999. Fluid mechanics of vascular systems, diseases, and thrombosis. *Annu Rev Biomed Eng 1:299*.
178. Geiger, J., and U. Walter. 1993. Properties and regulation of human platelet cation channels. *Exs 66:281*.
179. Watson, S. P., J. M. Auger, O. J. McCarty, and A. C. Pearce. 2005. GPVI and integrin alphaIIb beta3 signaling in platelets. *J Thromb Haemost 3:1752*.
180. Jackson, S. P., and S. M. Schoenwaelder. 2003. Antiplatelet therapy: in search of the 'magic bullet'. *Nat Rev Drug Discov 2:775*.
181. Rosado, J. A., and S. O. Sage. 2001. Role of the ERK pathway in the activation of store-mediated calcium entry in human platelets. *J Biol Chem 276:15659*.
182. Broad, L. M., T. R. Cannon, A. D. Short, and C. W. Taylor. 1999. Receptors linked to polyphosphoinositide hydrolysis stimulate Ca2+ extrusion by a phospholipase C-independent mechanism. *Biochem J 342 (Pt 1):199*.
183. Dobrydneva, Y., and P. Blackmore. 2001. 2-Aminoethoxydiphenyl borate directly inhibits store-operated calcium entry channels in human platelets. *Mol Pharmacol 60:541*.
184. Lee, S. B., A. K. Rao, K. H. Lee, X. Yang, Y. S. Bae, and S. G. Rhee. 1996. Decreased expression of phospholipase C-beta 2 isozyme in human platelets with impaired function. *Blood 88:1684*.
185. Rhee, S. G. 2001. Regulation of phosphoinositide-specific phospholipase C. *Annu Rev Biochem 70:281*.
186. Kim, S., J. Jin, and S. P. Kunapuli. 2004. Akt activation in platelets depends on Gi signaling pathways. *J Biol Chem 279:4186*.
187. Saklatvala, J., L. Rawlinson, R. J. Waller, S. Sarsfield, J. C. Lee, L. F. Morton, M. J. Barnes, and R. W. Farndale. 1996. Role for p38 mitogen-activated protein kinase in platelet aggregation caused by collagen or a thromboxane analogue. *J Biol Chem 271:6586*.
188. Steen, V. M., and H. Holmsen. 1987. Current aspects on human platelet activation and responses. *Eur J Haematol 38:383*.
189. Le Blanc, K., A. Berg, J. Palmblad, and J. Samuelsson. 2000. Defective platelet aggregation in polycythaemia vera is not caused by impaired calcium signaling, phospholipase D activation or decreased amounts of focal adhesion proteins. *Eur J Haematol 65:322*.
190. Fuse, I., W. Higuchi, Y. Uesugi, A. Hattori, and Y. Aizawa. 1999. Relationship between intracellular calcium-dependent process and protein-tyrosine phosphorylation in human platelets: studies of platelets from a patient with defective A23187-induced platelet aggregation. *Clin Lab Haematol 21:29*.
191. Werz, O., and D. Steinhilber. 2005. Development of 5-lipoxygenase inhibitors--lessons from cellular enzyme regulation. *Biochem Pharmacol 70:327*.
192. Rouzer, C. A., A. W. Ford-Hutchinson, H. E. Morton, and J. W. Gillard. 1990. MK886, a potent and specific leukotriene biosynthesis inhibitor blocks and reverses the membrane association of 5-lipoxygenase in ionophore-challenged leukocytes. *J Biol Chem 265:1436*.

193. Chen, X., S. Wang, N. Wu, S. Sood, P. Wang, Z. Jin, D. G. Beer, T. J. Giordano, Y. Lin, W. C. Shih, R. A. Lubet, and C. S. Yang. 2004. Overexpression of 5-lipoxygenase in rat and human esophageal adenocarcinoma and inhibitory effects of zileuton and celecoxib on carcinogenesis. *Clin Cancer Res 10:6703*.
194. Pommery, J., N. Pommery, and J. P. Henichart. 2005. Modification of eicosanoid profile in human blood treated by dual COX/LOX inhibitors. *Prostaglandins Leukot Essent Fatty Acids 73:411*.
195. Mao, J. T., I. H. Tsu, S. M. Dubinett, B. Adams, T. Sarafian, F. Baratelli, M. D. Roth, and K. J. Serio. 2004. Modulation of pulmonary leukotriene B4 production by cyclooxygenase-2 inhibitors and lipopolysaccharide. *Clin Cancer Res 10:6872*.
196. Romano, M., and J. Claria. 2003. Cyclooxygenase-2 and 5-lipoxygenase converging functions on cell proliferation and tumor angiogenesis: implications for cancer therapy. *FASEB J 17:1986*.
197. Grosch, S., T. J. Maier, S. Schiffmann, and G. Geisslinger. 2006. Cyclooxygenase-2 (COX-2)-independent anticarcinogenic effects of selective COX-2 inhibitors. *J Natl Cancer Inst 98:736*.
198. Tong, W. G., X. Z. Ding, and T. E. Adrian. 2002. The mechanisms of lipoxygenase inhibitor-induced apoptosis in human breast cancer cells. *Biochem Biophys Res Commun 296:942*.
199. Fan, X. M., S. P. Tu, S. K. Lam, W. P. Wang, J. Wu, W. M. Wong, M. F. Yuen, M. C. Lin, H. F. Kung, and B. C. Wong. 2004. Five-lipoxygenase-activating protein inhibitor MK-886 induces apoptosis in gastric cancer through upregulation of p27kip1 and bax. *J Gastroenterol Hepatol 19:31*.
200. Mezhybovska, M., K. Wikstrom, J. F. Ohd, and A. Sjolander. 2005. Pro-inflammatory mediator leukotriene D4 induces transcriptional activity of potentially oncogenic genes. *Biochem Soc Trans 33:698*.
201. Tong, W. G., X. Z. Ding, M. S. Talamonti, R. H. Bell, and T. E. Adrian. 2005. LTB4 stimulates growth of human pancreatic cancer cells via MAPK and PI-3 kinase pathways. *Biochem Biophys Res Commun 335:949*.
202. Charlier, C., and C. Michaux. 2003. Dual inhibition of cyclooxygenase-2 (COX-2) and 5-lipoxygenase (5-LOX) as a new strategy to provide safer non-steroidal anti-inflammatory drugs. *Eur J Med Chem 38:645*.
203. Singh, V. P., C. S. Patil, and S. K. Kulkarni. 2005. Effect of licofelone against mechanical hyperalgesia and cold allodynia in the rat model of incisional pain. *Pharmacol Rep 57:380*.
204. Fiorucci, S., R. Meli, M. Bucci, and G. Cirino. 2001. Dual inhibitors of cyclooxygenase and 5-lipoxygenase. A new avenue in anti-inflammatory therapy? *Biochem Pharmacol 62:1433*.
205. Mamdani, M., P. A. Rochon, D. N. Juurlink, A. Kopp, G. M. Anderson, G. Naglie, P. C. Austin, and A. Laupacis. 2002. Observational study of upper gastrointestinal haemorrhage in elderly patients given selective cyclo-oxygenase-2 inhibitors or conventional non-steroidal anti-inflammatory drugs. *BMJ 325:624.*
206. Hippisley-Cox, J., C. Coupland, and R. Logan. 2005. Risk of adverse gastrointestinal outcomes in patients taking cyclo-oxygenase-2 inhibitors or conventional non-steroidal anti-inflammatory drugs: population based nested case-control analysis. *BMJ 331:1310*.
207. Schneeweiss, S., D. H. Solomon, P. S. Wang, J. Rassen, and M. A. Brookhart. 2006. Simultaneous assessment of short-term gastrointestinal benefits and cardiovascular risks of selective cyclooxygenase 2 inhibitors and nonselective nonsteroidal antiinflammatory drugs: an instrumental variable analysis. *Arthritis Rheum 54:3390*.

9 Presentations

9.1 Poster presentation

Tausch L, Poeckel D, Altmann A, Werz O
Studies on the anti-inflammatory mode of action of boswellic acids in human platelets
DPhG PhD student meeting, Leipzig, 2005

Tausch L, Siemoneit U, Poeckel D, Kather N, Franke L, Schneider G, Holtmeier W, Beckhaus, T, Karas M, Jauch J, Werz O
Identification of targets and molecular modes of action of boswellic acids
DPhG Weihrauch Symposium 2008

9.2 Oral presentations

Tausch L, Werz O
Protein pulldown with immobilized boswellic acids and characterisation of fished targets. Plenary lecture
Summerschool of Pharmceutical Institute, University of Tuebingen, Arnsburg/Oberjoch, September 2006

Tausch L, Werz O
Target identification of boswellic acids
Seminar of the Institute of Pharmaceutical Chemistry, Frankfurt, February 2007

Tausch L
Short oral presentations at work group seminars of AK Steinhilber

10 Publications

1. Poeckel D, **Tausch L**, Kather N, Jauch J, Werz O.
   Boswellic acids stimulate arachidonic acid release and 12-lipoxygenase activity in human platelets independent of Ca^{2+} and differentially interact with platelet-type 12-lipoxygenase.
   Mol Pharmacol. 2006 Sep;70(3):1071-8..

2. Poeckel D, **Tausch L**, George S, Jauch J, Werz O.
   3-O-acetyl-11-keto-boswellic acid decreases basal intracellular Ca^{2+} levels and inhibits agonist-induced Ca^{2+} mobilization and mitogen-activated protein kinase activation in human monocytic cells.
   J Pharmacol Exp Ther. 2006 Jan;316(1):224-32.

3. Michaelis M, Suhan T, Michaelis UR, Beek K, Rothweiler F, **Tausch L**, Werz O, Eikel D, Zornig M, Nau H, Fleming I, Doerr HW, Cinatl J Jr.
   Valproic acid induces extracellular signal-regulated kinase 1/2 activation and inhibits apoptosis in endothelial cells.
   Cell Death Differ. 2006 Mar;13(3):446-53.

4. Poeckel D, **Tausch L**, Altmann A, Feisst C, Klinkhardt U, Graff J, Harder S, Werz O.
   Induction of central signalling pathways and select functional effects in human platelets by beta-boswellic acid.
   Br J Pharmacol. 2005 Oct;146(4):514-24.

5. Maier TJ, **Tausch L**, Hörnig M, Coste O, Schmidt R, Angioni C, Metzner J, Grösch S, Steinhilber D; Werz O, Geisslinger G
   Celecoxib is a 5-LO inhibitor
   Biochem Pharmacol;, accepted2008

6. Poeckel D, Greiner C, Verhoff M, Rau O, **Tausch L**, Hörnig C, Steinhilber D, Schubert-Zsilavecz M, Werz O
   Carnosic acid and carnosol potently inhibit human 5-lipoxygenase and suppress pro-inflammatory responses of stimulated human polymorphonuclear leukocytes
   Biochem Pharmacol; accepted2008

7. **Tausch L**, Kather N, Franke L, Schneider G, Beckhaus T, Karas M, Chen J, Jauch J, Werz O.
   Identification of human cathepsin G as a functional target of boswellic acids from the anti-inflammatory remedy frankincense.
   Nature Chemical Biology, presubmission accepted

8. **Tausch L**, Kather N, Jauch J, Werz O.
   Molecular interference of boswellic acids with Akt/protein kinase B and DNA-dependent protein kinase.
   Manuscript

9. **Tausch L**, Siemoneit U, Jauch J, Werz O.
   3-O-Acetyl-11-keto-β-boswellic acid potently antagonises select agonist-induced Ca^{2+} mobilisation and aggregation of human platelets.
   Manuscript

10. Kather N, **Tausch L**, Poeckel D, Werz O, Herdtweck E, Jauch J
    Immobilization of Boswellic acids at EAH Sepharose® for "target fishing"
    Manuscript

11 Acknowledgements

Mein besonderer Dank gilt folgenden Personen:

Meinem Betreuer Prof. Dr. Oliver Werz

Meinem Doktorvater Prof. Dr. Dieter Steinhilber

Meinem „Mentor“ Dr. Daniel Pöckel

Meinem Labornachbarn Michael Ermisch

Meiner ehemaligen Labornachbarin Kirsten Stoffers

den „Achtsemestlern“ Michi und Tina Hörnig, Marika Hoffmann, Dr. Beate Firla

Prof. Dr. Olof Rådmark, Yilmaz Mahsid, Karin Tholander, Maria Rakonjac und Sven Pawelzik für die exzellente Zeit in Schweden

Dr. Thorsten J. Maier

Den Doktores Christian Feißt und Adriane Lechtken

allen aktuellen und ehemaligen Mitarbeitern im AK Steinhilber sowie den „Startern“ im AK Werz: Uli, Ulf, Dagmar und Andreas und Arne, vor allem fürs Korrekturlesen

Dr. Gentner aus dem Eigenblutspendelabor des St.Markus-Krankenhauses

Kristallographie: Prof. Dr. Julian Chen, Dr. Christoph Kyritsis, Umar Jan Rashid, Stephanie Körber

AK Müller: Christian Fehske, Dr. Kristina Leuner, Dr. Gunter Eckert, „Hebbes“, Kathrin Schulz

Massenspektrometrie: Tobias Beckhaus

Der Burg- Apotheke mit allen Mitarbeitern, die mich immer und vor allem samstags ertragen haben und Herrn Rose für die Bereitstellung der Weihrauchkapseln

Prof. Dr. Walter Sauer (Wasa)

Dem Fähnlein Edelweiß im Orden der Kaiserjäger, Nerother Wandervogel, insbesondere Kalki, Hippl, Quassel, Gnom, Thorsten und FM Schulz

Meinen Freunden Hagen, Imme, Kevin, Roman, Svenni sowie Janko & Melle

Meinen Eltern, meiner Schwester, Peter, Lorena und Rilana

und Müpfe

12 Curriculum vitae

Persönliche Daten

Name	Lars Tausch
Geburtsdatum, -ort	27.04.1979, Bad Nauheim
Familienstand	ledig
Nationalität	deutsch

Ausbildung

Juli 2004 – Dez 2007	Promotion an der J.W.-Goethe-Universität, Frankfurt, Thema: "Novel anti-inflammatory targets and mechanisms of boswellic acids and celecoxib"
Mai 2004	Approbation als Apotheker
Nov 2003 - April 2004	Zweite Hälfte des Praktischen Jahres in der Burg-Apotheke, Königstein
Mai 2003 - Nov 2003	Erste Hälfte des Praktischen Jahres am Karolinska Institutet Stockholm, Schweden, Forschungsaufenthalt am Institut für Medizinische Chemie II
1998 - 2003	Pharmaziestudium an der J.W.-Goethe-Universität, Frankfurt, 2.Staatsexamen, Note: 1,75
1991 - 1998	Christian-Wirth-Schule, Gymnasium, Usingen Abitur, Note: 1,7

Berufliche Tätigkeiten, Weiterbildung

Seit Jan 2008	Wissenschaftlicher Produktmanager bei INFECTOPHARM Arzneimittel und Consilium GmbH
Juli 2004 - Sept 2007	Weiterbildung zum Fachapotheker für Pharmazeutische Analytik
Juli 2004 – Dez 2007	Betreuung des Achten Semesters Pharmazie als Wissenschaftlicher Mitarbeiter an der J.W.-Goethe-Universität, Frankfurt
Nov 2003 – Dez 2007	Burg-Apotheke, Königstein, Germany Apotheker
1995 - 2003	Körbers Montageservice, Grävenwiesbach - Laubach Schreiner, Holzmontage

Wehrersatzdienst

1998 - 2004	Dienst im Katastrophenschutzzug LZR 10/14 Grävenwiesbach (ehem. 1. LZR Hochtaunus, Bundeszug des Katastrophenschutzes)

Kenntnisse und Fähigkeiten

Fremdsprachen	Englisch in Wort und Schrift, verhandlungssicher Französisch in Wort und Schrift Russisch und Schwedisch Grundkenntnisse
EDV	MS Office, Outlook, DOS, Windows 98/2000/XP/Vista, Sigma-Plot, Graph-Prism, Labor-Software Millenium, Empower Pro und Odyssey, Hardware- und Netzwerktechnik

Engagement, Mitgliedschaften

Seit 2005	Mitglied im Verein Alumni und Freunde der Pharmazeutischen Institute, Frankfurt
Seit 2003	Mitglied in der Deutschen Pharmazeutischen Gesellschaft
2006 - 2008	Gruppenführer in der Freiwilligen Feuerwehr Grävenwiesbach-Laubach
Seit 1996	Mitglied in der Einsatzabteilung der Freiwilligen Feuerwehr Grävenwiesbach-Laubach
1998 - 2003	Fähnleinführer im Nerother Wandervogel

Akademische Lehrer

Neben Prof. Dr. Oliver Werz und Prof. Dr. Dieter Steinhilber waren meine Lehrer:

Prof. Dr. Theo Dingermann
Prof. Dr. T. Winkler
Prof. Dr. R. Marschalek
Prof. Dr. J. Dressman
Prof. Dr. J. Kreuter
Prof. Dr. M. Karas
Prof. Dr. M. Schubert-Zsilavecs
Prof. Dr. H. Stark
Prof. Dr. H. Blume
Prof. Dr. G. Lambrecht
Prof. Dr. W.E. Müller
Prof. Dr. Linde †
Prof. Dr. E. Ehlers